

**Superthermal particle effects on solitons in a symmetric four-species
electron-positron plasma**

by

Tamirat Gebeyehu Gogo

Submitted in fulfilment of the requirements for the degree of Master of Science

in the School of Chemistry and Physics

University of KwaZulu-Natal

Durban, South Africa, December, 2014

As the candidate's Supervisor I have/have not approved this dissertation for submission

Signed:

Name:

Date:

Preface

The work described in this dissertation was carried out by the author from August 2013 to September 2014, in the School of Chemistry and Physics, University of KwaZulu-Natal, Durban, under the supervision of Professor Manfred A. Hellberg, with Professor Richard L. Mace as co-supervisor.

These studies represent original work by the author and have not otherwise been submitted in any form for a degree or diploma to another tertiary institution. Where use was made of the work of others, it has been duly acknowledged in the text.

Declaration 1 - Plagiarism

I, Tamirat Gebeyehu Gogo, declare that

1. The research reported in this dissertation, except where otherwise indicated, is my original research.
2. This dissertation has not been submitted for any degree or examination at any other university.
3. This dissertation does not contain other persons' data, pictures, graphs or other information, unless specifically acknowledged as being sourced from other persons.
4. This dissertation does not contain other persons' writing, unless specifically acknowledged as being sourced from other researchers. Where other written sources have been quoted, then: (a) Their words have been re-written but the general information attributed to them has been referenced (b) Where their exact words have been used, then their writing has been placed in italics and inside quotation marks, and referenced.
5. This dissertation does not contain text, graphics or tables copied and pasted from the Internet, unless specifically acknowledged, and the source being detailed in the dissertation and in the References section.

Signed:

Declaration 2 - Publication

Based on the research described in this thesis, a poster has been presented at an international conference, and an article is in preparation for an appropriate international journal.

1. International Conference Presentation:

T.G. Gogo and M.A. Hellberg 2014, “Superthermal particle effects on solitons in a symmetric four-species electron-positron plasma”, *International Congress on Plasma Physics (Lisbon, Portugal)*, (2014); poster presented by the second author. The Supervisor devised and guided the research. The candidate derived the equations, wrote the computer programs and carried out all the calculations. He then produced a first draft of the poster under guidance. The supervisor edited the poster and ensured that the presentation of the physics was optimized.

2. Journal Article:

An article entitled “**Superthermal particle effects on solitons in a symmetric four-species electron-positron plasma**”, by **T.G. Gogo and M.A. Hellberg** is in preparation for the journal *Astrophysics and Space Science*. The calculations and interpretation of results are complete. Writing is in progress.

Acknowledgements

Foremost, I would like to express my sincere gratitude to my MSc thesis supervisor Professor Manfred A. Hellberg for his patience, understanding, immense knowledge, enthusiasm, and more importantly, his friendship approach in the important discussions we have had together. His guidance helped me in all the time of writing of this thesis. I have been extremely lucky to have a supervisor like him who cared so much about my work, who responded my questions and queries so quickly. Thank you very much.

Secondly, I would like to thank my co-supervisor Professor Richard L. Mace. My special thanks also go to my officemates Reginald Abdul, Francois Nsengiyumva, Harry Pillay and Farran Henning for their help when I needed it.

Finally, I would like to thank the National Astrophysics and Space Science Programme (NASSP) for a scholarship and providing funding to take up my MSc study components of course and research works at University of Cape Town and University of KwaZulu Natal, respectively.

Abstract

Electron-positron (EP) plasmas have been observed in active galactic nuclei, in the pulsar magnetosphere, at the center of our galaxy and in solar flares. Such plasmas are usually characterized as a fully ionized gas consisting of electrons and positrons, both constituent species possessing the same absolute charge to mass ratio. Because of this high symmetry it follows that a simple EP plasma cannot support acoustic waves. Hence, in this work we have investigated acoustic solitons in a symmetric four-species EP plasma, consisting of equal densities, N_h of hot electrons and positrons at temperature T_h , and cold electrons and positrons (density N_c) at temperature T_c . Such a plasma models the mixing of two, separately created, EP-pair plasmas, on a timescale short enough that full thermalization has not yet taken place.

The dynamics of the cold component has been studied using the non-relativistic multi-fluid approach (momentum and continuity equations). This investigation extends the study of Verheest et al. (1996), in which the hot species were assumed to be Maxwellian distributions, by considering the effects of excess superthermal particles.

The linear dispersion relation has been obtained using the usual Fourier methods. The reductive perturbation technique was used so as to study small amplitude nonlinear waves. Because of the symmetry of the model, a modified Korteweg-de Vries (mKdV) equation was obtained, and hence, a standard stationary solution representing a solitary wave was found.

In order to investigate arbitrary amplitude nonlinear waves we have used the fully nonlinear Sagdeev pseudopotential approach. Analytical and numerical calculations were employed to evaluate the upper and lower limits of the Mach number, defining existence domains for solitary waves in the plasma model under investigation. Based on that information, individual solitons were plotted. Moreover, the dependence of the soliton amplitude on

different plasma parameters was investigated both numerically and graphically. It was found that low kappa plasmas support solitons over a wider range of N_c/N_h parameter values than in the Maxwellian case. The amplitude at fixed true Mach number are somewhat smaller than found earlier by Verheest et al. (1996) for Maxwellian hot components, but for fixed absolute soliton speed, low kappa values yield larger amplitudes than found for higher kappa values, and hence Maxwellians.

Contents

1	General introduction	1
1.1	The magnetosphere of a pulsar	2
1.1.1	Electron-positron plasma generation	5
1.1.2	Primary and secondary plasmas	7
1.2	Justifications of our plasma model	8
1.3	Kappa velocity distribution function	10
1.3.1	Overview of the mathematical aspects of the kappa distribution . . .	11
1.4	Solitons	13
1.4.1	Methods employed in the investigation of solitary structures	14
1.4.2	Existence conditions of solitary structures	18
1.4.3	Outline of this thesis	20
2	Linear waves	23
2.1	Basic equations	25
2.2	Linear waves	29
2.3	Model equations	31
2.4	Waves in related plasma models	33
2.4.1	Hot kappa electrons and positrons	34
2.4.2	Cool adiabatic electrons and positrons	35

2.4.3	Kappa electrons and adiabatic positrons	35
2.4.4	A three component model	38
2.5	The symmetric four component model	41
3	Nonlinear waves	51
3.1	Small amplitude analysis	51
3.1.1	Derivation of the Korteweg de Vries (KdV) equation	52
3.1.2	The modified Korteweg de Vries (mKdV) equation	57
3.1.3	Reductive perturbation method for mKdV analysis	58
3.1.4	Stationary solution of the mKdV equation	60
3.2	Arbitrary amplitude analysis	63
3.2.1	The generalized Sagdeev pseudopotential	66
4	Results and discussions	69
4.1	Numerical results of the small amplitude analysis	69
4.2	Numerical results of the arbitrary amplitude analysis	75
4.2.1	The existence domain of the soliton	75
4.2.2	Comparison between mKdV and arbitrary amplitude results	87
5	Conclusion	89
5.1	Summary	89
	Appendix A	93
	Appendix B	99

List of Figures

1.1	Schematic representation of the creation of electron-positron pairs in the magnetosphere of a pulsar near its surface. Particles are accelerated by the electric field, move along the magnetic field lines, and radiate curvature photons which, by crossing the magnetic field, produce the electron(e^-) - positron(e^+) pairs (from Beskin et al. (1993), p. 98).	6
1.2	A typical solitary structure. The amplitude and width of the solitary structure are represented by H and w , respectively. The vertical axis represents the amplitude of the solitary structure while the horizontal axis represents the coordinate in the laboratory frame.	14
2.1	A plot of the dispersion relation shown in Eq. (2.49) for the plasma of adiabatic cold electrons and positrons. Dashed curve for $k \rightarrow 0$, while solid red line for large k	36
2.2	Solid blue and black curved lines generated from Eq. (2.53), respectively, for $\kappa = 2$ and $\kappa = 100$, showing an acoustic mode supported by an electron-positron plasma of hot kappa electrons and cool adiabatic positrons. The solid blue and black straight lines generated from Eq. (2.55), respectively, for $\kappa = 2$ and $\kappa = 100$ in the limit k very small. For large κ (Maxwellian limit) it is seen that all harmonics travels with the sound speed V when k is smaller. For $\kappa = 2$ it is observed that the harmonics doesn't travel with the same speed for all k	38

- 2.3 The dispersion relation for a plasma consisting of cold electrons and positrons at $T_c = 0$ and, hot kappa positrons at temperature T_h , as found from Eq. (2.62), the black and red curves for $\kappa = 2$ and $\kappa = 100$, respectively. For small k , the dotted and dashed lines show that $\omega \propto k$ 40
- 2.4 Dispersion relation (Eq. 2.70) for different kappa κ values for acoustic waves in a symmetric-four component electron-positron plasma of hot kappa distributed electrons and positrons, and cool adiabatic electrons and positrons. For small k , the dotted and dashed lines show that $\omega \propto k$ 44
- 2.5 Dispersion relation (Eq. (2.70)) evaluated for a plasma with very small cool component, $N_c = 0.01$, for $\kappa = 2$ (green curve) and $\kappa = 100$ (red). The dashed lines are from the small- k limit, Eq. (2.74). 46
- 2.6 Black and red curves for $\kappa = 2$ and $\kappa = 100$, respectively, generated from the dispersion relation, Eq. (2.70), for plasmas with very small hot components, $N_h = 0.001$. The dotted and dashed lines for $\kappa = 2$ and $\kappa = 100$, respectively, generated from the dispersion relation for low- k approximation, Eq. (2.74). 46
- 2.7 Figure shows the dependence of α on κ for the chosen values of α to c_1 ratios. 48
- 4.1 The regions of plasma parameters (α and κ) determining the sign of the nonlinear coefficient B in the mKdV equations when $\sigma \rightarrow 0$. The solid red curve corresponds to singular solution with an infinite amplitude of the electrostatic excitation. 72
- 4.2 Figure shows the effect of variations of different plasma parameters on the width w and amplitude ϕ of the hump-like electrostatic potential excitation found from mKdV theory, using a fixed true Mach number, M/M_s 73
- 4.3 Figure shows the effect of variations of different plasma parameters on the width w and amplitude ϕ of the hump-like electrostatic potential excitation found from mKdV theory, using a fixed normalized soliton speed, M 74

4.4 Figure shows the existence region of arbitrary amplitude solitons. The upper figure shows the soliton existence domain in the (α, M) space, whereas the lower figure shows the (κ, M) space. Solitons may exist between the lower and upper curves of the same style/color. 78

4.5 Sagdeev pseudopotential confirmation of the existence domain of solitary waves for chosen parametric values of plasma in accordance with our model. 79

4.6 The dependence of amplitude on α and κ for various values of M and M/M_s . 81

4.7 The dependence of the solitary wave amplitude ϕ on κ and α for fixed soliton speed, M (upper panels) and fixed Mach number, M/M_s (lower panels). . . 84

4.8 Figure shows the variation of ϕ_m with Mach number M for different values of α and κ 85

4.9 Figure shows the variation of the amplitude of soliton of the electrostatic potential ϕ_m with “true“Mach number $\frac{M}{M_s}$ 86

4.10 The variation of ϕ_m with $M - M_s$ for various values of α and κ 87

4.11 Comparison between the small amplitude and arbitrary amplitude results. . 88

Chapter 1

General introduction

The predominant presence of electron-positron (EP) plasma in the pulsar magnetosphere, active galactic nuclei and in the early universe (Beskin et al., 1983; Popel et al., 1995; Moslem et al., 2007; Misner et al., 1973) and the production of EP plasma in the laboratory (Greaves et al., 1994; Greaves and Surko, 1995) has attracted the attention of many authors to study the electrodynamics of this plasma.

A possibility for the co-existence of two types of cold and hot electron-positron populations in the pulsar magnetosphere has been suggested by Bharuthram (1992). Electrostatic waves in asymmetric unmagnetized electron-positron plasmas comprising hot and cool components, in which the hot components (hot electrons and positrons) followed the Maxwellian distribution whereas the cool inertial components (cold electrons and positrons) were governed by fluid equations have been studied by Pillay and Bharuthram (1992). In this model they have, however, assumed that the equilibrium number densities for each of the species in both hot and cool components are not equal, and the temperature of the cool components is strictly zero. In accordance to the physical conditions of the electron-positron plasma creation in the pulsar magnetosphere, this model is not a valid one, because of the asymmetry in number densities.

On the other hand, linear and nonlinear waves in a four component unmagnetized EP plasma in the pulsar magnetosphere have been investigated by Verheest et al. (1996). Zank and Greaves (1995) have studied the linear and nonlinear modes in a non-relativistic magnetized EP plasma. Linear electrostatic waves were considered by Lazarus et al. (2012) in a symmetric four component magnetized EP plasma. A theory for large amplitude compressional electromagnetic solitary pulses in a magnetized EP plasma have been presented by Shukla et al. (2011). More recently, Lu et al. (2014) have investigated nonrelativistic nonlinear wave solutions in a magnetized EP plasma.

Moreover, nonlinear phenomenon such as solitons in a plasma consisting of electrons and positrons with a component of other species such as ions and dust have been the subject of theoretical studies by a great number of authors in the recent past. For instance, (Popel et al., 1995; Alinejad et al., 2006; El-Awady et al., 2010; Baluku and Hellberg, 2011) have studied ion-acoustic solitary waves in an electron-positron-ion (epi) plasma. Solitary structures in electron-positron-ion-dust (epid) plasmas have been investigated by (Jehan et al., 2009; Guo et al., 2012; Wang and Zhang, 2014). Hence, stimulated specifically by the study of Verheest et al. (1996), we present the linear and nonlinear structures in a kappa distributed EP plasma in the pulsar magnetosphere in this work; starting with the investigation of the electrodynamics of a pulsar magnetosphere, and the mechanisms by which an EP plasma can be generated in the pulsar magnetosphere.

1.1 The magnetosphere of a pulsar

A pulsar is a highly magnetized, rapidly spinning neutron star which is small in size, an incredibly dense remnant of a much more massive star, that emits a beam of electromagnetic radiation with a wider range of energy. That rapidly spinning massive object generates extremely strong magnetic fields. The beam originates from the rotational energy of the neutron star, which generates an electrical field from the movement of the very strong

magnetic field, resulting in the acceleration of protons and electrons on the star surface. And we see that those accelerating particles emit electromagnetic energies in the form of gamma rays, x-rays and radio waves.

The magnetosphere of a pulsar is the region around the pulsar where its magnetic field dominates. The magnetic field strength near the pulsar surface is about $B_0 \approx 10^{12}\text{G}$ (Istomin and Sobyanin, 2007). That region consists of an electron-positron plasma (Beskin et al., 1993). This plasma can affect the radiation produced in the inner region of the magnetosphere or at the stellar surface. Therefore, Urpin (2011) has stated that *“understanding the plasma properties of the pulsar magnetosphere is of crucial importance for the interpretation of the observations”*.

Basic physical process By following the discussions of Beskin (2010) for the vacuum model approximation, i.e, the electrical conductivity of the star is large enough, the magnetic field may be assumed to be frozen-in in the neutron star. And the basic parameters defining the properties of the magnetosphere are the magnetic field B_0 , the star radius R , and the angular rotational velocity Ω . Therefore, in the internal region of the star the condition

$$\mathbf{E}_{\text{in}} + \frac{\boldsymbol{\Omega} \times \mathbf{r}}{c} \times \mathbf{B}_{\text{in}} = \mathbf{0}, \quad (1.1)$$

must hold, where c is the speed of light and \mathbf{r} is the radius vector from the star center. Because of the rotational motion of the star there is an electric field \mathbf{E} that arises due to the charge re-distribution inside the pulsar.

Beskin et al. (1993) approximated the component of electric field parallel to the magnetic field ($E_{\parallel} = \mathbf{E} \cdot \mathbf{B}/B$) in the neighbourhood of the star surface as

$$E_{\parallel} \approx \frac{\Omega R}{c} B_0 \approx 10^{10} - 10^{12} \text{V cm}^{-1}. \quad (1.2)$$

It is important to notice that E_{\parallel} appears to be of the same order of magnitude as the magnetic field B_0 defined earlier. Therefore, particles which find themselves in such a

strong electric field experience an enormous force, larger than the gravitational force of the pulsar, and have to be ejected from the star surface and, accelerated along the curvilinear magnetic field of the star, emitting hard gamma ray quanta (γ -quanta)(Beskin et al., 1993). These high energy curvature photons, i.e γ -ray quanta, propagating in the curved magnetic field reach the particle generation threshold, which occurs when photons in their motion cross the magnetic field lines (Sturrock, 1971) and, create electron-positron pairs (see Fig. 1.1 for the schematic representation of this process)

$$\gamma + B \rightarrow e^+ + e^- + B.$$

Thus, Beskin et al. (1993) have stated that *“the pulsar magnetosphere appears formed by the electron (e^-)-positron (e^+) plasma in the strong magnetic field of the neutron star”* .

Co-rotation of pulsar The electron-positron plasma, which fills the pulsar magnetosphere, screens the component of the electric field parallel to the magnetic field in the magnetosphere of pulsars. In other words, light electrons and positrons can always be redistributed so as to screen the longitudinal electric field

$$\mathbf{E}_{\parallel} \approx 0, \quad \varphi = \varphi(\mathbf{r}_{\text{perp}}) \quad (1.3)$$

where φ and \mathbf{r}_{perp} are the electric potential and the coordinate perpendicular to the magnetic field line, respectively. Because of the screening, the plasma starts to corotate along with the pulsar neutron star as a solid body. This rotational motion of the plasma across the magnetic field, is induced by the electric field (Beskin et al., 1993)

$$\mathbf{E}_c(\mathbf{r}) = -\frac{\boldsymbol{\Omega} \times \mathbf{r}}{c} \times \mathbf{B}, \quad (1.4)$$

where $\mathbf{E}_c(\mathbf{r})$ is the corotation electric field generated by the polarization of plasma that fills the magnetosphere. The charge density corresponding to the polarization of electric charge is obtained from

$$\rho_c = \frac{1}{4\pi} \nabla \cdot \mathbf{E}_c = -\frac{\Omega B}{2\pi c}, \quad (1.5)$$

where ρ_c is the corotation charge density or the Goldreich-Julian density (Goldreich and Julian, 1969). This density near the neutron star surface is about 10^{12} particles/cm³ (Is-tomin, 2008). The corotation charges rotates along with the magnetospheric plasma. This

rotation of the charge ρ_c leads to the appearance of electric currents.

Because of these currents, two distinctly different regions are known to be identified in the magnetosphere of neutron stars according to Istomin and Sobyanin (2007): *“the regions of open and closed field lines. In the region of closed field lines, the particles rotate synchronously with the field because of high plasma and magnetic field freezing-in. However, along the open lines, the particles can move freely and escape from the neutron star magnetosphere. Continuous plasma outflow from the magnetosphere requires the presence of electron-positron pair generation processes compensating for it”*.

1.1.1 Electron-positron plasma generation

Because of the outflow of plasma along the open magnetic field lines, along with it the co-rotation charge screening the longitudinal electric field in the equatorial region, a significant longitudinal potential difference (Beskin et al., 1993), $\varphi \approx 10^{13} - 10^{15}$ V, appears near the polar cap. In this region, the longitudinal electric field

$$\mathbf{E}_{\parallel} = -\nabla_{\parallel}\varphi, \quad (1.6)$$

accelerates positively charged particles (say, positrons) in the same direction as the electric field (away from the star), while negatively charged particles (say, electrons) are accelerated in the direction opposite to the field (towards the star).

Consequently, the charged particles start to move along the curved path because of the curvature of the strong magnetic field lines over the surface of the pulsar. During this motion, the particles acquire sufficient energy from the field. This gives rise to the emission of hard γ -quanta due to the so called curvature radiation (Zheleznyakov, 1996). These quanta (photons) will be radiated in the direction of the magnetic field lines. Because of the curvature of the magnetic field, the photons start to cross the magnetic field lines and, consequently, they reach the electron-positron generation threshold angle (Gurevich and Istomin, 1985).

These newly created particles (electron-positron pairs) start to accelerate in opposite directions depending on the signs of the charges. The electrons are accelerated toward the

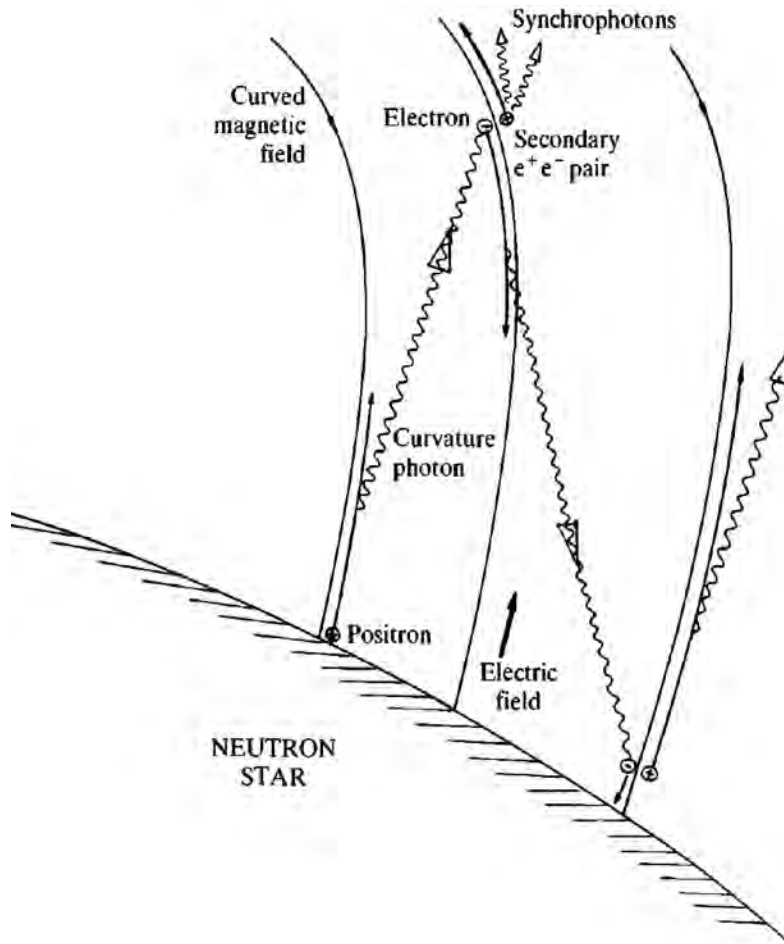


Figure 1.1: Schematic representation of the creation of electron-positron pairs in the magnetosphere of a pulsar near its surface. Particles are accelerated by the electric field, move along the magnetic field lines, and radiate curvature photons which, by crossing the magnetic field, produce the electron(e^-) - positron(e^+) pairs (from Beskin et al. (1993), p. 98).

star surface (opposite to the electric field direction), and produce a photon near the star surface. This photon now starts to cross the curved field and hence generates the new

pairs. Now the newly born positrons begin to accelerate away from the star's surface. Thus, through the repeated action of these processes, the electron-positron production will be sustained in the pulsar magnetosphere as shown schematically in Fig. 1.1.

Double layer Because of the accumulation of excess charges with opposite polarities over the star surface and the magnetosphere, an electric field will be produced. The existence of the electric field provides the potential difference, about $10^{13} - 10^{15}$ V, between the star surface and its magnetosphere. This potential difference is called a “double layer” or a “vacuum gap”. In this layer the plasma will not exist owing to the escape along the open magnetic field lines. The potential drop across the double layer will accelerate electrons and positrons in opposite directions. The magnitude of the potential drop determines the acceleration of the charged particles and hence particles acquire the high energy necessary for the radiation of curvature photons capable of generating electron-positron plasmas.

Vacuum breakdown These particles generated near the star surface can be accelerated by the double layer and produce photons. Before reaching the upper limit of the double layer, the photons create an electron-positron pair plasma. The newly generated electron will be picked up by the electric field and then it is accelerated towards the star surface. Near the neutron star surface this electron emits γ -quanta, which in turn produces electron-positron pairs. Then, the positrons are caught by the field to move away from the star surface, while the electrons are moving towards the surface. With such repeating processes the vacuum gap will break down. This process is known as the vacuum breakdown.

1.1.2 Primary and secondary plasmas

The plasma particles generated (ejected) from the surface of the star are accelerated by the strong potential gap. These fast moving plasmas are capable of producing so-called curvature photons (see Fig. 1.1). Then, these photons are absorbed by the magnetic field of the star to produce the electron-positron pairs discussed earlier. These pairs of plasmas

are known as the primary plasma.

Outside the double layer (potential gap) of the polar cap of the star surface the production of electron-positron (EP) plasma increases. Although this increase in concentration of EP plasma starts to screen the longitudinal component of electric field, i.e., $E_{\parallel} = 0$, EP pair production occurs due to synchrotron radiation (see Figure 1).

The EP pairs produced due to the curvature photons find themselves in a non-zero Landau level for a very short period of time of about 10^{-19} s (Beskin et al. (1993), p. 101). After this extremely short period of time, the pair plasmas moves down to zero Landau level. During this transition, from non-zero Landau level to zero Landau level, they emit synchrophotons (see Fig. 1.1). These photons have very low energy relative to the energy of the parent curvature photons due to their large mean free path length as compared to the curvature photons mean free path length (Gurevich and Istomin, 1985). Now, the synchrophoton has to be absorbed by the magnetic field to produce the EP pair plasma. These pairs produced by synchrophotons are called the secondary plasmas. It is important to notice here that the energy of the secondary plasma is less than that of the primary plasmas. This is because of the fact that the mean energy of curvature photons (responsible for the primary plasmas production) is much less than that of the synchrophoton radiation (responsible for the secondary plasmas production).

1.2 Justifications of our plasma model

In this work we have considered four-component electron-positron plasmas. In these, we have hot electrons and positrons at the same temperature T_h , and cool positrons and electrons at another temperature T_c . In an unperturbed state both the hot and cool components have the number density N_h and N_c , respectively. Note that the subscripts h and c , respectively, stands for the hot and cool plasma species.

The electron and positron pairs which have been created from curvature photons in the primary plasma production process are assumed to be a hot species with equilibrium number density N_h and temperature T_h . The other pairs of electrons and positrons which were produced from synchrophotons by the secondary plasma generation process can be taken as a cold species having the number density N_c and temperature T_c . Because of the high symmetry between electrons and positrons it is assumed that both species (electrons and positrons) must have the same number density and temperature in the equilibrium hot and cold states, respectively.

The relative terms “hot” and “cold” come from the fact that the plasma formed by the primary process has more energy (thermal) than the plasma generated by the secondary process as described in Section 1.1.1 above. Therefore, relatively the secondary plasma is in a cool thermal state compared to the plasma produced by the primary generation process, which is found in a relatively hot thermal state.

We shall not take into account the influence of the magnetic field, although there is a strong magnetic field in the pulsar magnetosphere. This is because, the motion of EP pairs is mainly along the magnetic field lines, therefore, these pairs will not feel the effect of the magnetic field. In addition, any transverse momentum, that the particles may have, with respect to the magnetic field of the pulsar will be radiated away because of the strength of this field. Hence, these assumptions restrict our analysis of plasma dynamics to electrostatic disturbances propagating in an unmagnetized electron-positron plasma.

Although the extreme situations in the pulsar magnetosphere would allow the relativistic environment for an EP plasma, given the effect of cooling of EP plasmas by cyclotron emission it is likely that non-relativistic astrophysical EP plasmas may exist (Zank and Greaves, 1995). With this assumption, we have considered a non-relativistic EP plasma in the pulsar magnetosphere in this work.

1.3 Kappa velocity distribution function

Introduction

Livadiotis and McComas (2011) have described that “*the Maxwell-Boltzmann (MB) statistical mechanics describes successfully classical system in thermal equilibrium - a state where any flow of heat (e.g. thermal conduction, thermal radiation) is in balance. Any system in thermal equilibrium has its distribution function of velocities stabilized into the Maxwellian distribution*”. However, these distributions are not very common in space and astrophysical plasmas because there is a lack of thermal equilibrium in general (Hammond et al., 1995). Instead, most of these plasmas reside in stationary states (that is their statistics do not depend explicitly on time, and thus all the macroscopic thermal observables have ceased to change with time), that are typically not well described by Maxwell distributions, and are thus often power law-like, not in thermal equilibrium (Hellberg et al., 2009; Livadiotis and McComas, 2013).

Different observational outcomes confirmed that the space plasmas from the solar wind to planetary magnetosphere are largely collisionless systems of particles, with long-range electromagnetic interactions, in non-thermal equilibrium stationary states. The plasmas in these states do not follow the usual Maxwellian distribution (Formisano et al., 1973; Scudder et al., 1981; Marsch et al., 1982; Leubner, 2004). Instead these have been characterized by the empirical velocity distributions introduced by Vasyliunas (1968). This function is known as the generalized Lorentzian or kappa distribution, which is parametrized by the spectral index kappa (κ) (Hellberg et al., 2009).

Moreover, Livadiotis and McComas (2011) pointed out that such stationary states are characterized by their values of the superthermality index κ , and that smaller values of kappa are associated with systems that are further from equilibrium. In other words, lower kappas have excess superthermal particles compared to a Maxwellian distribution. That is, low values of κ represent a strong non-Maxwellian tail with more superthermal

particles in the tail of the distribution function. They also have more slow particles, but a reduction in the range when the speed of particles v approaches the thermal speed v_{th} . In contrast, $\kappa \rightarrow \infty$ represents the equilibrium condition (the Maxwellian distribution). Similarly, Livadiotis and McComas (2010) have categorized the region of space plasmas into two based on kappa indices: the “near-equilibrium” region with $\kappa \in (2.5, \infty]$ and the “far-equilibrium” region with indices $\kappa \in (1.5, 2.5]$.

Since the introduction of the kappa distribution to fit satellite data by Vasyliunas (1968), many authors have used it in their studies of waves in space plasmas. To investigate the effect of Landau damping on various plasma modes (Summers and Thorne, 1991; Mace and Hellberg, 1993; Hellberg and Mace, 2002) have employed the kappa distribution. Moreover, Formisano et al. (1973) have used the kappa distribution to fit proton data measured in the Earth’s bow shock. Similarly, the analysis of high resolution HELIOS observations by Marsch et al. (1982) confirmed the ubiquitous presence of high energy proton populations that generate non-Maxwellian halos in the distribution.

The evidence of kappa distributions of charged particles (electrons, protons and heavy ions) which are far away from their thermodynamic equilibrium in space plasmas is clear and unambiguous (Shukla et al., 1986; Ghosh and Bharuthram, 2008). There is much evidence that the kappa distribution provides a straightforward replacement for the Maxwellian distribution when dealing with systems in stationary states out of thermal equilibrium, commonly found in space and astrophysical plasmas. Such kappa functions gives the best fit to the observed velocity distribution functions (Pierrard and Lazar, 2010).

1.3.1 Overview of the mathematical aspects of the kappa distribution

Conventionally, a three dimensional isotropic kappa velocity distribution function for a free particle of mass m will be represented by (Vasyliunas, 1968; Summers and Thorne,

1991)

$$f_{\kappa}(v) = A_{\kappa} \left[1 + \frac{v^2}{\kappa\theta^2} \right]^{-(\kappa+1)}, \quad (1.7)$$

where A_{κ} is a normalization parameter, $v^2 = v_x^2 + v_y^2 + v_z^2$ (velocity of the particle in 3D), κ is the spectral index which measures the deviation of the superthermal particles from the Maxwellian distribution, and the parameter θ is a characteristic speed. In fact, this “effective speed” is the most probable speed it is related to the Maxwellian most probable speed $v_{mp} = (2k_B T_k/m)^{1/2}$ through $\theta = [(\kappa - \frac{3}{2})/\kappa]^{1/2} v_{mp}$ (Summers and Thorne, 1991; Hellberg et al., 2009), where k_B and T_k are the Boltzmann constant and the kinetic temperature of the particles, respectively. Note that this relation is only valid for $\kappa > 3/2$ and thus the κ distribution function can be used to model the superthermal (non-Maxwellian) plasma. The Maxwellian most probable speed will be recovered for $\kappa \rightarrow \infty$. Moreover, the parameter κ is a free parameter, which means that it does not depend on a parameter like temperature (Livadiotis and McComas, 2011), while the parameters A_{κ} and θ are constrained by the lowest (even) moments of the distribution function (Hellberg et al., 2009).

The total equilibrium number density N_o can be calculated by taking the integral of Eq. (1.7) over the velocity space \mathbf{v} . That is,

$$N_o = \int_{-\infty}^{\infty} f_{\kappa}(\mathbf{v}) d^3v = A_{\kappa} (\pi\kappa\theta^2)^{3/2} \frac{\Gamma(\kappa - 1/2)}{\Gamma(\kappa + 1)}. \quad (1.8)$$

That yields

$$A_{\kappa} = \frac{N_o}{(\pi\kappa\theta^2)^{3/2}} \frac{\Gamma(\kappa + 1)}{\Gamma(\kappa - 1/2)}, \quad (1.9)$$

where Γ is the usual gamma function, $\Gamma(a) = \int_0^{\infty} t^{a-1} e^{-t} dt$.

Using Eq. (1.9) into Eq. (1.7), the generalized isotropic three dimensional kappa distribution (generalized Lorentzian) function takes the form

$$f_{\kappa}(v) = \frac{N_o}{(\pi\kappa\theta^2)^{3/2}} \frac{\Gamma(\kappa + 1)}{\Gamma(\kappa - 1/2)} \left[1 + \frac{v^2}{\kappa\theta^2} \right]^{-(\kappa+1)}. \quad (1.10)$$

By integrating Eq. (1.10) of kappa distribution over the velocity space, Baluku and Hellberg (2008) have derived an expression for the number density n_j of species j with equilibrium density N_{j0} , charge q_j , mass m_j and spectral index κ_j , which moves in an electrostatic potential difference φ as

$$n_j = N_{j0} \left(1 + \frac{2q_j\varphi}{m_j\kappa_j\theta_j^2} \right)^{-(\kappa_j - \frac{1}{2})}, \quad (1.11)$$

where θ_j is the characteristic speed and q_j is the particle charge of species j . Using the relationship between v_{mp} and θ discussed earlier in this subsection, Eq. (1.11) take the form

$$n_j = N_{j0} \left(1 + \frac{q_j\varphi}{(\kappa_j - \frac{3}{2})k_B T_k} \right)^{-(\kappa_j - \frac{1}{2})}. \quad (1.12)$$

1.4 Solitons

General introduction

A soliton is a special form of solitary wave. The solitary wave/soliton represents, not a periodic wave, but the propagation of a single isolated symmetrical hump/dip-like structure of unchanged form (Shukla and Mamun, 2002). To sustain a stable nonlinear solitary wave, dispersive effects are in balance with the steeping effect of nonlinearity, assuming that the dissipation effects are negligible. Solitons do not interact strongly with other solitons so that they effectively pass through one another, unchanged and retaining their form. This means that solitons do not obey the superposition principle and can travel long distances with little loss of energy or structure. In Fig. 1.2 a typical solitary structure is shown in terms of its height H and width w . This solitary structure is characterized by a single hump at the origin.

Historically, John Scott Russell first experimentally observed the solitary wave, or “great wave of translation” propagating without change in shape, on the Edinburgh-Glasgow canal in 1834 (Drazin, 1983). Based on his experimental findings, Russell discovered, empirically, one of the most important relations between the speed U of a solitary wave and

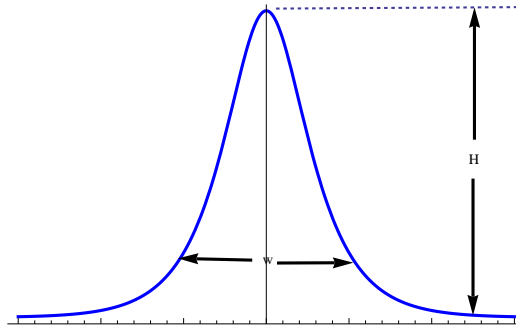


Figure 1.2: A typical solitary structure. The amplitude and width of the solitary structure are represented by H and w , respectively. The vertical axis represents the amplitude of the solitary structure while the horizontal axis represents the coordinate in the laboratory frame.

its maximum amplitude H above the free surface of liquid of finite depth a in the form

$$U^2 = g(H + a),$$

where g is acceleration due to gravity.

After Russell observed the solitary structure in the canal, series of investigations was carried out to provide the explanation of the water wave. Among these, the mathematical model equation which was derived by two Dutch physicists, Korteweg and de Vries (KdV) in 1895 to provide an explanation of the phenomenon observed by Scott Russell has been used widely by a great number of authors from other disciplines to study weakly nonlinear small amplitude solitary structures. In line with this, the new concept of the *soliton*, a name intended to signify particle-like qualities, was discovered by Zabusky and Kruskal (1965) in connection with the numerical integration of KdV equation.

1.4.1 Methods employed in the investigation of solitary structures

To study the propagation of the solitary structure of the electrostatic potential pulse in our plasma model under the perturbed state, we have employed two approaches. The

reductive perturbation technique that corresponds to small amplitude (weakly nonlinear soliton) and *Sagdeev pseudopotential* approach that corresponds to an arbitrary amplitude (fully nonlinear soliton).

Reductive perturbation theory

This method is widely applicable to waves that are weakly nonlinear, if their linear counterparts have acoustic like dispersion at low frequencies. The method was employed for the first time to study the propagation of small amplitude ion acoustic solitary structures in a plasma of cold ions and hot electrons by Washimi and Taniuti (1966). Since then this method has been used by a great number of authors in order to investigate small amplitude solitary structures in different plasma models.

The technique (reductive perturbation method) is commonly employed to derive the nonlinear KdV equation using the stretched coordinates $\zeta = \varepsilon^{1/2}(x - Vt)$ and $\tau = \varepsilon^{3/2}t$ (Washimi and Taniuti, 1966; Verheest, 2000; Shukla and Mamun, 2002), where ε is the smallness parameter ($\varepsilon < 1$) measuring the weakness of perturbation and V is the linear phase velocity of the wave in the limit where the wave number $k \rightarrow 0$. The detail of the derivation of the KdV equation is presented in Appendix A.

The general form of the KdV equation is given in Swanson (2003) as

$$\frac{\partial \varphi_1}{\partial \tau} + A\varphi_1 \frac{\partial \varphi_1}{\partial \zeta} + B \frac{\partial^3 \varphi_1}{\partial \zeta^3} = 0, \quad (1.13)$$

where φ_1 is the perturbed electrostatic potential pulse, A and B are constants, and τ and ζ are space-like and time-like variables, respectively. It is a simple and useful model for describing the long time evolution of dispersive wave phenomena in which the steepening effect of the nonlinear term (second term in Eq. (1.13)) is counterbalanced by the dispersion (third term in Eq. (1.13)). It was originally introduced by Korteweg and de Vries (1895) to describe the propagation of unidirectional shallow water waves. It admits the exact solution called the soliton. Note that the explicit form of A and B are model

dependent (see Chapter 3 for detail).

A is the coefficient of the nonlinear term in the middle of Eq. (1.13) and B is the coefficient of the dispersive term. The trade-off between these terms, the nonlinear (second term) and the dispersive (third term) in Eq. (1.13), is the condition responsible for sustaining the solitary structure (soliton) without breakdown. The stationary soliton solution of the KdV equation (1.13) can be obtained by applying a transformation $\eta(\tau, \zeta) = \zeta - U_0\tau$, where U_0 is the constant phase speed in the laboratory frame Chen (1983) normalised by sound speed c_s , and imposing the boundary conditions for localized perturbations, namely, φ_1 , $d\varphi_1/d\zeta$ and $d^2\varphi_1/d\zeta^2 \rightarrow 0$ as $\zeta \rightarrow \infty$ as (Verheest, 2000)

$$\varphi_1 = \varphi_m \operatorname{sech}^2(\eta/w). \quad (1.14)$$

This function is a so called soliton solution; it describes a stationary bell-shaped solitary wave pulse propagating at velocity U_0 without change of form (see Fig. 1.2). Here $\varphi_m = 3U_0/A$ is the amplitude and $w = \sqrt{4B/U_0}$ is the width of the soliton. The stationary soliton solution (Eq. 1.14) for the KdV equation is valid for $A \neq 0$ and $B/U_0 > 0$. Note that the sign of the potential soliton depends on the sign of A if we assume that $U_0 > 0$. For a positive soliton ($\varphi_m > 0$) the sign of A must be greater than zero, whereas for the negative soliton ($\varphi_m < 0$) the sign of A must be less than zero. We also note that for a given set of plasma parameter values we can have only a single sign of the nonlinear coefficient A , and thus of φ_m . Hence, for a given plasma, KdV solitons can only have a specific polarity, and coexistence of solitons of both polarities can not occur.

However, for some plasma models (like the model in this work) the nonlinear coefficient A in the KdV equation vanishes (see chapter 3, section 3.1). In such a case, the amplitude of the potential solitary pulse becomes infinitely large, and this leads to the wave breakdown because of the absence of trade-off between the nonlinear and dispersive terms in the KdV equation.

In order to avoid such a scenario it is appropriate to introduce the modified Korteweg

de-Vries (mKdV) equation, for instance by following Verheest (2000). In this case the stretched coordinates are considered as $\zeta = \varepsilon(x - Vt)$ and $\tau = \varepsilon^3 Vt$ (Verheest, 1988) instead of the stretched coordinate used earlier in the derivation of the KdV equation. Therefore, using this approach, the mKdV equation takes the form (see the detailed derivation of the mKdV equation in the Appendix B)

$$\frac{\partial \varphi_1}{\partial \tau} + C \frac{\partial \varphi_1^3}{\partial \zeta} + B \frac{\partial^3 \varphi_1}{\partial \zeta^3} = 0, \quad (1.15)$$

where the coefficient B in Eq. (1.15) has the same role as in Eq. (1.13), the explicit form of C is model dependent, and φ_1 is the perturbed electrostatic potential pulse to the first order. The mKdV equation is valid only when the nonlinear coefficient in the KdV equation goes to zero. Details of the stationary soliton solution of Eq. (1.15) are given in Section (3.3) of Chapter 3.

Sagdeev pseudopotential method

One of the important and widely used methods in the investigation of the nonlinear arbitrary amplitude (large) solitary structures in a given plasma model is the Sagdeev pseudopotential approach (Sagdeev, 1966). This method takes advantage of the fact that the nonlinear wave equations can be reduced to a pseudo-energy conservation equation, which is similar to the energy equation of a unit mass particle in classical mechanics. Both electrostatic and electromagnetic waves in collisionless plasmas have been studied by this method by several authors. For instance, (Verheest and Pillay, 2008; Baluku et al., 2010a; Baluku and Hellberg, 2011) have used this method in their study of acoustic solitary structures in different plasma models. The method gives the necessary condition (see subsection 1.4.2) for the existence of solitary structures (McKenzie and Doyle, 2003).

Using the Poisson equation, we can start this approach as

$$\epsilon_0 \frac{\partial^2 \varphi}{\partial x^2} + \sum_j n_j q_j = 0, \quad (1.16)$$

where φ , x , n_j , and q_j are the unnormalized electrostatic potential, coordinate, number density of species j , and charge of species j , respectively. After multiplication of both

sides of Eq. (1.16) by $d\varphi/dx$, the second term in this equation can be represented as the derivative of the Sagdeev pseudopotential, Ψ , which in this case is a function of the electrostatic potential φ . It becomes explicit in the pseudo-energy conservation law

$$\frac{\epsilon_0}{2} \left(\frac{d\varphi}{dx} \right)^2 + \Psi(\varphi) = 0. \quad (1.17)$$

In this equation, the Sagdeev pseudopotential $\Psi(\varphi) = -\int G(\varphi)d\varphi$, where $G(\varphi) = \sum_j n_j q_j$. Note that $G(\varphi)$ is not a function of φ only through $n_j = n_j(\varphi)$ (for example see Eq. (1.12) for n_j above), rather it is also a function of different plasma parameters depending on the plasma model under investigation (see Eq. (3.92) in Section (3.2) of Chapter 3 in this thesis) and of the soliton speed. It is also important to notice that because the first term in Eq. (1.17) is a positive quantity, a soliton solution exists only under the condition that the Sagdeev pseudopotential Ψ forms a well, that is, Ψ is negative, in the region of electrostatic potential space $\varphi < |\varphi_m|$, where φ_m is the amplitude of the solitary pulse of the electrostatic potential.

Equation (1.17) is analogous to the equation, $\frac{1}{2} \left(\frac{dx}{dt} \right)^2 + V(x) = 0$, that governs the motion of a classical particle of unit mass which moves along the x -axis in a conservative potential field $V(x)$. Here, in Eq. (1.17), x , φ , and $\Psi(\varphi)$ plays the role of time t , coordinate x , and the potential field $V(x)$, respectively, for the classical particle.

1.4.2 Existence conditions of solitary structures

From the Sagdeev pseudopotential method, the following conditions must hold in order that the perturbation will propagate as a solitary structure:

- At the origin ($\varphi = 0$), from the Sagdeev pseudoenergy conservation law in Eq.(1.17), we have, $\Psi(\varphi = 0) = 0$. This can be easily verified from the expression derived for the pseudopotential Ψ in this work in Eqs. (3.93-94), Section 3.2 of Chapter 3. Note that, in those equations Eqs. (3.93-94), the electrostatic potential φ is written in a normalized form designated by ϕ . Moreover, the condition, $\frac{d\Psi(\varphi)}{d\varphi}(\varphi = 0) = 0$, must

hold at the origin in order that Eq. (1.17) has a solitary wave solution (Baboolal et al., 1988; Mace and Hellberg, 1993; Verheest, 2000). This means that the condition

$$\Psi(\varphi = 0) = \frac{d\Psi(\varphi = 0)}{d\varphi} = 0,$$

must hold in order to have a solitary wave solution.

- The origin ($\varphi = 0$) must be unstable for a soliton solution to Eq. (1.17) to exist (Verheest et al., 2008). The condition for this is that the Sagdeev potential $\Psi(\varphi)$ must have a second derivative such that

$$\frac{d^2\Psi(\varphi)}{d\varphi^2}(\varphi = 0) < 0. \quad (1.18)$$

Often this condition is called the soliton condition. It implies that there is an unstable local maximum at the origin, such that the pseudoparticle comes to rest, at the origin $\varphi = 0$ ($\eta = \pm\infty$) (Baboolal et al., 1990). This condition (1.18) is used to calculate the minimum speed of the solitary structure from

$d^2\Psi(\varphi)/d\varphi^2(\varphi = 0) = 0$ (Verheest et al., 2008). Below this speed the plasma under study no longer supports the solitary structures. Therefore, the speed that will be calculated from this condition can be used as a lower critical speed M_s of the soliton. Actually, this speed is equal to the corresponding normalized linear phase velocity or acoustic speed in the limit of large wavelength (see Eq. (2.75) of Chapter 2 in this thesis), supported by the four-component symmetric electron-positron plasma, the model this work is mainly concerned with. For such a case, the amplitude of the solitary structures of the electrostatic potential pulse goes to zero when the speed of the structure is approaching the critical speed which corresponds to the global acoustic speed for the model envisaged (Verheest et al., 2008). In general, both KdV and Sagdeev theories require that solitons be strictly superacoustic ($M > M_s$). However, recently it was found that in some plasmas, finite amplitude solitons may occur at the critical speed M_s , in contradiction to both KdV theory and standard Sagdeev theory (Baluku et al., 2010a,b; Baluku and Hellberg, 2011). Hence, from this we conclude that the condition $\Psi''(\varphi = 0) \leq 0$ is a better formulation of this condition.

- There exists a maximum potential φ_m at which the Sagdeev pseudopotential $\Psi(\varphi)$ in Eq. (1.17) goes to zero. That is,

$$\Psi(\varphi_m) = 0, \quad (1.19)$$

where φ_m is the value of the electrostatic potential beyond which the density of a species is either infinite or complex. This condition is used to calculate the maximum speed (upper limit) of the solitary structures. Beyond this speed, solitons will not exist in the model under investigation for given values of the plasma parameters. Therefore, the solitons are expected to exist between the critical speed that will be derived from Eq. (1.18) and maximum speed which will be calculated from Eq. (1.19).

- To ensure the real soliton solution in Eq. (1.17), one requires to have

$$\Psi(\varphi) < 0 \quad \text{for} \quad 0 < |\varphi| < |\varphi_m|. \quad (1.20)$$

1.4.3 Outline of this thesis

This thesis is organized in the following way. It starts with the brief introduction in Chapter 1 that covers the basic plasma processes in the pulsar magnetosphere and justification of our plasma model. In this chapter we have also described briefly superthermality effects through the kappa distribution, what the solitary structure/soliton is, and the methods that we have used to investigate this structure in our model.

In Chapter 2 we discuss the linear waves in various multi-component electron-positron plasma, deriving the linear dispersion relations for different models of EP plasmas. We also present the dispersion relations for different linear EP plasma models in graphical form. This includes our symmetric four component EP model.

The reductive perturbation method is employed in Chapter 3 to investigate small amplitude nonlinear solitary structures in our four component symmetric electron-positron

plasma. Using this method the mKdV equation is derived, from which the stationary soliton solution is obtained. In order to study the arbitrary amplitude solitary waves in our plasma model we have used the Sagdeev pseudopotential method, obtaining the Sagdeev pseudo-energy conservation equation.

The numerical evaluation of the mathematical results obtained from Chapter 3 is discussed in detail in Chapter 4, including graphical visualizations. In particular, based on the Sagdeev potential, we consider the dependence of the solitary structure on different plasma parameters, such as number density ratio α , superthermality parameter κ , and temperature ratio σ . Finally, the conclusion is given in Chapter 5.

Chapter 2

Linear waves in multispecies electron-positron plasmas

In this chapter we will discuss linear electrostatic waves in which the wave propagation vector \mathbf{k} is parallel to the electric field vector \mathbf{E} , in multi-species electron-positron plasmas in the pulsar magnetosphere. The dimensionless basic governing equations will be developed for both cool and hot components of EP plasma from the multi-fluid equations of motion and kappa velocity distribution function, respectively. From these equations, the dispersion relations will be derived for each of the related plasma models using the usual Fourier mode for small oscillation follows that of Chen (1983).

Introduction

We have considered the electron-positron plasma pairs formed in the pulsar magnetosphere. The temperature of both electrons and positrons formed from the curvature photons by the primary plasma generation process is T_h (density N_h). And, the temperature of the electron-positron pairs formed from synchrophotons in the secondary plasma generation process is T_c (number density N_c). Since the electrons and positrons are highly

symmetric in absolute charge to mass ratio, both species are assumed to have equal temperatures in the hot and cool states at equilibrium, that is,

$$\underbrace{T_{eh} = T_{ph} = T_h}_{\text{hot EP plasma (hot state)}} \quad \text{and} \quad \underbrace{T_{ec} = T_{pc} = T_c}_{\text{cool EP plasma (cool state)}},$$

where T_{eh} , T_{ph} , T_{ec} and T_{pc} are the temperature of the hot electrons, hot positrons, cool electrons and cool positrons, respectively. We define the number density of the electrons and positrons in the hot and cool states as n_{eh} (hot electrons), n_{ec} (cool electrons), n_{ph} (hot positrons) and n_{pc} (cool positrons). At equilibrium, the densities of both hot and cool species can be defined as

$$\underbrace{n_{eh0} = n_{ph0} = N_h}_{\text{hot EP Plasma (hot equilibrium state)}} \quad \text{and} \quad \underbrace{n_{ec0} = n_{pc0} = N_c}_{\text{cool EP plasma (cool equilibrium state)}},$$

where the subscript 0 refers to the equilibrium (unperturbed) state. Thus, n_{eh0} is the equilibrium number density of the hot electrons, n_{ph0} the equilibrium number density of the hot positrons, n_{ec0} the equilibrium number density of the cool electrons, and n_{pc0} the equilibrium number density of the cool positrons. At equilibrium, N_h and N_c refer to the hot and cool component number densities, respectively. Since the plasma is uniform and electrically neutral in the unperturbed (equilibrium) state, then the following charge neutrality condition holds:

$$n_{e0} = n_{p0} = n_0 = N_0 \implies \underbrace{n_{eh0} + n_{ec0}}_{n_{e0}} = \underbrace{n_{ph0} + n_{pc0}}_{n_{p0}} = \underbrace{N_h + N_c}_{n_0} = N_0, \quad (2.1)$$

where n_{e0} , n_{p0} , n_0 , and N_0 are the equilibrium number density of the electrons, the equilibrium number density of the positrons, the overall number density of the plasma, and the equilibrium number density of the plasma, respectively.

Or, in general,

$$N_h + N_c = N_0. \quad (2.2)$$

The particles' motion in the pulsar magnetosphere is largely in the direction of the magnetic field, with a negligible amount of transverse motion as compared to the longitudinal

motion. It follows that the effect of the magnetic field has not been considered in our plasma model. We shall also consider only the electrostatic oscillation (the wave propagation vector \mathbf{k} is parallel to the electric field vector \mathbf{E}). Moreover, in an unperturbed state the electrostatic potential $\phi_0 = 0$ because of the plasma screening effect of the electrostatic field in the pulsar magnetosphere at equilibrium. It follows that the drift velocity u_0 of the particles in an unperturbed state is equal to zero. This means that the plasma is stationary in an equilibrium state.

2.1 Basic equations

We consider a plasma consisting of two pairs of electron-positron species, with the hot electrons and positrons found at temperature T_h with equilibrium number density N_h , and the cool electrons and positrons found at temperature T_c with the equilibrium number density N_c . The inertial cool component of the EP plasma has to be governed by fluid equations of motion (continuity and momentum equations), while the velocity of the inertialess hot component of the EP plasma will follow the kappa distribution law. It follows that for the cool species we can write the governing continuity and momentum equations, respectively, as

$$\frac{\partial n_{jc}}{\partial t} + \frac{\partial}{\partial x}(n_{jc}u_{jc}) = 0 \quad (2.3)$$

and

$$m_j n_{jc} \left[\frac{\partial u_{jc}}{\partial t} + u_{jc} \frac{\partial u_{jc}}{\partial x} \right] + \frac{\partial p_{jc}}{\partial x} = -Z_j e n_{jc} \frac{\partial \varphi}{\partial x}, \quad (2.4)$$

where n_{jc} is the number density of the cool species, u_{jc} the average speed of the particles of cool component, p_{jc} the partial pressure of the cool species, m_j the mass of the species, e is the charge on an electron which is equal to the charge carried by a positron in magnitude but opposite in sign, and φ is the electrostatic potential; m_j is the mass of the electron which is equal to the mass of the positron, it follows that $m_j = m$ for both species. The subscript j represents either electrons or positrons, that is, $j = e$ (electrons), p (positrons).

In general,

$$Z_j = \begin{cases} +1 & , \text{ if } j=p \text{ (positron)} \\ -1 & , \text{ if } j=e \text{ (electron)} \end{cases} \quad (2.5)$$

From the thermodynamic equation of state relating p_{jc} to n_{jc} , we shall write

$$p_{jc}n_{jc}^{-\gamma} = C. \quad (2.6)$$

From the ideal gas law we know that

$$p_{jc0} = n_{jc0}k_B T_c, \quad (2.7)$$

where C is a constant and γ is the ratio of specific heats C_p/C_v (where C_p and C_v are the specific heat capacities at constant pressure and volume, respectively), k_B is the Boltzmann constant, T_c is the temperature of the cool component, and n_{jc0} and p_{jc0} are the number density and partial pressure of the cold species at equilibrium, respectively.

Moreover, in an equilibrium state,

$$p_{jc} = p_{jc0}, \quad (2.8)$$

hence, using Eq. (2.6) in the equilibrium state relation for pressure in Eq. (2.8) above, one will have

$$p_{jc}n_{jc}^{-\gamma} = p_{jc0}n_{jc0}^{-\gamma}. \quad (2.9)$$

From Eq. (2.7) and Eq. (2.9), we get

$$p_{jc}n_{jc}^{-\gamma} = n_{jc0}k_B T_c n_{jc0}^{-\gamma}.$$

This gives

$$p_{jc} = \left(\frac{k_B T_c}{n_{jc0}^{\gamma-1}} \right) n_{jc}^{\gamma}. \quad (2.10)$$

Substituting Eq. (2.10) into Eq. (2.4) one obtains

$$mn_{jc} \left[\frac{\partial u_{jc}}{\partial t} + u_{jc} \frac{\partial u_{jc}}{\partial x} \right] + \left(\frac{k_B T_c}{n_{jc0}^{\gamma-1}} \right) \gamma n_{jc}^{\gamma-1} \frac{\partial n_{jc}}{\partial x} = -Z_j e n_{jc} \frac{\partial \varphi}{\partial x}. \quad (2.11)$$

For the adiabatic case, the value of γ is greater than one. If N is the number of degrees of freedom, then γ is given by

$$\gamma = \frac{N + 2}{N}.$$

Since a one dimensional displacement of the plasma particles about the equilibrium position is assumed say, along the x -axis, $N = 1$. It follows that $\gamma = 3$ from the above relation.

Hence, using $\gamma = 3$ in Eq. (2.11), the momentum Eq. (2.4) takes the form

$$mn_{jc} \left[\frac{\partial u_{jc}}{\partial t} + u_{jc} \frac{\partial u_{jc}}{\partial x} \right] + 3k_B T_c \frac{n_{jc}^2}{n_{jc0}^2} \frac{\partial n_{jc}}{\partial x} = -Z_j e n_{jc} \frac{\partial \phi}{\partial x}. \quad (2.12)$$

The velocity distribution of the inertialess hot component of EP plasma species is taken to follow a kappa distribution law. This assumption of an effectively inertialess species is only justified if the hot species thermal velocity v_{th} is much greater than the speed of the wave form v_ϕ supported by the plasma, so that v_{th} is considered as infinite compared to v_ϕ . It follows that the hot component must be isothermal and, assumed to be distributed according to a kappa distribution law. For such a fluid, the number density from this distribution function has been derived by Baluku and Hellberg (2008) as

$$n_{jh} = N_h \left[1 + \frac{Z_j e \varphi}{(\kappa - \frac{3}{2}) k_B T_h} \right]^{-\kappa+1/2}, \quad (2.13)$$

where n_{jh} and T_h , respectively, are the perturbed number density and the temperature of the hot species, κ is the spectral kappa index that measures the deviation of particle velocities from the thermal Maxwellian distribution, k_B is the Boltzmann constant, and $N_h = n_{eho} = n_{pho}$ is the hot species number density at equilibrium in the absence of any disturbances.

Finally, the set of equations which are governing the whole system of our plasma dynamics can be coupled by Poisson's equation:

$$\epsilon_o \frac{\partial^2 \varphi}{\partial x^2} = \sum_{j=e,p} \sum_{k=c,h} -Z_j n_{jk}, \quad (2.14)$$

where k is either a cool (c) or hot (h) species.

To make each of the variables in the set of equations (that is, in Eqs. (2.3), (2.12), (2.13) and Eq. (2.14)) dimensionless, we need to normalize the number density by the total equilibrium number density N_0 , cold species velocity by the hot species thermal speed $v_{th} = \left(\frac{k_B T_h}{m}\right)^{1/2}$, the electrostatic potential by $\frac{e\varphi}{k_B T_h}$, and temperature by the hot species temperature T_h . The time and space variables will be normalized by the inverse plasma frequency $\omega_p = \left(\frac{N_0 e^2}{\epsilon_0 m}\right)^{1/2}$ and the Debye length $\lambda_D = \left(\frac{\epsilon_0 k_B T_h}{N_0 e^2}\right)^{1/2}$, respectively. That is, we have the normalized variables, marked by a tilde where appropriate,

$$\tilde{x} = \frac{x}{\lambda_D}, \quad \tilde{t} = t\omega_p, \quad \tilde{n}_{jk} = \frac{n_{jk}}{N_0}, \quad \tilde{u}_{jc} = \frac{u_{jc}}{v_{th}}, \quad \sigma = \frac{T_c}{T_h}, \quad \phi = \frac{e\varphi}{k_B T_h} \quad (2.15)$$

We have already defined the total equilibrium number density of the plasma as

$$N_0 = N_h + N_c.$$

In dimensionless (the normalization has taken over N_0) form this can be written as

$$N_c + N_h = 1, \quad (2.16)$$

where here N_c and N_h are now normalized quantities.

Using the respective variables from Eq. (2.15) in Eq. (2.3), Eq. (2.12), Eq. (2.13) and Eq. (2.14), the following dimensionless set of the governing equations for both hot and cool components are obtained as :

Normalized continuity equation:

$$\frac{\partial n_{jc}}{\partial t} + \frac{\partial}{\partial x}(n_{jc} u_{jc}) = 0. \quad (2.17)$$

Normalized momentum equation:

$$\frac{\partial u_{jc}}{\partial t} + u_{jc} \frac{\partial u_{jc}}{\partial x} + 3\sigma \frac{n_{jc}}{n_{jco}^2} \frac{\partial n_{jc}}{\partial x} = -Z_j \frac{\partial \phi}{\partial x}. \quad (2.18)$$

Normalized number density for kappa distribution:

$$n_{jh} = N_h \left[1 + \frac{Z_j \phi}{\left(\kappa - \frac{3}{2}\right)} \right]^{-\kappa+1/2}. \quad (2.19)$$

Normalized Poisson's equation:

$$\frac{\partial^2 \phi}{\partial x^2} = \sum_{j=e,p} \sum_{k=c,h} -Z_j n_{jk} \implies \frac{\partial^2 \phi}{\partial x^2} = n_{eh} + n_{ec} - n_{ph} - n_{pc}, \quad (2.20)$$

where σ is the cool (T_c) to hot (T_h) temperature ratio. Note that we have omitted the tildes over some of the variables in the above set of equations for convenience. From here onwards, we will omit the tilde for dimensionless variables.

2.2 Linear waves

Any periodic motion of a fluid can be decomposed by Fourier analysis into a superposition of sinusoidal oscillations with different frequencies ω and wavenumbers k . A simple wave is any one of these components. When the oscillation amplitude is small the wave form is generally sinusoidal; and there is only one component.

Small amplitude oscillations permit the wave fields to be represented by a sinusoidal wave. A plane wave is defined as a wave whose direction of propagation and amplitude is the same everywhere. For a monochromatic plane wave disturbance with frequency ω , a sinusoidal varying quantity in space and time is represented by

$$s(\mathbf{r}, t) = \mathbf{s}_0 e^{i(\mathbf{k} \cdot \mathbf{r} - \omega t)}, \quad (2.21)$$

where \mathbf{s}_0 is a constant vector defining the amplitude of the wave, $i = \sqrt{-1}$ is the imaginary index, \mathbf{k} is the wave vector (specifies the direction of wave propagation), and t is time. The measurable quantity is understood to be the real part of this complex expression.

Phase velocity A point of constant phase (think of wave crests or troughs) is displaced with a phase velocity, which is obtained by taking the total time derivative of the phase and setting it equal to zero. Thus $d(\mathbf{k} \cdot \mathbf{r} - \omega t)/dt = 0$ yields

$$\mathbf{v}_\phi = \frac{\omega}{k^2} \mathbf{k}, \quad (2.22)$$

where the phase velocity is a vector with magnitude $v_\phi = \omega/k$ and the vector has the same orientation as the wave vector \mathbf{k} .

Dispersion relation The phase velocity can be calculated if a relation exists between ω and k . The relation, $\omega = \omega(k)$, is known as the dispersion relation. The dispersion relation contains the physical parameters of a given medium in which a wave exists and propagates. Hence, the dispersion relation contains all relevant information on how the medium responds to a given wave. One of the main tasks of this chapter is the derivation of the dispersion relation for our model, as well as for related plasma models.

Small amplitude perturbation equations If plane harmonic wave solutions are assumed for the dynamical variables like velocity u , number density n , electrostatic field E , and the electrostatic potential ϕ , we can write a one dimensional sinusoidal Fourier form for each of the variable as

$$u = u_0 e^{i(kx - \omega t)} \quad n = n_0 e^{i(kx - \omega t)} \quad E = E_0 e^{i(kx - \omega t)} \quad \phi = \phi_0 e^{i(kx - \omega t)}, \quad (2.23)$$

where x is a 1D spatial variable. The time and spatial derivatives can be represented by

$$\frac{\partial}{\partial t} \rightarrow -i\omega \quad \nabla \rightarrow ik \quad \nabla \cdot \rightarrow ik, \quad \nabla \times \rightarrow ik \times, \quad (2.24)$$

where $\nabla = \hat{x} \frac{\partial}{\partial x}$, for one dimensional spatial analysis. When only small amplitude perturbations are considered, the dynamic variables can be expressed in terms of their equilibrium and perturbed parts, by neglecting the contribution of second and higher order terms. It follows that

$$u = u_0 + u_1 = u_1 \quad n = n_0 + n_1 \quad \phi = \phi_0 + \phi_1 = \phi_1 \quad E = E_0 + E_1 = E_1, \quad (2.25)$$

where the subscripts 0 and 1 refer to the equilibrium and perturbed parts of the dynamical dependent quantities, respectively. In equilibrium, $u_0 = \phi_0 = E_0 = 0$. The fluid velocity u , electrostatic field E , and the electrostatic potential ϕ arise from perturbing an equilibrium fluid and, hence, they are first order quantities (higher order terms are regarded as small

and they are neglected). Our interest in this chapter is to retain quantities only to first order, ignoring higher order terms.

2.3 Model equations

In this section we will consider the normalized equations that govern our plasma dynamics. As we have already discussed earlier, the dynamics of the cool component of our plasma model will be governed by the momentum and continuity equations (normalized), respectively:

$$\frac{\partial n_{jc}}{\partial t} + \frac{\partial}{\partial x}(n_{jc}u_{jc}) = 0 \quad (2.26)$$

and

$$\frac{\partial u_{jc}}{\partial t} + u_{jc} \frac{\partial u_{jc}}{\partial x} + 3\sigma \frac{n_{jc}}{N_c^2} \frac{\partial n_{jc}}{\partial x} = -Z_j \frac{\partial \phi}{\partial x}. \quad (2.27)$$

Using Eq. (2.23), Eq. (2.24) and Eq. (2.25), that is, assuming sinusoidal small perturbations of dynamical variables to the first order from their equilibrium state, Eq. (2.26) takes the form

$$-i\omega n_{jc1} + N_c i k u_{jc1} = 0,$$

which implies that,

$$u_{jc1} = \frac{\omega}{k} \frac{n_{jc1}}{N_c}. \quad (2.28)$$

By using similar reasoning, from Eq. (2.27), we have

$$-i\omega u_{jc1} + 3\sigma \frac{n_{jc1}}{N_c} = -Z_j i k \phi_1. \quad (2.29)$$

Using Eq. (2.28) in Eq. (2.29), and after some rearrangement, we obtain

$$n_{jc1} = Z_j \frac{\phi_1 N_c}{\frac{\omega^2}{k^2} - 3\sigma}. \quad (2.30)$$

For each of the species (cool electrons and positrons), Eq. (2.30) becomes,

$$n_{ec1} = -\frac{\phi_1 N_c}{\frac{\omega^2}{k^2} - 3\sigma} \quad \text{and} \quad n_{pc1} = \frac{\phi_1 N_c}{\frac{\omega^2}{k^2} - 3\sigma}, \quad (2.31)$$

where n_{ec1} and n_{pc1} , respectively, are the first order perturbed number density for cool electrons and positrons.

To model the dynamics of the hot component of our plasma model, we are using a kappa velocity distribution function. From that, the normalized number density for the species of hot electrons and positrons, respectively, has been calculated by Baluku and Hellberg (2008) as

$$n_{eh} = N_h \left[1 - \frac{\phi}{(\kappa - \frac{3}{2})} \right]^{-\kappa+1/2} \quad (2.32)$$

and

$$n_{ph} = N_h \left[1 + \frac{\phi}{(\kappa - \frac{3}{2})} \right]^{-\kappa+1/2}. \quad (2.33)$$

The above set of density equations (i.e, Eqs. (2.26), (2.27), (2.32) and (2.33)) are coupled by the normalized Poisson equation:

$$\frac{\partial^2 \phi}{\partial x^2} = n_{eh} + n_{ec} - n_{ph} - n_{pc}. \quad (2.34)$$

If we consider a small perturbation of the electrostatic potential ϕ (that is, $\phi \ll 1$), one can employ a Taylor power series expansion, respectively, in Eq. (2.32) and Eq. (2.33).

So that

$$n_{eh} = N_h \left[1 + \left(\frac{\kappa - \frac{1}{2}}{\kappa - \frac{3}{2}} \right) \phi + \frac{(\kappa - \frac{1}{2})(\kappa + \frac{1}{2})}{2(\kappa - \frac{3}{2})^2} \phi^2 + \frac{(\kappa - \frac{1}{2})(\kappa + \frac{1}{2})(\kappa + \frac{3}{2})}{6(\kappa - \frac{3}{2})^3} \phi^3 + \dots \right] \quad (2.35)$$

and

$$n_{ph} = N_h \left[1 - \left(\frac{\kappa - \frac{1}{2}}{\kappa - \frac{3}{2}} \right) \phi + \frac{(\kappa - \frac{1}{2})(\kappa + \frac{1}{2})}{2(\kappa - \frac{3}{2})^2} \phi^2 - \frac{(\kappa - \frac{1}{2})(\kappa + \frac{1}{2})(\kappa + \frac{3}{2})}{6(\kappa - \frac{3}{2})^3} \phi^3 + \dots \right]. \quad (2.36)$$

Using the following substitutions;

$$c_1 = \left(\frac{\kappa - \frac{1}{2}}{\kappa - \frac{3}{2}} \right), \quad (2.37)$$

$$c_2 = \frac{(\kappa - \frac{1}{2})(\kappa + \frac{1}{2})}{2(\kappa - \frac{3}{2})^2}, \quad (2.38)$$

$$c_3 = \frac{(\kappa - \frac{1}{2})(\kappa + \frac{1}{2})(\kappa + \frac{3}{2})}{6(\kappa - \frac{3}{2})^3}. \quad (2.39)$$

Eq. (2.35) and Eq. (2.36), becomes

$$n_{eh} = N_h(1 + c_1\phi + c_2\phi^2 + c_3\phi^3 + \dots) \quad \text{and} \quad n_{ph} = N_h(1 - c_1\phi + c_2\phi^2 - c_3\phi^3 + \dots). \quad (2.40)$$

For small perturbations about the equilibrium point, we can apply linearization to the dynamical variables of number density (n_{eh} and n_{ph}) and the electrostatic potential ϕ in Eq. (2.40). Hence,

$$N_h + n_{eh1} + n_{eh2} + \dots = N_h[1 + c_1\phi_1 + c_2\phi_1^2 + c_3\phi_1^3 + \dots] \quad (2.41)$$

and

$$N_h + n_{ph1} + n_{ph2} + \dots = N_h[1 - c_1\phi_1 + c_2\phi_1^2 - c_3\phi_1^3 + \dots], \quad (2.42)$$

where n_{eh1} , n_{ph1} and ϕ_1 are the first order perturbed number density for hot electrons, hot positrons, and the electrostatic potential, respectively, whereas n_{eh2} and n_{ph2} are the second order perturbed number densities for hot electrons and positrons, respectively. Here we have used the assumption that in an unperturbed state the electrostatic potential $\phi_0 = 0$, and the hot component number density $n_{eho} = N_h$. By ignoring the second and all higher order terms in Eq. (2.41) and Eq. (2.42), we have

$$N_h + n_{eh1} = N_h[1 + c_1\phi_1] \quad \text{and} \quad N_h + n_{ph1} = N_h[1 - c_1\phi_1],$$

which implies that,

$$n_{eh1} = N_h c_1 \phi_1 \quad (2.43)$$

and

$$n_{ph1} = -N_h c_1 \phi_1. \quad (2.44)$$

2.4 Waves in related plasma models

In this section we will consider related simple electron-positron plasma models, and we shall derive linear wave dispersion relations for each of them. These studies will enable us to recognize the model requirements to obtain an acoustic dispersion relation, while bearing in mind the obvious physical constraint associated with the symmetry of the electron-positron pair creation process. At the same time, they will lead us naturally to the model that we have adopted in this study, namely, a symmetric four-species electron-positron plasma.

2.4.1 Hot kappa electrons and positrons

In this model we consider a two-species symmetric plasma, for which we have assumed that the temperature of both electrons and positrons is hot, and both species are assumed to be distributed according to a kappa velocity distribution law. The thermal speed of both species is much greater than the phase speed supported by the model. Since the particles are highly mobile we may ignore their inertia. So, for this particular model, Eq. (2.34) takes the form

$$\frac{d^2\phi}{dx^2} = n_{eh} - n_{ph}.$$

After linearization, this equation can be written as

$$\frac{d^2\phi_1}{dx^2} = n_{eh1} - n_{ph1}. \quad (2.45)$$

Perturbation from equilibrium is assumed to be sinusoidal and, therefore, applying a Fourier mode sinusoidal plane wave discussed in Eq. (2.23) and Eq. (2.24) to the left hand side of Eq. (2.45), and using Eq. (2.43) and Eq. (2.44), we get

$$-k^2\phi_1 = 2c_1\phi_1N_h \implies k^2 = -2c_1N_h.$$

In this model, $N_c = 0$ since we are dealing with the hot species only. Hence, from Eq. (2.16) one obtain that $N_h = 1$. Therefore,

$$k^2 = -2c_1.$$

Substituting for c_1 (see Eq. (2.37)), this equation can be written in terms of the superthermal parameter κ as

$$k^2 = -2 \left(\frac{\kappa - 1/2}{\kappa - 3/2} \right). \quad (2.46)$$

We recall that the kappa distribution is valid for $\kappa > 3/2$ (Vasyliunas, 1968; Hellberg et al., 2009) and hence, for any derived physical quantity (e.g., the density), we are restricted to values of κ that satisfy $\kappa > 3/2$ (Baluku et al., 2010a). Hence, the term inside the bracket in Eq. (2.46) is always positive and, hence, k is indeterminate in the dispersion relation of the model in Eq. (2.46). This signifies that the wave is not supported by an isothermal hot electron-positron plasma in the absence of the inertial cool species. Clearly, an inertial species is required to support oscillatory behaviour, and hence a wave.

2.4.2 Cool adiabatic electrons and positrons

In this model we will consider a two-species plasma consisting of electrons and positrons found at a single cool temperature T_c , and with equilibrium number density N_c . The cool species thermal velocity v_{tc} is much smaller than the phase velocity v_ϕ for the model. The dynamics of both the electrons and positrons is governed by the normalized continuity, momentum and Poisson equations (note that normalization for temperature was taken with respect to T_c because only cold species are involved in this model and, hence, $\sigma = 1$ in the normalized fluid equations). Therefore, for this particular model, Eq. (2.34) can be rewritten as

$$\frac{\partial^2 \phi}{\partial x^2} = n_{ec} - n_{pc}. \quad (2.47)$$

After linearization and Fourier mode analysis, Eq. (2.47) reads

$$-k^2 \phi_1 = n_{ec1} - n_{pc1}. \quad (2.48)$$

In this equation we have used an assumption $n_{eco} = n_{pco} = N_c$ in the equilibrium state. Then substituting Eq. (2.31) into Eq. (2.48), and keeping in mind that the total cool species equilibrium number density $N_c = 1$ (see Eq. (2.16)) in normalized form in the absence of the hot species, the dispersion relation takes the form

$$\omega^2 = 2 + 3k^2. \quad (2.49)$$

This shows that the medium may support a plasma-like wave, with phase velocity v_ϕ , greater than the particle thermal velocity. Importantly, this model cannot support an acoustic wave, characterized by $\omega/k \rightarrow V_o$ as $k \rightarrow 0$.

2.4.3 Kappa electrons and adiabatic positrons

In this model we have considered an electron-positron (EP) plasma consisting of hot inertialess electrons distributed according to the kappa distribution law and cool inertial adiabatic positrons governed by the fluid equations of motion (continuity and momentum equations). The hot electrons are at temperature T_h (number density N_c) whereas the

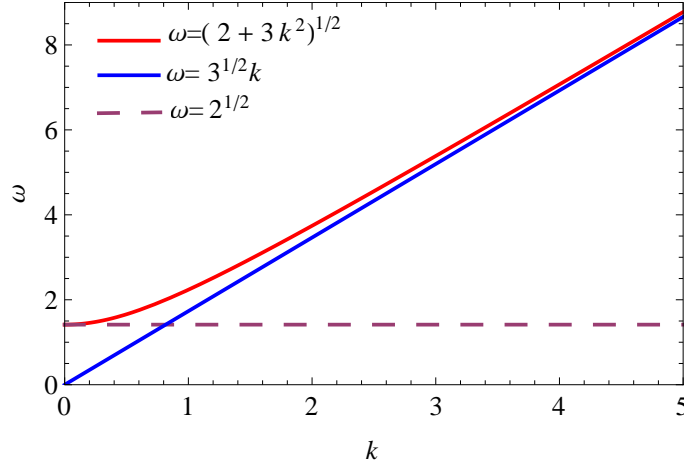


Figure 2.1: A plot of the dispersion relation shown in Eq. (2.49) for the plasma of adiabatic cold electrons and positrons. Dashed curve for $k \rightarrow 0$, while solid red line for large k .

cool positrons have temperature T_c (number density N_c), and we assume that $T_h \gg T_c$. In an unperturbed state the condition,

$$N_c = N_h$$

holds. Moreover, it is assumed that the hot species thermal velocity v_{th} is much larger than the phase velocity v_ϕ supported by the plasma, which in turn is much larger than the thermal speed of the cool species v_{tc} (i.e., $v_{th} \gg v_\phi \gg v_{tc}$) to reduce Landau damping in our model following Watanabe and Taniuti (1977). Hence, for this particular model, Eq. (2.34) reads

$$\frac{d^2 \phi}{dx^2} = n_{eh} - n_{pc}. \quad (2.50)$$

where n_{eh} and n_{pc} are the perturbed number densities of hot kappa electrons and adiabatic cool positrons, respectively.

After linearization, Eq. (2.50) becomes

$$-k^2 \phi_1 = n_{eh1} - n_{pc1}. \quad (2.51)$$

Using Eq. (2.43) and Eq. (2.31) in Eq. (2.51), we obtain

$$-k^2\phi_1 = N_h c_1 \phi_1 - \frac{N_c \phi_1}{\frac{\omega^2}{k^2} - 3\sigma}. \quad (2.52)$$

Rearranging this gives us the following dispersion relation,

$$\frac{\omega^2}{k^2} = \frac{N_c}{N_h c_1 + k^2} + 3\sigma. \quad (2.53)$$

In the limit of very small k (that is, $k^2 \ll N_h c_1$), Eq. (2.53) reduces to

$$\omega = \left(\frac{N_c}{N_h c_1} + 3\sigma \right)^{1/2} k. \quad (2.54)$$

Using the definition of c_1 , and the neutrality condition in the equilibrium state ($N_c = N_h$), Eq. (2.54) becomes

$$\omega = \left(\frac{2\kappa - 3}{2\kappa - 1} + 3\sigma \right)^{1/2} k \implies \omega = V k, \quad (2.55)$$

where $V = \left(\frac{2\kappa - 3}{2\kappa - 1} + 3\sigma \right)^{1/2}$ is the normalized sound speed in such a plasma. Fig. 2.2 shows a plot of the dispersion relation, Eq. (2.53), for the hot kappa distributed electrons and the cool adiabatic positrons. In the large wavelength (very small k) limit, all the harmonics travel nearly with the normalized sound speed V when the superthermality parameter $\kappa = 100$ (Maxwellian regime). However, for high superthermality ($\kappa = 2$) it is seen that all the harmonics travel with different speeds for all k as displayed in Fig. 2.2. Although this two-species model does support an acoustic wave, it is based on the assumption that $T_e \gg T_p$. In view of the expected symmetry between electrons and positrons derived from pair creations, this does not appear to be a realistic model.

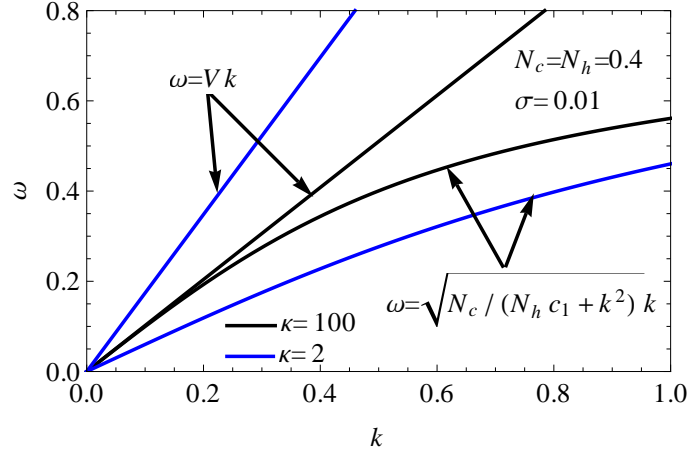


Figure 2.2: Solid blue and black curved lines generated from Eq. (2.53), respectively, for $\kappa = 2$ and $\kappa = 100$, showing an acoustic mode supported by an electron-positron plasma of hot kappa electrons and cool adiabatic positrons. The solid blue and black straight lines generated from Eq. (2.55), respectively, for $\kappa = 2$ and $\kappa = 100$ in the limit k very small. For large κ (Maxwellian limit) it is seen that all harmonics travels with the sound speed V when k is smaller. For $\kappa = 2$ it is observed that the harmonics doesn't travel with the same speed for all k .

2.4.4 A three component model

Here we will investigate linear electrostatic waves in a three component plasma model consisting of cold inertial electron and positron fluids at a cold temperature $T_c = 0$ (density N_c), with a component of a kappa-distributed energetic positrons at hot temperature T_h (density N_h).

In an unperturbed state where $\phi_0 = 0$, the charge neutrality condition dictates that

$$n_{ec0} = n_{ph0} + n_{pc0},$$

where n_{ec0} , n_{ph0} and n_{pc0} are densities of the cold electrons, hot positrons and cool positrons in the equilibrium state, respectively. For this particular model, Poisson's equa-

tion reads

$$\frac{d^2\phi}{dx^2} = n_{ec} - n_{pc} - n_{ph}, \quad (2.56)$$

where n_{ec} , n_{pc} , and n_{ph} are the number densities of cold electrons, cold positrons and hot positrons, respectively, in the perturbed state. The linearized Poisson's equation finally takes the form

$$\frac{d^2\phi_1}{dx^2} = n_{ec1} - n_{pc1} - n_{ph1}. \quad (2.57)$$

Employing the Fourier modes and using Eq. (2.31) and Eq. (2.44) in Eq. (2.57), gives

$$-k^2\phi_1 = -n_{eco}\frac{k^2}{\omega^2}\phi_1 - n_{pco}\frac{k^2}{\omega^2}\phi_1 + n_{ph0}c_1\phi_1. \quad (2.58)$$

After rearranging, Eq. (2.58) yields

$$\omega^2 = \left[\frac{n_{eco} + n_{pco}}{k^2 + n_{ph0}c_1} \right] k^2. \quad (2.59)$$

Substituting for $n_{eco} = n_{pco} + n_{ph0}$, Eq. (2.59) becomes

$$\omega^2 = \left[\frac{2n_{pco} + n_{ph0}}{k^2 + n_{ph0}c_1} \right] k^2. \quad (2.60)$$

This can also be written, using $n_{pco} = N_c$ and $n_{ph0} = N_h$ in an equilibrium state, as

$$\omega^2 = \left[\frac{1 + \frac{2N_c}{N_h}}{c_1 + \frac{k^2}{N_h}} \right] k^2. \quad (2.61)$$

Replacing c_1 , the dispersion relation in Eq. (2.61) for a three component model takes the form

$$\omega = \left[\frac{1 + \frac{2N_c}{N_h}}{\frac{2\kappa-1}{2\kappa-3} + \frac{k^2}{N_h}} \right]^{1/2} k. \quad (2.62)$$

For large wavelength (small k), that is, $\frac{k^2}{N_h} \ll c_1$, this becomes

$$\omega = \left[\left(\frac{2\kappa-3}{2\kappa-1} \right) \left(1 + \frac{2N_c}{N_h} \right) \right]^{1/2} k. \quad (2.63)$$

This is the dispersion relation for the large wavelength limit with the normalized sound speed (acoustic mode):

$$V = \left[\left(\frac{2\kappa-3}{2\kappa-1} \right) \left(1 + \frac{2N_c}{N_h} \right) \right]^{1/2}.$$

With this replacement, one can write Eq. (2.63) as

$$\omega = Vk. \quad (2.64)$$

Again, this model supports an acoustic wave, but is suspect because of its lack of symmetry between electrons and positrons. The dispersion relation (2.62) is illustrated in Fig. 2.3 for extreme values of κ . For small k , the acoustic speed (Eq. (2.64)) is seen to be larger for a quasi-Maxwellian plasma ($\kappa = 100$) than for a low- κ plasma

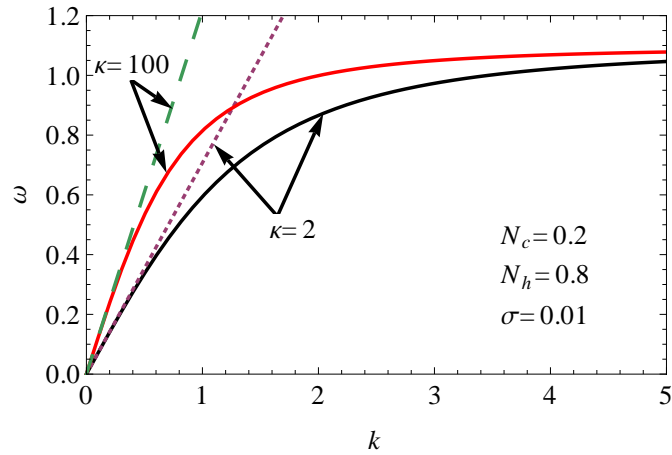


Figure 2.3: The dispersion relation for a plasma consisting of cold electrons and positrons at $T_c = 0$ and, hot kappa positrons at temperature T_h , as found from Eq. (2.62), the black and red curves for $\kappa = 2$ and $\kappa = 100$, respectively. For small k , the dotted and dashed lines show that $\omega \propto k$.

2.5 The symmetric four component model

Having considered some related plasma models, we now turn to our main area of interest, the symmetric, four-component electron-positron plasma model.

In this model we have considered an EP pair plasma consisting of hot electrons and positrons which are generated from the curvature photons by the primary plasma production process, and cool electrons and positrons generated from the synchrophotons in the secondary plasma generation process in the pulsar magnetosphere. Because the two species have the same absolute charge to mass ratio, both electrons and positrons in the hot component of the EP plasma will exist at the same temperature T_h (number density N_h), and in the cool component of the EP plasma they will be found at the cool temperature T_c (number density N_c). It is assumed that the thermal speed of the hot species v_{th} is much greater than the phase speed v_ϕ supported by the model, which in turn is much greater than the cool species thermal speed v_{tc} , i.e., $v_{th} \gg v_\phi \gg v_{tc}$. This assumption is justified in the light of the large energy difference between the secondary and primary plasmas in the pulsar magnetosphere. Furthermore, the inertialess hot species are assumed to follow a kappa velocity distribution function, and the cool species are governed by the multi-fluid equations (momentum and continuity equations).

The set of equations governing the whole system in this model are coupled by the normalized Poisson's equation as

$$\frac{d^2\phi}{dx^2} = n_{eh} + n_{ec} - (n_{ph} + n_{pc}). \quad (2.65)$$

Linearizing the dynamical variables to the first order, Eq. (2.65) may be written as

$$\frac{d^2\phi_1}{dx^2} = \underbrace{N_h + n_{eh1}}_{n_{eh}} + \underbrace{N_c + n_{ec1}}_{n_{ec}} - \left(\underbrace{N_h + n_{ph1}}_{n_{ph}} + \underbrace{N_c + n_{pc1}}_{n_{pc}} \right). \quad (2.66)$$

Taking the Fourier transform by assuming small sinusoidal oscillations of the variables about their equilibrium state in Eq. (2.66), we get

$$-k^2\phi_1 = n_{eh1} + n_{ec1} - n_{ph1} - n_{pc1}. \quad (2.67)$$

Using Eq. (2.31), Eq. (2.43) and Eq. (2.44) in Eq. (2.67), one obtains

$$-k^2\phi_1 = c_1 N_h \phi_1 - \frac{\phi_1}{\frac{\omega^2}{k^2} - 3\sigma} N_c + c_1 N_h \phi_1 - \frac{\phi_1}{\frac{\omega^2}{k^2} - 3\sigma} N_c,$$

which implies that

$$k^2 = \frac{2N_c}{\frac{\omega^2}{k^2} - 3\sigma} - 2c_1 N_h. \quad (2.68)$$

Rearranging of Eq. (2.68) gives us the dispersion relation for a symmetric four-component EP plasma model as

$$\omega^2 = \left[\frac{2N_c}{2N_h c_1 + k^2} + 3\sigma \right] k^2. \quad (2.69)$$

Using the definition for c_1 , this dispersion relation in terms of superthermal parameter κ can take the form

$$\omega = \left[\frac{2N_c}{2N_h \left(\frac{2\kappa-1}{2\kappa-3} \right) + k^2} + 3\sigma \right]^{1/2} k. \quad (2.70)$$

In unnormalized form, this will take the form

$$\omega^2 = \frac{\alpha k^2 v_{th}^2}{\frac{\alpha k^2 \lambda_{Dh}^2}{2} + c_1} + 3k^2 v_{tc}^2,$$

where $\alpha = N_c/N_h$, $\lambda_{Dh} = \left(\frac{\epsilon_0 k_B T_h}{N_h e^2} \right)^{1/2}$, $v_{th} = \left(\frac{k_B T_h}{m} \right)^{1/2}$ and $v_{tc} = \left(\frac{k_B T_c}{m} \right)^{1/2}$.

This is reminiscent of the unnormalized dispersion relation for the electron-acoustic wave given by Danehkar et al. (2011) in their Eq. (18), although in the unnormalized form of Eq. (2.70) there is an additional factor 1/2 in the coefficient of k^2 in the denominator, related to the fact that in the present case the total number of particles (electrons + positrons) providing inertia is $2N_c$. Danehkar et al. (2011) had considered a plasma composed of hot-kappa distributed electrons, cool inertial electrons (density N_c) and immobile ions.

Eq. (2.70) can also be written as

$$\omega^2 = \left[\frac{2N_c}{2N_h c_1} \left(1 + \frac{k^2}{2N_h c_1} \right)^{-1} + 3\sigma \right] k^2. \quad (2.71)$$

For $\frac{k^2}{2N_h c_1} \ll 1$ (very small wave number k), we can employ a Taylor power series expansion in Eq. (2.71) to obtain

$$\omega^2 = \left[\frac{N_c}{N_h c_1} \left(1 - \frac{k^2}{2N_h c_1} \right) + 3\sigma \right] k^2. \quad (2.72)$$

This can also be written as

$$\omega^2 = \left(\frac{N_c}{N_h c_1} + 3\sigma \right) k^2 - \frac{N_c}{2N_h^2 c_1^2} k^4. \quad (2.73)$$

This equation is in the form of a general acoustic dispersion relation (Chen, 1983)

$$\omega^2 = v_s k^2 + \gamma k^4,$$

where γ is some constant, and $v_s = \omega/k$ is the sound speed of the acoustic wave in the long wavelength limit $k \rightarrow 0$. This form of the dispersion relation is directly related to the nonlinear Korteweg-de Vries equation which will be discussed in Chapter 3.

For very long wavelengths (small k), the second term on the right hand side of Eq. (2.73) goes to zero more rapidly than the first term, so that for very long wavelengths (small k) Eq. (2.73) will be reduced to

$$\omega^2 = \left(\frac{N_c}{N_h c_1} + 3\sigma \right) k^2.$$

Substituting for c_1 , we have

$$\omega = \left[\left(\frac{2\kappa - 3}{2\kappa - 1} \right) \frac{N_c}{N_h} + 3\sigma \right]^{1/2} k. \quad (2.74)$$

This is the dispersion relation of acoustic waves in our four-component symmetric model in the limit of small k :

$$V = \left[\left(\frac{2\kappa - 3}{2\kappa - 1} \right) \frac{N_c}{N_h} + 3\sigma \right]^{1/2}, \quad (2.75)$$

where $V = v_\phi/v_{th}$ ($v_\phi = \frac{\omega}{k}$), is the normalized (with respect to the hot species thermal speed v_{th}) sound speed. Before considering some aspects of this dispersion relation, we note that Eq. (2.75) has the same form as the characteristic phase speed for small k of the electron-acoustic wave as may have been seen by comparing with Eq. (16) of Danekar et al. (2011).

Fig. 2.4 shows a plot of the dispersion relation (Eq. 2.70) for a symmetric four-component plasma at two different extreme values of κ . It is seen that for large wavelength (small k) all frequencies travel with the same speed, V .

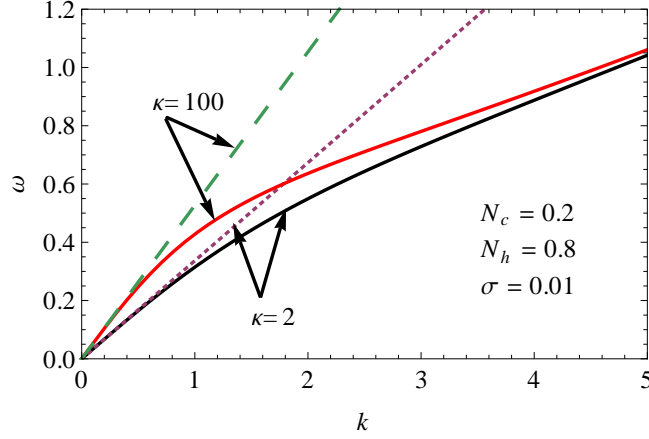


Figure 2.4: Dispersion relation (Eq. 2.70) for different kappa κ values for acoustic waves in a symmetric-four component electron-positron plasma of hot kappa distributed electrons and positrons, and cool adiabatic electrons and positrons. For small k , the dotted and dashed lines show that $\omega \propto k$.

From Eq. (2.74) it is clear that when the number density of the cold species goes to zero ($N_c = 0$), the dispersion relation reduces to

$$\omega^2 = 3\sigma k^2.$$

This implies that ω depends on the non-existent parameter $\sigma = T_c/T_h$ through the cold species temperature T_c . In order to resolve this paradox, we need to refer to Eq. (2.68). There, if $N_c = 0$ ($N_h = 1$) it can take the form,

$$k^2 = -2c_1.$$

This is the same as the dispersion relation in Eq. (2.46) that was derived for the simple two-species model of hot kappa electrons and positrons. In that case, it was shown that in the absence of the cool inertial component, the model cannot support waves. Thus, when

there are no cool particles we get a breakdown of wave formation in the plasma.

Furthermore, in the absence of the hot species, Eq. (2.70) will be reduced to

$$\omega^2 = 2 + 3\sigma k^2, \quad (2.76)$$

where the temperature ratio $\sigma = T_c/T_h$. But, largely, for $N_h = 0$, the normalization with non-existent hot species temperature T_h is meaningless. Hence, by taking a normalization for this particular case with respect to T_c , we then have $\sigma = 1$. Thus, Eq. (2.76) becomes

$$\omega^2 = 2 + 3k^2,$$

which is the same as the dispersion relation in Eq. (2.49) derived for a plasma consisting of cool adiabatic electrons and positrons. Hence, in the absence of the hot species, the symmetric four component model will be reduced to the two-species EP plasma model consisting of cool adiabatic electrons and positrons only, yielding an electron plasma-like wave.

Following discussions in Gray (1998), now let us consider the cases when either of the cold or hot species number densities tends to zero. Fig. 2.5 shows that the plasma purely supports an acoustic wave as the number density of the cool species are getting low. The particular value used for the cold species number density was $N_c = 0.01$ and temperature $T_c = 0.01$.

On the other hand, as the hot species number density tends to zero, the plasma starts to support the plasma-like wave for larger k . However, the plasma supports an acoustic mode for smaller k . This effect is seen in Fig. 2.6 for the hot species equilibrium number density $N_h = 0.001$ and the temperature $\sigma = 0.01$.

However, this analysis is not valid in accordance with the assumption imposed by the model to reduce the Landau damping. That is,

$$v_{th} \gg v_\phi \gg v_{tc},$$

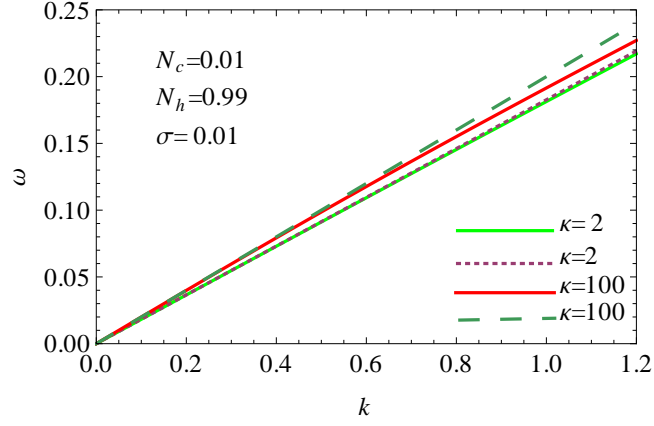


Figure 2.5: Dispersion relation (Eq. (2.70)) evaluated for a plasma with very small cool component, $N_c = 0.01$, for $\kappa = 2$ (green curve) and $\kappa = 100$ (red). The dashed lines are from the small- k limit, Eq. (2.74).

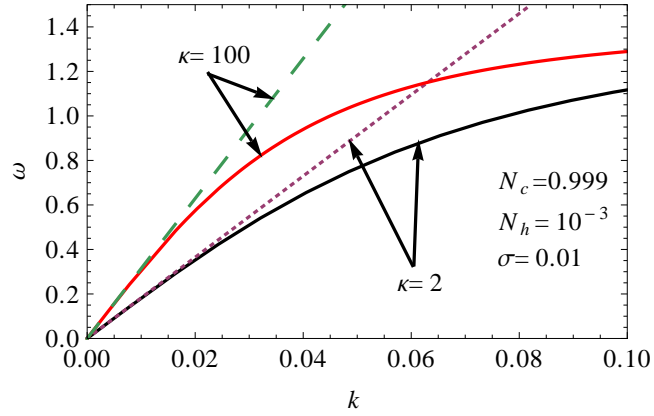


Figure 2.6: Black and red curves for $\kappa = 2$ and $\kappa = 100$, respectively, generated from the dispersion relation, Eq. (2.70), for plasmas with very small hot components, $N_h = 0.001$. The dotted and dashed lines for $\kappa = 2$ and $\kappa = 100$, respectively, generated from the dispersion relation for low- k approximation, Eq. (2.74).

where v_{th} , v_ϕ and v_{tc} are the thermal speed of the hot species, the phase velocity and the thermal speed of the cool species, respectively. This implies a requirement that

$$1 \gg V,$$

where $V = v_\phi/v_{th}$. Using Eq. (2.75) and the previous relation, we have

$$\left(\left[\frac{2\kappa - 3}{2\kappa - 1} \right] \frac{N_c}{N_h} + 3\sigma \right)^{1/2} \ll 1. \quad (2.77)$$

In principle, this relation provides an important constraint on valid parameter values for this model. The values used in Fig. 2.6 lie outside the permitted range.

When σ tends to zero, the above constraint can be written as

$$\frac{\alpha}{c_1} \ll 1, \quad (2.78)$$

where $c_1 = \frac{2\kappa-1}{2\kappa-3}$ and $\alpha = \frac{N_c}{N_h}$. By keeping this designation in mind and using Eq. (2.16) we can write expressions for N_c and N_h in terms of α as

$$N_h = \frac{1}{\alpha + 1} \quad \text{and} \quad N_c = \frac{\alpha}{\alpha + 1}. \quad (2.79)$$

For convenience we shall use α as the ratio of cool (N_c) to hot (N_h) normalized equilibrium number density hereinafter wherever necessary. In the light of Eq. (2.78), we can determine the parametric values of α for which the model supports an acoustic wave without appreciable Landau damping for the given values of κ . Fig. 2.7, generated from Eq. (2.78), shows the dependence of limiting values of α on κ for a chosen ratio of α to c_1 in accordance with our model. In the early work of Verheest et al. (1996) that investigated acoustic nonlinear waves in a symmetric four component EP plasma, the hot components were assumed to follow the Maxwellian distribution. It was found that the model supports the waves without Landau damping if the cold species normalized number density $N_c \leq 0.2$ ($\alpha \leq 0.25$).

However, in our model, the lower κ (higher superthermality) permits the model to support acoustic waves over a much wider range of hot to cold number density ratios α . For example, from Table 2.1 ($\alpha/c_1 = 0.3 \implies (\alpha/c_1)^{1/2} \approx 0.5 \ll 1$), it is seen that the model allows the cold species number density $N_c \approx 0.76$ ($\alpha = 3.3$) at $\kappa = 1.6$. This result is well beyond the upper limit of N_c obtained by Verheest et al. (1996), that is $N_c = 0.2$

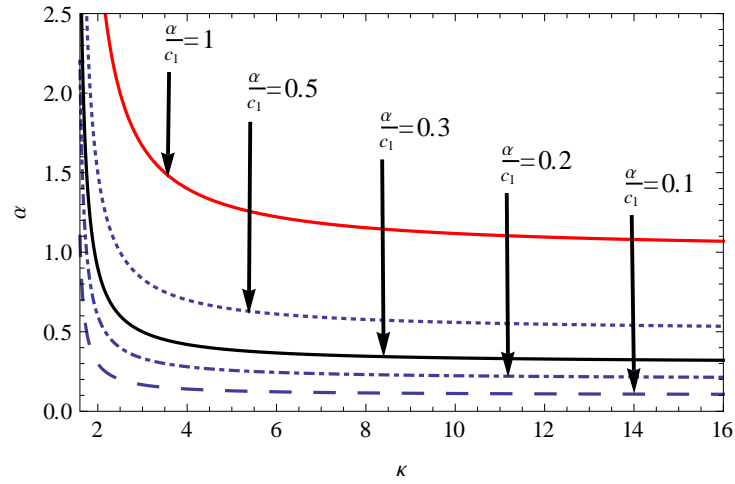


Figure 2.7: Figure shows the dependence of α on κ for the chosen values of α to c_1 ratios.

($\alpha = 0.25$).

For convenience, most of the limiting values of α for the corresponding κ in the forthcoming discussions will be constrained to those values of α and κ below a black curve in Fig. 2.7 (i.e., $\alpha/c_1 = 0.3$). Thus, all soliton existence domains are subject to this cut-off. Moreover, for numerical visualization purposes, the corresponding numerical values of α for given κ at various chosen α to c_1 ratios are displayed in Table (2.1).

Table 2.1: Parametric limiting values of α for corresponding κ , generated from the various chosen values of α to c_1 ratios (Eq. 2.78) when $\sigma \rightarrow 0$.

$\frac{\alpha}{c_1} = 1$		$\frac{\alpha}{c_1} = 0.5$		$\frac{\alpha}{c_1} = 0.3$		$\frac{\alpha}{c_1} = 0.2$	
κ	α	κ	α	κ	α	κ	α
1.6	11	1.6	5.5	1.6	3.3	1.6	2.2
2.6	1.90909	2.6	0.954545	2.6	0.572727	2.6	0.381818
3.6	1.47619	3.6	0.738095	3.6	0.442857	3.6	0.295238
4.6	1.32258	4.6	0.66129	4.6	0.396774	4.6	0.264516
5.6	1.2439	5.6	0.621951	5.6	0.373171	5.6	0.24878
6.6	1.19608	6.6	0.598039	6.6	0.358824	6.6	0.239216
7.6	1.16393	7.6	0.581967	7.6	0.34918	7.6	0.232787
8.6	1.14085	8.6	0.570423	8.6	0.342254	8.6	0.228169
9.6	1.12346	9.6	0.561728	9.6	0.337037	9.6	0.224691
10.6	1.10989	10.6	0.554945	10.6	0.332967	10.6	0.221978
11.6	1.09901	11.6	0.549505	11.6	0.329703	11.6	0.219802

Having studied linear waves in a four component system, as well as in some related models in this chapter, we next turn to the main aspect of this thesis, namely the investigation of nonlinear solitary waves.

Chapter 3

Nonlinear acoustic waves in the electron-positron plasma

In this chapter we will investigate nonlinear waves in an unmagnetized, collisionless and non-relativistic four species plasma consisting of hot electrons and positrons at temperature T_h (number density N_h), and cool electrons and positrons at temperature T_c (number density N_c). To study small amplitude nonlinear waves in the model, we will employ the reductive perturbation technique to derive a modified Korteweg de Vries (mKdV) equation which yields a standard soliton solution. To investigate fully nonlinear (arbitrary amplitude) solitary waves, the Sagdeev pseudopotential approach will be employed.

3.1 Small amplitude analysis

We shall first derive the Kortweg de Vries (KdV) equation using the reductive perturbation expansion. However, because of the symmetry of the problem, the nonlinear term vanishes in the KdV equation. Hence, we go to the next step to derive the mKdV equation that allows a higher degree of nonlinearity. From that equation (mKdV), the standard stationary soliton solution is given in terms of plasma parameters.

3.1.1 Derivation of the Korteweg de Vries (KdV) equation

We assume weak nonlinearity, that is, the amplitude of the electrostatic potential is small $|\phi| < 1$, and the perturbation in the densities and velocities are all small compared to unity. So it permits use of the reductive perturbation technique that follows Washimi and Taniuti (1966) to derive the evolutionary KdV equation describing weakly nonlinear EP acoustic waves from the system of equations governing a four species symmetric EP plasma.

Coordinate stretching Following the ideas of Washimi and Taniuti (1966) to recover the specific coordinate stretching to the reductive perturbation expansion for the case of a symmetric four component electron-positron plasma, we may write the linear dispersion relation in Eq. (2.71) in the limit $\sigma \rightarrow 0$ as

$$\omega = \left(\frac{N_c}{N_h c_1} \right)^{1/2} \left(1 + \frac{k^2}{2N_h c_1} \right)^{-1} k.$$

Using the binomial expansion, this can be reduced to

$$\omega = \left(\frac{N_c}{N_h c_1} \right)^{1/2} \left(k - \frac{k^3}{2N_h c_1} \right).$$

We consider a plane wave moving from left to right in the positive x-direction with a phase argument

$$kx - \omega t = kx - \left(\frac{N_c}{N_h c_1} \right)^{1/2} \left(k - \frac{k^3}{4N_h c_1} \right),$$

which implies that

$$kx - \omega t = k \left(x - \left(\frac{N_c}{N_h c_1} \right)^{1/2} t \right) + \left(\frac{N_c}{N_h c_1} \right)^{1/2} \frac{1}{4N_h c_1} k^3 t. \quad (3.1)$$

In unnormalized terms Eq. (3.1) takes the form

$$kx - \omega t = k \lambda_{Dh} \left(\frac{x}{\lambda_{Dh}} - \left(\frac{N_c}{N_h c_1} \right)^{1/2} t \omega_p \right) + \left(\frac{N_c}{N_h c_1} \right)^{1/2} \frac{N_o}{4N_h c_1} k^3 \lambda_{Dh}^3 t \omega_p, \quad (3.2)$$

where the Debye length $\lambda_{Dh} = \left(\frac{k_B T_h}{\epsilon_o N_o e^2} \right)^{1/2}$, and plasma frequency $\omega_p = \left(\frac{N_o e^2}{\epsilon_o m} \right)^{1/2}$. Recalling that $V = \frac{v_\phi}{v_{th}} = \left(\frac{N_c}{N_h c_1} \right)^{1/2}$, in the limit $\sigma \rightarrow 0$, we have

$$kx - \omega t = \beta \left(\frac{x}{\lambda_{Dh}} - V t \omega_p \right) + \beta^3 \frac{N_o}{4N_h c_1} V t \omega_p,$$

which implies the following coordinate stretching

$$\xi = \beta(x - Vt), \quad \tau = \beta^3 Vt, \quad (3.3)$$

where the parameter $\beta = k\lambda_{Dh}$, a measure of wave dispersion is considered small, $\beta^2 \ll 1$. Using the smallness parameter $\varepsilon < 1$ measuring the weakness of perturbation (weak nonlinearity) of dynamical variables (density, velocity and electrostatic potential) leads to $\beta^2 \approx O(\varepsilon)$ (here O is an expansion order). This shows the relation between the nonlinearity and dispersion of the wavepacket, linking the opposing effects so that a balance is attained. Thus, coordinate stretching in Eq. (3.3) becomes

$$\xi = \varepsilon^{1/2}(x - Vt), \quad \zeta = \varepsilon^{3/2}Vt. \quad (3.4)$$

This coordinate stretching follows that of Verheest (1988). Here ε , ξ and ζ are the parameters that measure the smallness of the nonlinearity, space-like and time-like coordinates in the wave frame, respectively.

Applying the chain rule to the above coordinate stretching, one obtains

$$\frac{\partial}{\partial x} = \frac{\partial}{\partial \xi} \frac{\partial \xi}{\partial x} + \frac{\partial}{\partial \zeta} \frac{\partial \zeta}{\partial x} = \varepsilon^{3/2} \frac{\partial}{\partial \xi} \quad (3.5)$$

$$\frac{\partial}{\partial t} = \frac{\partial}{\partial \xi} \frac{\partial \xi}{\partial t} + \frac{\partial}{\partial \zeta} \frac{\partial \zeta}{\partial t} = -V\varepsilon^{1/2} \frac{\partial}{\partial \xi} + \varepsilon^{3/2} \frac{\partial}{\partial \zeta}. \quad (3.6)$$

Later on we will use these relations in deriving the KdV equation.

Model equations

We consider a homogeneous, collisionless, unmagnetized four-component electron-positron plasma consisting of superthermal kappa-distributed hot electrons and positrons at equilibrium temperature T_h , and adiabatic cool electrons and positrons at equilibrium temperature T_c governed by fluid equations of motion. The equilibrium number densities for the hot and cool components are N_h and N_c , respectively.

The normalized basic equations governing the dynamics of the cool-component of the EP plasma are

$$\frac{\partial n_{jc}}{\partial t} + \frac{\partial}{\partial x}(n_{jc}u_{jc}) = 0. \quad (3.7)$$

$$\frac{\partial u_{jc}}{\partial t} + u_{jc} \frac{\partial u_{jc}}{\partial x} + 3\sigma \frac{n_{jc}}{N_c^2} \frac{\partial n_{jc}}{\partial x} = -z_j \frac{\partial \phi}{\partial x}, \quad (3.8)$$

and the dynamics of the hot component is governed by the kappa distribution law. For each of the hot species, the number density can take the form following that of Baluku and Hellberg (2008),

$$n_{eh} = N_h \left[1 - \frac{\phi}{\kappa - \frac{3}{2}} \right]^{-\kappa+1/2}, \quad (3.9)$$

$$n_{ph} = N_h \left[1 + \frac{\phi}{\kappa - \frac{3}{2}} \right]^{-\kappa+1/2}. \quad (3.10)$$

For small ϕ we can introduce Taylor power series expansions to Eq. (3.9) and Eq. (3.10).

Thus,

$$n_{eh} = N_h(1 + c_1\phi + c_2\phi^2 + c_3\phi^3 + \dots). \quad (3.11)$$

$$n_{ph} = N_h(1 - c_1\phi + c_2\phi^2 - c_3\phi^3 + \dots). \quad (3.12)$$

Here we have defined c_1 , c_2 and c_3 in Eq. (2.37), Eq. (2.38) and Eq. (2.39), respectively.

These sets of equations are closed by Poisson's equation

$$\frac{\partial^2 \phi}{\partial x^2} = n_{eh} - n_{ph} + \sum_j -Z_j n_{jc}. \quad (3.13)$$

Using Eq. (3.11) and Eq. (3.12) in Eq. (3.13), Poisson's equation takes the form

$$\frac{\partial^2 \phi}{\partial x^2} = 2N_h c_1 \phi + 2N_h c_3 \phi^3 + \dots + \sum_j -Z_j n_{jc}. \quad (3.14)$$

Reductive perturbation analysis

Now we can expand the dependent variables n_{jc} , u_{jc} and ϕ near their equilibrium values in a power series in ε as

$$n_{jc} = N_c + \varepsilon n_{jc1} + \varepsilon^2 n_{jc2} + \dots \quad (3.15)$$

$$u_{jc} = \varepsilon u_{jc1} + \varepsilon^2 u_{jc2} + \dots \quad (3.16)$$

$$\phi = \varepsilon\phi_1 + \varepsilon^2\phi_2 + \dots \quad (3.17)$$

Note that $\phi_o = u_{jco} = 0$ and $n_{jco} = N_c$ in the equilibrium state.

We obtain for the perturbed number density n_{jc1} and velocity u_{jc1} to the first order (see Appendix A for the full derivation)

$$n_{jc1} = \frac{Z_j N_c}{V^2 - 3\sigma} \phi_1, \quad (3.18)$$

$$u_{jc1} = \frac{Z_j V}{V^2 - 3\sigma} \phi_1, \quad (3.19)$$

where V is the normalized sound speed (acoustic speed), and satisfies the long wavelength linear dispersion relation

$$\left(2N_h c_1 - \sum_j \frac{Z_j^2 V}{V^2 - 3\sigma} \right) \phi_1 = 0. \quad (3.20)$$

Since $\phi_1 \neq 0$, Eq. (3.20) becomes

$$2N_h c_1 - \sum_j \frac{Z_j^2 V}{V^2 - 3\sigma} = 0. \quad (3.21)$$

In terms of the superthermal parameter κ , this equation yields

$$V^2 = \left(\frac{2\kappa - 3}{2\kappa - 1} \right) \frac{N_c}{N_h} + 3\sigma. \quad (3.22)$$

From the expansion to order $O(\varepsilon^{5/2})$ of the momentum equation (see A.19 in Appendix A), we obtain

$$N_c \frac{\partial u_{jc2}}{\partial \xi} = V \frac{\partial n_{jc2}}{\partial \xi} - V \frac{\partial n_{jc1}}{\partial \zeta} - \frac{\partial (u_{jc1} n_{jc1})}{\partial \xi}. \quad (3.23)$$

Multiplying both sides of the expansion to order $O(\varepsilon^{5/2})$ of the momentum equation (A.21) by N_c gives us

$$-V N_c \frac{\partial u_{jc2}}{\partial \xi} + N_c V \frac{\partial u_{jc1}}{\partial \zeta} + N_c u_{jc1} \frac{\partial u_{jc1}}{\partial \zeta} + 3\sigma \frac{\partial n_{jc2}}{\partial \xi} + \frac{3T\sigma}{N_c} n_{jc1} \frac{\partial n_{jc1}}{\partial \xi} = -Z_j N_c \frac{\partial \phi_2}{\partial \xi}. \quad (3.24)$$

Comparison between Eq. (3.23) and Eq. (3.24) yields

$$(V^2 - 3\sigma) \frac{\partial n_{jc2}}{\partial \xi} = N_c V \frac{\partial u_{jc1}}{\partial \xi} + V^2 \frac{\partial n_{jc1}}{\partial \zeta} + V \frac{\partial(n_{jc1} u_{jc1})}{\partial \zeta} + N_c u_{jc1} \frac{\partial u_{jc1}}{\partial \xi} + \frac{3\sigma}{N_c} n_{jc1} \frac{\partial n_{jc1}}{\partial \xi} + Z_j N_c \frac{\partial \phi_2}{\partial \xi}. \quad (3.25)$$

Using Eq. (3.18) and Eq. (3.19) in Eq. (3.25), one obtains that

$$\frac{\partial n_{jc2}}{\partial \xi} = \frac{2Z_j N_c V^2}{(V^2 - 3\sigma)^2} \frac{\partial \phi_1}{\partial \zeta} + \frac{3Z_j^2 N_c (V^2 + \sigma)}{(V^2 - 3\sigma)^3} \phi_1 \frac{\partial \phi_1}{\partial \xi} + \frac{Z_j N_c}{(V^2 - 3\sigma)} \frac{\partial \phi_2}{\partial \zeta}. \quad (3.26)$$

Taking the derivative of the expansion to order $O(\epsilon^2)$ of Poisson's equation in A.24 (see Appendix A) by ξ gives

$$\sum_j Z_j \frac{\partial n_{jc2}}{\partial \xi} = 2N_h c_1 \frac{\partial \phi_2}{\partial \xi} - \frac{\partial^3 \phi_1}{\partial \xi^3}. \quad (3.27)$$

Multiplying both sides of Eq. (3.26) by $\sum_j Z_j$, we have

$$\sum_j Z_j \frac{\partial n_{jc2}}{\partial \xi} = 2 \sum_j \frac{Z_j^2 N_c V^2}{(V^2 - 3\sigma)^2} \frac{\partial \phi_1}{\partial \zeta} + 3 \sum_j \frac{Z_j^3 N_c (V^2 + \sigma)}{(V^2 - 3\sigma)^3} \phi_1 \frac{\partial \phi_1}{\partial \xi} + \sum_j \frac{Z_j^2 N_c}{(V^2 - 3\sigma)} \frac{\partial \phi_2}{\partial \zeta}. \quad (3.28)$$

Comparison between Eq. (3.27) and Eq. (3.28), gives

$$\frac{\partial^3 \phi_1}{\partial \xi^3} = \left[2N_h c_1 - \sum_j \frac{Z_j^2 N_c}{V^2 - 3\sigma} \right] \frac{\partial \phi_2}{\partial \zeta} - \left[2 \sum_j \frac{Z_j^2 N_c V^2}{(V^2 - 3\sigma)^2} \right] \frac{\partial \phi_1}{\partial \zeta} - \left[3 \sum_j \frac{Z_j^3 N_c (V^2 + \sigma)}{(V^2 - 3\sigma)^3} \right] \phi_1 \frac{\partial \phi_1}{\partial \xi}. \quad (3.29)$$

From Eq. (3.21), the coefficient of $\frac{\partial \phi_2}{\partial \zeta}$ in Eq. (3.29) becomes zero. We can write Eq. (3.29) as a KdV form

$$\boxed{\frac{\partial \phi_1}{\partial \zeta} + A \phi_1 \frac{\partial \phi_1}{\partial \xi} + B \frac{\partial^3 \phi_1}{\partial \xi^3} = 0}, \quad (3.30)$$

where

$$A = \frac{3 \sum_j Z_j^3 N_c (V^2 + \sigma)}{2 \sum_j Z_j^2 N_c V^2} \quad \text{and} \quad B = \frac{1}{2 \sum_j \frac{Z_j^2 N_c V^2}{(V^2 - 3\sigma)^2}}. \quad (3.31)$$

However, in general,

$$\sum_j Z_j^n = \begin{cases} 2 & \text{if } n=\text{even} \\ 0 & \text{if } n=\text{odd} \end{cases} \quad (3.32)$$

With this property, the coefficient of the nonlinear term $\phi_1 \frac{\partial \phi_1}{\partial \xi}$, that is, A in Eq. (3.30) vanishes. Therefore, finally, the KdV expression in Eq. (3.30) becomes

$$\frac{\partial \phi_1}{\partial \zeta} + B \frac{\partial^3 \phi_1}{\partial \xi^3} = 0. \quad (3.33)$$

This equation is purely a dispersive one without the nonlinear term. The reason for this loss of nonlinearity is the anti-symmetry in the charge carried by positrons and electrons. In order to avoid such a scenario we can include a higher order nonlinearity, which results in the modified KdV equation (Watanabe, 1984).

3.1.2 The modified Korteweg de Vries (mKdV) equation

In order to allow for a higher degree of nonlinearity, we thus need to consider the modified Korteweg de Vries equation (Watanabe, 1984) with a different stretching, to obtain quadratic and cubic nonlinear terms on an equal footing. Following the approach of Verheest (1988), we thus have the following stretched coordinates

$$\xi = \varepsilon(x - Vt) \quad \text{and} \quad \zeta = \varepsilon^3 Vt,$$

where V is the phase velocity normalized with respect to the hot species thermal speed. In this case the nonlinear parameter $\beta^2 = k^2 \lambda_D^2 = O(\varepsilon^2)$. The above stretchings allow for the incorporation of even higher wavenumber harmonics in the wavepackets, $k \lambda_D \approx \varepsilon$, as opposed to the KdV stretching which has β^2 of order ε . The larger wavenumber allows stronger wave dispersion, which for balance implies a greater degree of nonlinearity (Baboolal, Bharuthram and Hellberg, 1988). So, from the above stretching, we have

$$\frac{\partial}{\partial x} = \varepsilon \frac{\partial}{\partial \xi} \quad \text{and} \quad \frac{\partial}{\partial t} = -\varepsilon V \frac{\partial}{\partial \xi} + \varepsilon^3 V \frac{\partial}{\partial \tau}. \quad (3.34)$$

3.1.3 Reductive perturbation method for mKdV analysis

Now we can expand the dependent variables n_{jc} , u_{jc} and ϕ near their equilibrium values in a power series in ε as

$$n_{jc} = N_c + \varepsilon n_{jc1} + \varepsilon^2 n_{jc2} + \varepsilon^3 n_{jc3} + \dots \quad (3.35)$$

$$u_{jc} = \varepsilon u_{jc1} + \varepsilon^2 u_{jc2} + \varepsilon^3 u_{jc3} \dots \quad (3.36)$$

$$\phi = \varepsilon \phi_1 + \varepsilon^2 \phi_2 + \varepsilon^3 \phi_3 \dots, \quad (3.37)$$

which in this case are expanded up to $O(\varepsilon^3)$. We obtain to $O(\varepsilon^2)$ from B.31 and B.32 (see Appendix B for the full derivation)

$$u_{jc1} = \frac{Z_j V}{V^2 - 3T_c} \phi_1, \quad (3.38)$$

$$n_{jc1} = \frac{Z_j N_c}{V^2 - 3T_c} \phi_1, \quad (3.39)$$

where V , the normalized sound speed, satisfies the long wavelength linear dispersion relation

$$2N_h c_1 - \sum_j \frac{Z_j^2 N_c}{V^2 - 3T_c} = 0. \quad (3.40)$$

Eq. (3.38) and Eq. (3.39) are expressions for the first order nonlinear perturbations in u and n .

To $O(\varepsilon^3)$ we obtain

$$n_{jc2} = \frac{Z_j N_c}{V^2 - 3\sigma} \phi_2 + \frac{3Z_j^2 N_c}{2(V^2 - 3\sigma)^3} (V^2 + \sigma) \phi_1^2 \quad (3.41)$$

$$u_{jc2} = \frac{1}{2} Z_j^2 \left[\frac{V(V^2 + 9T_c)}{(V^2 - 3\sigma)^3} \right] \phi_1^2 + \frac{Z_j V}{V^2 - 3\sigma} \phi_2. \quad (3.42)$$

At $O(\varepsilon^4)$ we obtain from the continuity equation in terms of perturbed variables and stretched coordinates in the wave frame (see B.19 in Appendix B)

$$V \frac{\partial n_{jc2}}{\partial \zeta} - V \frac{\partial n_{jc3}}{\partial \xi} + u_{jc1} \frac{\partial n_{jc2}}{\partial \xi} + u_{jc2} \frac{\partial n_{jc1}}{\partial \xi} + N_c \frac{\partial u_{jc3}}{\partial \xi} + n_{jc1} \frac{\partial u_{jc2}}{\partial \xi} + n_{jc2} \frac{\partial u_{jc1}}{\partial \xi} = 0. \quad (3.43)$$

From the momentum equation at $O(\epsilon^4)$

$$-V \frac{\partial u_{jc3}}{\partial \xi} + V \frac{\partial u_{jc1}}{\partial \zeta} + \frac{\partial(u_{jc1}u_{jc2})}{\partial \xi} + \frac{3\sigma}{N_c} \frac{\partial n_{jc3}}{\partial \xi} + \frac{3\sigma}{N_c^2} \frac{\partial(n_{jc1}n_{jc2})}{\partial \xi} = -Z_j \frac{\partial \phi_3}{\partial \xi}. \quad (3.44)$$

Eliminating u_{jc3} from Eq. (3.43), and using Eq. (3.38), Eq. (3.39), Eq. (3.41) and Eq. (3.42), gives an equation for $\frac{\partial n_{jc3}}{\partial \xi}$, which when substituted into $O(\epsilon^3)$ of Poisson's equation (B.26), after partial differentiation with respect to ξ gives the modified Korteweg de Vries (mKdV) equation:

$$\frac{\partial \phi_1}{\partial \zeta} + \frac{b}{a} \frac{\partial \phi_1^3}{\partial \xi} + \frac{1}{a} \frac{\partial^3 \phi_1}{\partial \xi^3} = 0. \quad (3.45)$$

This may be written as

$$\boxed{\frac{\partial \phi_1}{\partial \zeta} + B \frac{\partial \phi_1^3}{\partial \xi} + C \frac{\partial^3 \phi_1}{\partial \xi^3} = 0}, \quad (3.46)$$

where $B = b/a$ and $C = 1/a$ with

$$b = \frac{2N_c}{(V^2 - 3\sigma)^2} \left(\frac{V^2 + 3\sigma}{(V^2 - 3\sigma)^2} + \frac{9\sigma(V^2 + \sigma)}{(V^2 - 3\sigma)^3} + \frac{3(V^2 + 3\sigma)(V^2 + \sigma)}{2(V^2 - 3\sigma)^3} \right) - 2N_h c_3 \quad (3.47)$$

and

$$a = \frac{4N_c V^2}{(V^2 - 3\sigma)^2}. \quad (3.48)$$

Thus, the dispersive term, coefficient C , in the mKdV equation is defined as

$$C = \frac{(V^2 - 3\sigma)^2}{4N_c V^2}.$$

Using Eq. (2.75), this equation reads

$$C = \frac{N_c}{4N_h^2} \left[\frac{2\kappa - 3}{2\kappa - 1} \right]^2 \left[\frac{1}{\frac{N_c}{N_h} \left[\frac{2\kappa - 3}{2\kappa - 1} \right] + 3\sigma} \right].$$

Applying the definition,

$$\frac{N_c}{N_h} = \alpha \quad \text{and} \quad N_c + N_h = 1 \implies N_h = \frac{1}{\alpha + 1} \quad \text{and} \quad N_c = \frac{\alpha}{\alpha + 1}$$

the expression for C reads,

$$C = \frac{\alpha(\alpha + 1)}{4} \left[\frac{2\kappa - 3}{2\kappa - 1} \right]^2 \left[\frac{1}{\alpha \left[\frac{2\kappa - 3}{2\kappa - 1} \right] + 3\sigma} \right]. \quad (3.49)$$

After rearrangement Eq. (3.47), takes the form

$$b = \left[\frac{N_c(5V^4 + 30V^2\sigma + 9\sigma^2) - N_h(V^2 - 3\sigma)^5 c_3}{(V^2 - 3\sigma)^5} \right]. \quad (3.50)$$

So, using Eq. (3.48) and Eq. (3.50), we then have

$$B = \frac{b}{a} = \left[\frac{N_c(5V^4 + 30V^2\sigma + 9\sigma^2) - N_h(V^2 - 3\sigma)^5 c_3}{(V^2 - 3\sigma)^5} \right] \left[\frac{(V^2 - 3\sigma)^2}{4N_c V^2} \right]. \quad (3.51)$$

Using an expression for normalized sound speed V , that has been obtained in Eq. (2.75), in Eq. (3.51), we get

$$B = - \frac{2 \frac{c_3}{c_1^3} \left(\frac{N_c}{N_h}\right)^4 - 5 \frac{1}{c_1^2} \left(\frac{N_c}{N_h}\right)^2 - 60\sigma \left(\frac{1}{c_1}\right) \left(\frac{N_c}{N_h}\right) - 144\sigma^2}{4 \left(\frac{N_c}{N_h} \frac{1}{c_1} + 3\sigma\right) \left(\frac{N_c}{N_h} \frac{1}{c_1}\right)^3}. \quad (3.52)$$

Since we have already defined $N_c/N_h = \alpha$, then the coefficient of the nonlinear term in a mKdV equation becomes

$$B = - \frac{2 \frac{c_3}{c_1^3} \alpha^4 - 5 \frac{\alpha^2}{c_1^2} - 60\sigma \left(\frac{\alpha}{c_1}\right) - 144\sigma^2}{4 \left(\frac{\alpha}{c_1} + 3\sigma\right) \left(\frac{\alpha}{c_1}\right)^3}. \quad (3.53)$$

In terms of the kappa parameter κ , this equation is finally written as

$$B = - \frac{\left(\frac{16\kappa^4 - 16\kappa^3 - 48\kappa^2 + 36\kappa + 27}{16\kappa^4 - 32\kappa^3 + 24\kappa^2 - 8\kappa + 1}\right) \alpha^4 - \left(\frac{2\kappa - 3}{2\kappa - 1}\right)^2 15\alpha^2 - \left(\frac{2\kappa - 3}{2\kappa - 1}\right) 180\sigma\alpha - 432\sigma^2}{12 \left[\left(\frac{2\kappa - 3}{2\kappa - 1}\right)\alpha + 3\sigma\right] \left[\left(\frac{2\kappa - 3}{2\kappa - 1}\right)\alpha\right]^3}. \quad (3.54)$$

Note that the results in Eqs. (3.49) and (3.54) have reduced to Eqs. (3.53) and Eqs. (3.54) of Gray (1998), respectively, for $\kappa \rightarrow \infty$, in which the hot species was assumed to follow the Maxwellian distribution.

3.1.4 Stationary solution of the mKdV equation

In order to obtain small amplitude soliton solutions to the mKdV equation

$$\frac{\partial \phi_1}{\partial \zeta} + B \frac{\partial \phi_1^3}{\partial \xi} + C \frac{\partial^3 \phi_1}{\partial \xi^3} = 0,$$

we define a stationary wave frame following Mace (1991) as

$$\phi(\zeta, \xi) = \phi(\nu) = \phi(\xi - U\zeta),$$

where U is an incremental velocity of the soliton in the frame moving with the phase speed. So with this,

$$\frac{\partial\phi}{\partial\zeta} = -U\frac{d\phi}{d\nu} \quad \text{and} \quad \frac{\partial\phi}{\partial\xi} = \frac{d\phi}{d\nu}. \quad (3.55)$$

For the sake of mathematical simplicity we have suppressed the subscript “1” in ϕ . Using Eq. (3.55) in the mKdV equation above, we obtain that

$$U\frac{d\phi}{d\nu} + B\frac{d\phi^3}{d\nu} + C\frac{d^3\phi}{d\nu^3} = 0. \quad (3.56)$$

Integration can be done directly because Eq. (3.56) is a form of total derivative. It follows that

$$-U\phi + B\phi^3 + C\frac{d^2\phi}{d\nu^2} = K, \quad (3.57)$$

where K is the constant of integration. Multiplication of both sides of Eq. (3.57) by $d\phi$ gives

$$-U\phi d\phi + B\phi^3 d\phi + C\frac{d^2\phi}{d\nu^2} d\phi = K d\phi. \quad (3.58)$$

Integrating

$$-\frac{U\phi^2}{2} + \frac{B\phi^4}{4} + \frac{1}{2}C\left(\frac{d\phi}{d\nu}\right)^2 = K\phi + D, \quad (3.59)$$

where D is another constant of integration. The following boundary conditions must be satisfied to obtain a satisfactory soliton solution,

$$\phi, \quad \frac{d\phi}{d\nu} \quad \text{and} \quad \frac{d^2\phi}{d\nu^2} \rightarrow 0 \quad \text{as} \quad \nu \rightarrow \infty.$$

With this condition, K and D in Eq. (3.59) become zero, so that Eq. (3.59) takes the form

$$-\frac{U\phi^2}{2} + \frac{B\phi^4}{4} + \frac{1}{2}C\left(\frac{d\phi}{d\nu}\right)^2 = 0. \quad (3.60)$$

Rearranging this,

$$\frac{d\phi}{d\nu} = \frac{U}{C}\phi^2 - \frac{B}{2C}\phi^2.$$

It follows that

$$\frac{d\phi}{d\nu} = \pm \left(\frac{U}{C}\right)^{1/2} \phi \left[1 - \frac{B\phi^2}{2U}\right]^{1/2}. \quad (3.61)$$

By rearranging this one obtains that

$$d\nu = \pm \left(\frac{C}{U} \right)^{1/2} \frac{d\phi}{\phi \left[1 - \frac{B\phi^2}{2U} \right]^{1/2}}. \quad (3.62)$$

Integrating both sides of this, we have

$$\nu = \pm \left(\frac{C}{U} \right)^{1/2} \int \frac{d\phi}{\phi \left[1 - \frac{B\phi^2}{2U} \right]^{1/2}}. \quad (3.63)$$

Using the following substitution

$$\phi = \left(\frac{2U}{B} \right)^{1/2} \operatorname{sech} x, \quad (3.64)$$

and using Eq. (3.63), we see that

$$1 - \frac{B\phi^2}{2U} = 1 - \frac{B}{2U} \left(\frac{2U}{B} \operatorname{sech}^2 x \right) = 1 - \operatorname{sech}^2 x.$$

This implies that

$$1 - \frac{B\phi^2}{2U} = \tanh^2 x. \quad (3.65)$$

Here we have used the following trigonometric identity,

$$1 - \operatorname{sech}^2 x = \tanh^2 x.$$

Differentiating Eq. (3.64) with respect to x , one obtains

$$\frac{d\phi}{dx} = \left(\frac{2U}{B} \right)^{1/2} \frac{d}{dx}(\operatorname{sech} x) = - \left(\frac{2U}{B} \right)^{1/2} \operatorname{sech} x \tanh x. \quad (3.66)$$

Using Eq. (3.64), Eq. (3.65) and Eq. (3.66) in Eq. (3.63) we find that

$$\nu = \mp \left(\frac{C}{U} \right)^{1/2} \int dx.$$

This implies that

$$\nu = \mp \left(\frac{C}{U} \right)^{1/2} x. \quad (3.67)$$

From Eq. (3.64), we know that

$$x = \operatorname{sech}^{-1} \left[\left(\frac{B}{2U} \right)^{1/2} \phi \right]. \quad (3.68)$$

So, using Eq. (3.68) in Eq. (3.67), gives us

$$\nu = \mp \left(\frac{C}{U}\right)^{1/2} \operatorname{sech}^{-1} \left[\left(\frac{B}{2U}\right)^{1/2} \phi \right].$$

From this equation we finally have a soliton solution for ϕ_1 as

$$\phi_1 = \left(\frac{2U}{B}\right)^{1/2} \operatorname{sech} \left[\pm \left(\frac{U}{C}\right)^{1/2} (\xi - U\zeta) \right]. \quad (3.69)$$

This is a soliton solution to the mKdV equation. Here U , ξ and ζ are velocity, space-like and time-like coordinates in the wave frame, respectively. We recall that here,

$$B = -\frac{2\frac{c_3}{c_1^3}\alpha^4 - 5\frac{\alpha^2}{c_1^2} - 60\sigma\left(\frac{\alpha}{c_1}\right) - 144\sigma^2}{4\left(\frac{\alpha}{c_1} + 3\sigma\right)\left(\frac{\alpha}{c_1}\right)^3}$$

$$C = \frac{\alpha(\alpha + 1)}{4c_1^2} \left(\frac{1}{\frac{\alpha}{c_1} + 3\sigma}\right)$$

$$c_1 = \left(\frac{\kappa - \frac{1}{2}}{\kappa - \frac{3}{2}}\right)$$

$$c_3 = \frac{(\kappa - \frac{1}{2})(\kappa + \frac{1}{2})(\kappa + \frac{3}{2})}{6(\kappa - \frac{3}{2})^3}.$$

3.2 Arbitrary amplitude analysis

Anticipating stationary profile solitary waves moving at a constant speed, all the fluid variables in the evolution Eq. (2.17), Eq. (2.18) and Eq. (2.20) are assumed to depend on a single variable $\eta = x - Mt$ (Verheest and Hellberg, 1999; Roychoudhury and Maitra, 2002), where M is the dimensionless normalized solitary wave propagation velocity scaled by a fixed hot species speed v_{th} (often referred to as the ‘‘Mach number’’), x and t are space and time coordinates of the solitary structure in the laboratory frame, respectively.

With $\frac{\partial}{\partial x} = \frac{d}{d\eta}$; $\frac{\partial}{\partial t} = -M\frac{d}{d\eta}$ all the variables depends on η . With these substitutions, the normalized evolution equations (continuity, momentum and Poisson’s) becomes

$$-M\frac{dn_{jc}}{d\eta} + \frac{d}{d\eta}(n_{jc}u_{jc}) = 0 \quad (3.70)$$

$$-M \frac{du_{jc}}{d\eta} + u_{jc} \frac{du_{jc}}{d\eta} + 3\sigma \frac{n_{jc}}{N_c^2} \frac{dn_{jc}}{d\eta} = -Z_j \frac{d\phi}{d\eta} \quad (3.71)$$

$$\frac{d^2\phi}{d\eta^2} = n_{ec} + n_{eh} - n_{pc} - n_{ph}. \quad (3.72)$$

Integrating Eq. (3.70) by using the boundary conditions $n_{jc} = N_c$; $\phi, \frac{d\phi}{d\eta} = 0$, and $u_{jc} = 0$ at $\eta \rightarrow \infty$, we get

$$u_{jc} = M \left(1 - \frac{N_c}{n_{jc}} \right). \quad (3.73)$$

Differentiating Eq. (3.73) with respect to η gives us

$$\frac{du_{jc}}{d\eta} = M \frac{N_c}{n_{jc}^2} \frac{dn_{jc}}{d\eta}. \quad (3.74)$$

Using Eq. (3.73) and Eq. (3.74) in Eq. (3.71), we obtain

$$-M^2 \frac{N_c^2}{n_{jc}^3} \frac{dn_{jc}}{d\eta} + 3\sigma \frac{n_{jc}}{N_c^2} \frac{dn_{jc}}{d\eta} = -Z_j \frac{d\phi}{d\eta}. \quad (3.75)$$

Upon integration, Eq. (3.75) becomes

$$M^2 \frac{N_c^2}{2n_{jc}^2} + 3\sigma \frac{n_{jc}^2}{2N_c^2} = -Z_j\phi + K, \quad (3.76)$$

where K is the constant of integration and it can be evaluated using the above boundary conditions to get

$$K = \frac{M^2}{2} + \frac{3\sigma}{2}.$$

With this substitution, Eq. (3.76) takes the form

$$M^2 \left(\frac{N_c^2}{n_{jc}^2} - 1 \right) + 3\sigma \left(\frac{n_{jc}^2}{N_c^2} - 1 \right) = -Z_j 2\phi. \quad (3.77)$$

Rearranging of this gives

$$\frac{3\sigma}{N_c^2} n_{jc}^4 - (M^2 + 3\sigma - Z_j 2\phi) n_{jc}^2 + M^2 N_c^2 = 0.$$

This is a bi-quadratic equation which can be solved in n_{jc}^2 to get

$$\frac{n_{jc}^2}{N_c^2} = \frac{1}{6\sigma} \left[(M^2 - Z_j 2\phi + 3\sigma) \pm \sqrt{(M^2 - Z_j 2\phi + 3\sigma)^2 - 12M^2\sigma} \right] \quad (3.78)$$

This equation has been obtained previously by many authors (Verheest and Hellberg, 1999; Verheest et al., 1996; Roychoudhury and Bhattacharyya, 1987). Some of them have

used a numerical integration to obtain the corresponding pseudopotential. However, in order to obtain an integrable form of n_{jc} in deriving the corresponding Sagdeev potential analytically, we have followed the ideas of Ghosh et al. (1996) and written

$$\frac{n_{jc}}{N_c} = \sqrt{p} \pm \sqrt{q}. \quad (3.79)$$

Squaring both sides of Eq. (3.79), we have

$$\frac{n_{jc}^2}{N_c^2} = p + q \pm 2\sqrt{pq}. \quad (3.80)$$

Comparing Eq. (3.78) with Eq.(3.80), gives

$$(p + q) \pm 2\sqrt{pq} = \frac{1}{6\sigma} \left[(M^2 - Z_j 2\phi + 3\sigma) \pm \sqrt{(M^2 - Z_j 2\phi + 3\sigma)^2 - 12M^2\sigma} \right].$$

By collecting like terms, the above equation will be split into the following forms

$$p + q = \frac{[M^2 - Z_j 2\phi + 3\sigma]}{6\sigma} \quad (3.81)$$

and

$$2\sqrt{pq} = \frac{\sqrt{(M^2 - Z_j 2\phi + 3\sigma)^2 - 12M^2\sigma}}{6\sigma}. \quad (3.82)$$

Squaring both sides of Eq. (3.82) gives us

$$4pq = \frac{(M^2 - Z_j 2\phi + 3\sigma)^2 - 12M^2\sigma}{36\sigma^2}. \quad (3.83)$$

From Eq. (3.81) and Eq. (3.83), one obtains that

$$144\sigma^2 q^2 - 24\sigma (M^2 - Z_j 2\phi + 3\sigma) q + [(M^2 - Z_j 2\phi + 3\sigma)^2 - 12M^2\sigma] = 0.$$

This is a quadratic equation in q so that it can be solved, to get

$$q = \frac{(M^2 - Z_j 2\phi + 3\sigma) \pm 2M\sqrt{3\sigma}}{12\sigma}. \quad (3.84)$$

Using Eq. (3.84) in place of q in Eq. (3.81), we have

$$p = \frac{(M^2 - Z_j 2\phi + 3\sigma) \mp 2M\sqrt{3\sigma}}{12\sigma}. \quad (3.85)$$

Substituting Eq. (3.84) and Eq. (3.85) in Eq. (3.79), one obtains that

$$n_{jc} = \frac{N_c}{2\sqrt{3\sigma}} \left[\sqrt{(M^2 - Z_j 2\phi + 3\sigma) \mp 2M\sqrt{3\sigma}} \pm \sqrt{(M^2 - Z_j 2\phi + 3\sigma) \pm 2M\sqrt{3\sigma}} \right]. \quad (3.86)$$

This equation can also be written as

$$n_{jc} = \frac{N_c}{2\sqrt{3\sigma}} \left[\sqrt{(M \mp \sqrt{3\sigma})^2 - Z_j 2\phi} \pm \sqrt{(M \pm \sqrt{3\sigma})^2 - Z_j 2\phi} \right]. \quad (3.87)$$

The \pm sign in this equation indicates that there are two possible roots for each species. However, the positive root is misleading in the boundary condition that $n_{jc} \rightarrow N_c$ when the electrostatic potential ϕ is equal to zero. Therefore, we can reject the positive root from the above solution so as to get a physically acceptable solution for the number density at the boundaries. Thus, we can write Eq. (3.87) for each of the species as

$$n_{ec} = \frac{N_c}{2\sqrt{3\sigma}} \left[\sqrt{(M + \sqrt{3\sigma})^2 + 2\phi} - \sqrt{(M - \sqrt{3\sigma})^2 + 2\phi} \right] \quad (3.88)$$

and

$$n_{pc} = \frac{N_c}{2\sqrt{3\sigma}} \left[\sqrt{(M + \sqrt{3\sigma})^2 - 2\phi} - \sqrt{(M - \sqrt{3\sigma})^2 - 2\phi} \right]. \quad (3.89)$$

3.2.1 The generalized Sagdeev pseudopotential

To obtain fully nonlinear solutions for acoustic soliton, we can use the Sagdeev pseudopotential method (Sagdeev, 1966) by substituting Eq. (3.9), Eq. (3.10), Eq. (3.88) and Eq. (3.89) into Eq. (3.72). Hence,

$$\begin{aligned} \frac{d^2\phi}{d\eta^2} = & \frac{N_c}{2\sqrt{3\sigma}} \left[\sqrt{(M + \sqrt{3\sigma})^2 + 2\phi} - \sqrt{(M - \sqrt{3\sigma})^2 + 2\phi} \right] + N_h \left[1 - \frac{\phi}{\kappa - \frac{3}{2}} \right]^{-\kappa+1/2} \\ & - \frac{N_c}{2\sqrt{3\sigma}} \left[\sqrt{(M + \sqrt{3\sigma})^2 - 2\phi} - \sqrt{(M - \sqrt{3\sigma})^2 - 2\phi} \right] - N_h \left[1 + \frac{\phi}{\kappa - \frac{3}{2}} \right]^{-\kappa+1/2}. \end{aligned} \quad (3.90)$$

After multiplying this equation by $d\phi/d\eta$, we can integrate with respect to η and obtain an energy type equation for a classical unit mass particle moving in a conservative force field, if one defines η as a time and ϕ as a position

$$\frac{1}{2} \left(\frac{d\phi}{d\eta} \right)^2 + \Psi(\phi, M) = 0. \quad (3.91)$$

This is often called the Sagdeev equation. We have imposed the boundary conditions $\phi_0 = \phi'_0 = 0$ at $\eta = \pm\infty$ in Eq. (3.90) in order to arrive at Eq. (3.91). The Sagdeev pseudopotential $\Psi(\phi, \mu)$ in Eq. (3.91) is given by

$$\begin{aligned} \Psi(\phi, M) = & - \int_0^\phi \frac{N_c}{2\sqrt{3}\sigma} \left[\sqrt{(M + \sqrt{3}\sigma)^2 + 2\phi} - \sqrt{(M - \sqrt{3}\sigma)^2 + 2\phi} \right] d\phi \\ & + \int_0^\phi \frac{N_c}{2\sqrt{3}\sigma} \left[\sqrt{(M + \sqrt{3}\sigma)^2 - 2\phi} - \sqrt{(M - \sqrt{3}\sigma)^2 - 2\phi} \right] d\phi \\ & - \int_0^\phi N_h \left[1 - \frac{\phi}{\kappa - \frac{3}{2}} \right]^{-\kappa+1/2} d\phi + \int_0^\phi N_h \left[1 + \frac{\phi}{\kappa - \frac{3}{2}} \right]^{-\kappa+1/2} d\phi. \end{aligned} \quad (3.92)$$

Note that $\frac{d^2\phi}{d\eta^2} = -\Psi'(\phi, \mu)$, the prime denoting the derivative with respect to ϕ . After integration, Eq. (3.92) take the form

$$\begin{aligned} \Psi(\phi, M) = & \frac{N_c}{6\sqrt{3}\sigma} \left[2(M + \sqrt{3}\sigma)^3 - 2(M - \sqrt{3}\sigma)^3 + \left([M - \sqrt{3}\sigma]^2 - 2\phi \right)^{3/2} \right] \\ & + \frac{N_c}{6\sqrt{3}\sigma} \left[\left([M - \sqrt{3}\sigma]^2 + 2\phi \right)^{3/2} - \left([M + \sqrt{3}\sigma]^2 - 2\phi \right)^{3/2} - \left([M + \sqrt{3}\sigma]^2 + 2\phi \right)^{3/2} \right] \\ & + N_h \left\{ 2 - \left[1 - \frac{\phi}{\kappa - \frac{3}{2}} \right]^{\frac{3}{2}-\kappa} - \left[1 + \frac{\phi}{\kappa - \frac{3}{2}} \right]^{\frac{3}{2}-\kappa} \right\}. \end{aligned} \quad (3.93)$$

Using the definition in Eq. (2.79), and after some algebraic manipulation, Eq. (3.93) will be written as

$$\begin{aligned} \Psi(\phi, M) = & \frac{\alpha}{\alpha + 1} \left[2(M^2 + \sigma) + \frac{1}{6\sqrt{3}\sigma} \left\{ \left([M - \sqrt{3}\sigma]^2 - 2\phi \right)^{3/2} + \left([M - \sqrt{3}\sigma]^2 + 2\phi \right)^{3/2} \right\} \right] \\ & - \frac{\alpha}{(\alpha + 1)6\sqrt{3}\sigma} \left[\left([M + \sqrt{3}\sigma]^2 - 2\phi \right)^{3/2} + \left([M + \sqrt{3}\sigma]^2 + 2\phi \right)^{3/2} \right] \\ & + \frac{1}{\alpha + 1} \left\{ 2 - \left[1 - \frac{\phi}{\kappa - \frac{3}{2}} \right]^{\frac{3}{2}-\kappa} - \left[1 + \frac{\phi}{\kappa - \frac{3}{2}} \right]^{\frac{3}{2}-\kappa} \right\}. \end{aligned} \quad (3.94)$$

Here we recall that $\alpha = N_c/N_h$ is the ratio of cool to hot species densities in equilibrium, $\sigma = T_c/T_h$ is the temperature ratio of cool to hot species, M is the normalized solitary wave speed in the laboratory frame and κ is the superthermal parameter describing the hot species velocity distributions.

The Sagdeev pseudopotential in Eq. (3.94) satisfies the soliton condition $\Psi(0, M) = 0$ and $\Psi'(0, M) = 0$, where the two terms in that equation are the contributions to the pseudopotential, of cool adiabatic and hot kappa distributed species, respectively.

In Chapter 4, we will explore numerically the properties and characteristics of solitons arising from the Sagdeev potential approach, as well as make a comparison with the results from the small amplitude mKdV theory.

Chapter 4

Results and discussions

In this chapter we will investigate numerically the solutions for both mKdV (Eq. (3.69)) and arbitrary amplitude (Eq. (3.94)) solitary waves which have been derived in Chapter 3.

4.1 Numerical results of the small amplitude analysis

As a first step we consider small amplitude waves. Using the reductive perturbation method, the mKdV solution for a soliton profile has been obtained in Chapter 3 as

$$\phi_1 = \left(\frac{2U}{B}\right)^{1/2} \operatorname{sech} \left[\pm \left(\frac{U}{C}\right)^{1/2} (\xi - U\zeta) \right].$$

Returning to the laboratory frame, we use the following change of variables

$$\xi = \varepsilon(x - Vt) \quad \text{and} \quad \zeta = \varepsilon^3 Vt.$$

Hence,

$$\phi_1 = \left(\frac{2U}{B}\right)^{1/2} \operatorname{sech} \left[\pm \left(\frac{U}{C}\right)^{1/2} (\varepsilon x - \varepsilon Vt - U\varepsilon^3 Vt) \right].$$

After some re-arrangement, this can be written as

$$\phi_1 = \left(\frac{2U}{B}\right)^{1/2} \operatorname{sech} \left[\pm \left(\frac{U\varepsilon^2}{C}\right)^{1/2} (x - Vt(1 + U\varepsilon^2)) \right].$$

Using $\phi = \varepsilon\phi_1$, the above equation takes the form

$$\phi = \left(\frac{2U\varepsilon^2}{B}\right)^{1/2} \operatorname{sech} \left[\pm \left(\frac{U\varepsilon^2}{C}\right)^{1/2} (x - V(1 + U\varepsilon^2)t) \right]. \quad (4.1)$$

We have assumed that the arbitrary amplitude solitary wave is stationary in the frame $\eta = x - Mt$, so that from Eq. (4.1) we see that

$$M = V(1 + U\varepsilon^2), \quad (4.2)$$

which means

$$\frac{M}{V} = 1 + U\varepsilon^2 \implies U\varepsilon^2 = \frac{M}{M_s} - 1, \quad (4.3)$$

where $M_s = V$, that is the phase velocity of the wave form scaled by the hot species thermal velocity (Eq. 2.75). Using Eq. (4.3) in Eq. (4.1), we can write an expression for a soliton solution of the electrostatic potential pulse as

$$\phi = \left(\frac{2(M - M_s)}{M_s B}\right)^{1/2} \operatorname{sech} \left[\pm \left(\frac{M - M_s}{M_s C}\right)^{1/2} (x - Mt) \right], \quad (4.4)$$

where the dispersive coefficient C and the nonlinear coefficient B in the mKdV equations have been defined in Eq. (3.49) and Eq. (3.54), respectively. Since the sech function is even in x , we can omit \pm sign in Eq. (4.4). Hence, we can write Eq. (4.4) finally as

$$\phi = \left(\frac{2\delta M}{M_s B}\right)^{1/2} \operatorname{sech} \left[\left(\frac{\delta M}{M_s C}\right)^{1/2} \eta \right], \quad (4.5)$$

where $\delta M = M - M_s$, in which, M and M_s are soliton pulse speed and the acoustic speed, respectively, normalized to the hot species speed.

For a physically realistic thermal speed, the superthermal parameter $\kappa > 3/2$ (Mace and Hellberg, 1995). With this condition, M_s and C are greater than zero in Eq. (2.75) and Eq. (3.49), respectively. This implies that $\delta M > 0$ in Eq. (4.5) for a real soliton. Hence, for the real amplitude of the soliton of electrostatic potential pulse, the dispersive coefficient $B > 0$ in Eq. (4.5). With all these conditions, therefore, the model under investigation supports both a positive or negative super-acoustic ($M > M_s$) mKdV electrostatic potential excitation because of the symmetry of the model. On the other hand,

from Eq. (4.5) one can also see that at the acoustic point, where $M = M_s$, the mKdV soliton amplitude tends to zero, as expected.

Moreover, from Eq. (4.5) it is clear that the maximum amplitude $\phi_o = \left(\frac{2\delta M}{M_s B}\right)^{1/2}$ and the width of the electrostatic potential pulse (soliton) $w = \left(\frac{M_s C}{\delta M}\right)^{1/2}$ depends on the plasma parameters (number density ratio α , superthermal parameter κ , temperature ratio σ) through δM , the nonlinear coefficient B and the dispersive coefficient C which are complicated functions of α , κ and σ and are listed in conjunction with Eq. (3.69). It can be seen that as δM increases, the soliton amplitude increases with a square root dependence, while the width w decreases similarly.

Next, we will investigate the mKdV solution (Eq. (4.5)) graphically to see the effect of variations of various plasma parameters on the electrostatic potential excitation. To generate different curves which will be represented in Fig. 4.2, for convenience, the limiting values of α for the corresponding κ are determined from the chosen ratio of $\alpha/c_1 = 0.3$ (see the detailed discussions for this at the end of Chapter 2).

Before that, the region of parameters of α and κ which are determining the sign of the nonlinear coefficient B in the mKdV equation when $\sigma \rightarrow 0$ is represented in Fig. 4.1 along with the curves for different chosen values of α/c_1 . The real electrostatic excitations will exist only in the region (below red line in Fig. 4.1) where $B > 0$ as evidence from the mKdV soliton solution in Eq. (4.5). In the region where $B < 0$ the electrostatic potential excitation will not propagate because of the imaginary root in the mKdV solution. Therefore, all the parametric values of α and κ in the upcoming discussions of the mKdV analysis are restricted to the region (coloured in light gray) below the red curve.

Pictorially, the effect of the variation of the cold-to-hot number density ratio α , the superthermal parameter κ , the “true” Mach number M/M_s and the temperature ratio σ on the solitary wave amplitude ϕ and its width w is displayed in Fig. 4.2. From Fig. 4.2 (a) it

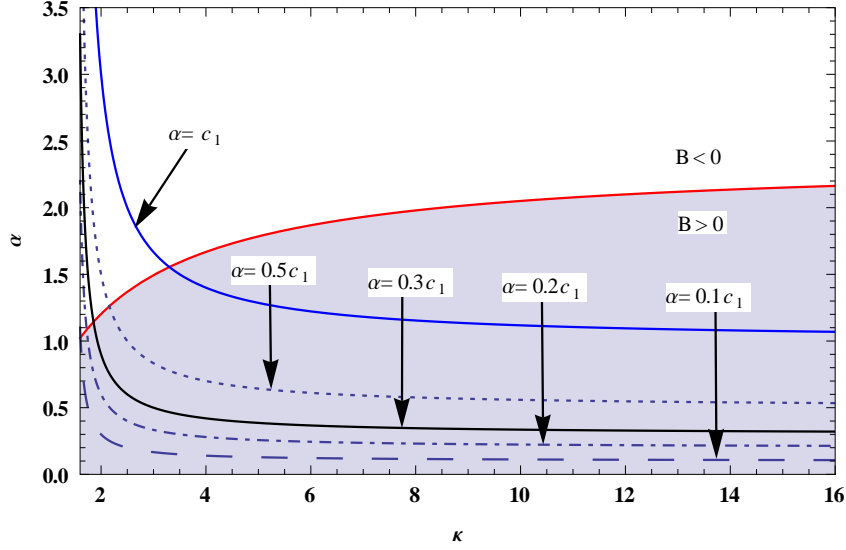


Figure 4.1: The regions of plasma parameters (α and κ) determining the sign of the nonlinear coefficient B in the mKdV equations when $\sigma \rightarrow 0$. The solid red curve corresponds to singular solution with an infinite amplitude of the electrostatic excitation.

can be seen that increasing α will result in the enhancement of both amplitude and width of the solitary structure at fixed κ , temperature ratio σ and the true Mach number M/M_s .

On the other hand, the effect of superthermality has a very significant role on the amplitude and width of the solitons. This effect is seen in Fig.4.2 (b), where the wave amplitude and width of the solitary structures are reduced with the decrease of κ . From this figure one can also observe that the amplitude of the electrostatic excitation decreases by about the same amount as κ is reduced from 20 to 6, and 6 to 4, but shows much larger drop as one goes from $\kappa = 4$ to 2. This implies that in the regime of very high superthermality (lower κ), the amplitude of the excitation is reduced considerably at fixed M/M_s , σ and α .

The dependence of the amplitude and width of a soliton on M/M_s and σ are shown in Fig. 4.2 (c) and Fig. 4.2 (d), respectively. It is seen that the wave amplitude (width) increases (shrinks) with the increase of true Mach number, whereas both the amplitude

and width are increased with the decrease of the temperature ratio σ .

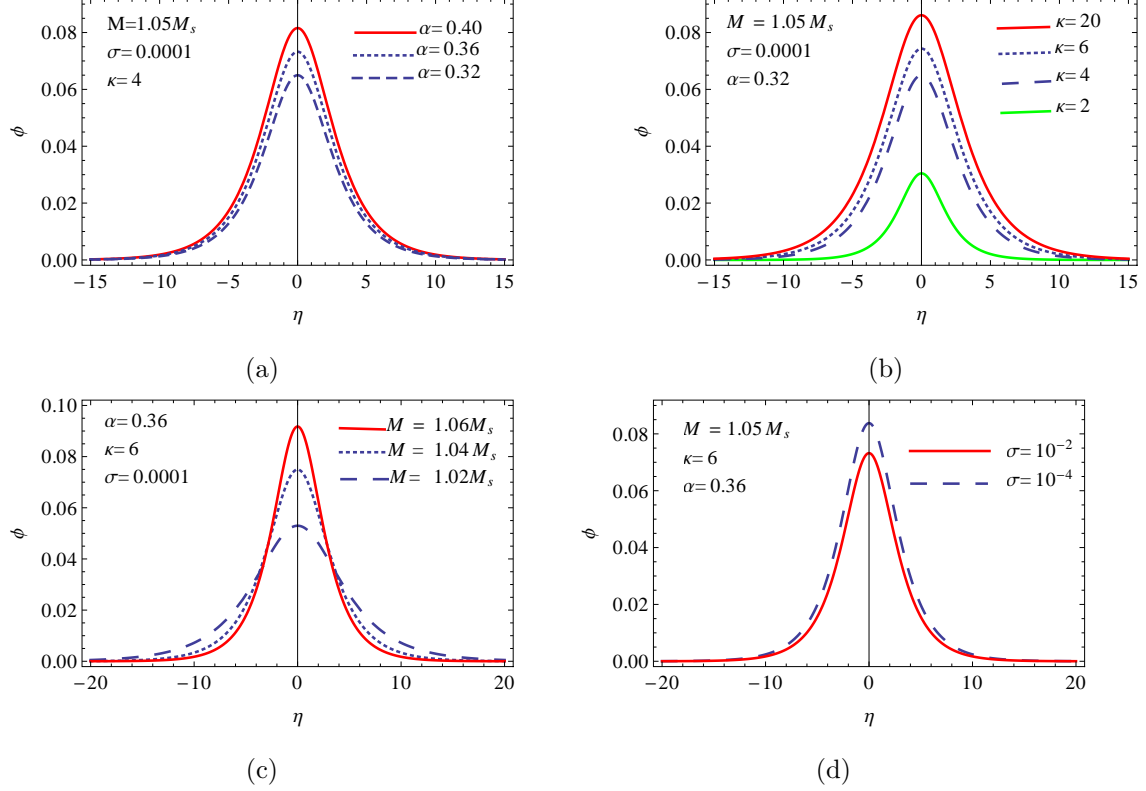


Figure 4.2: Figure shows the effect of variations of different plasma parameters on the width w and amplitude ϕ of the hump-like electrostatic potential excitation found from mKdV theory, using a fixed true Mach number, M/M_s .

In the above discussions we have considered fixed M/M_s (the true Mach number), that is, the normalized solitary wave speed measured with respect to the acoustic speed M_s , to study the effect of variations of different plasma parameters on the electrostatic excitation. Now, we will turn to the investigation of mKdV solitary wave excitation moving with the normalized speed M in a laboratory frame, as displayed in Fig. 4.3. From Fig. 4.3 (a) it can be seen that increasing the number density ratio α will result in the reduction of amplitude of the electrostatic excitation. This effect is in contrast to that observed in Fig. 4.2 (a), in which the amplitude was increasing with α .

The dependence of the mKdV electrostatic potential excitation on various values of the superthermal parameter κ is depicted in Fig. 4.3 (b). It is seen that for fixed M , σ and α , decreasing κ leads to the enhancement of the amplitude and reduction of the width of excitation, in contrast to that shown in Fig. 4.2 (b). However, this trend (increasing of amplitude with decreasing of κ) does not continue as one goes from $\kappa = 4$ to $\kappa = 2$. Rather, the amplitudes of the excitation for these two κ 's are close to equal as depicted in the dashed and green curves of Fig. 4.3 (b). Moreover, we have carried out calculations for $\kappa = 1.6$ as an academic exercise, and can confirm that the amplitude of the excitation

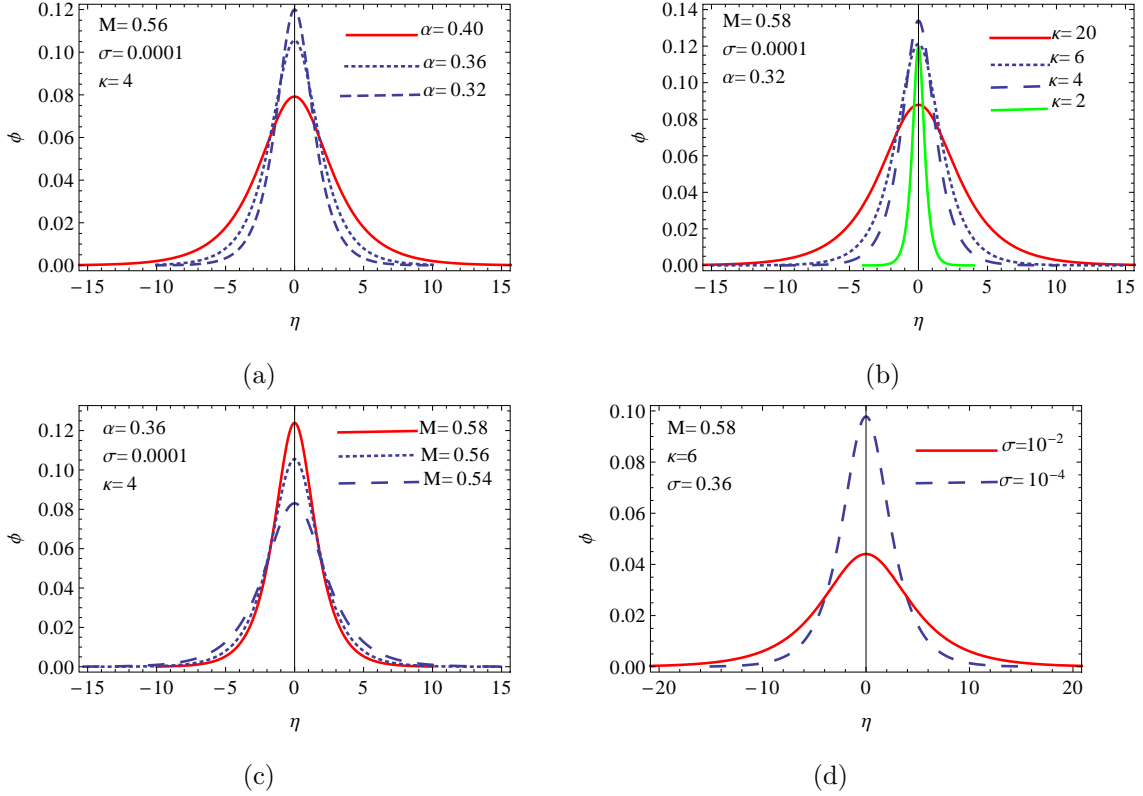


Figure 4.3: Figure shows the effect of variations of different plasma parameters on the width w and amplitude ϕ of the hump-like electrostatic potential excitation found from mKdV theory, using a fixed normalized soliton speed, M .

dropped by a significant amount. And, the width of the structure is diminishing as superthermality is increased (lower κ).

The effect of variation of normalized electrostatic potential excitation speed M and the temperature ratio σ on the amplitude of the excitation are displayed in Fig. 4.3 (c) and (d), respectively. From Fig. 4.3(c) it is seen that the amplitude of the excitation increases with the increase of M while its width shrinks. Similarly, the increasing of σ has a diminishing effect on the amplitude. These effects are consistent with the result shown in Eq. (4.8) that will be discussed in the next section.

4.2 Numerical results of the arbitrary amplitude analysis

In this section we will investigate numerically the properties and characteristics of arbitrary amplitude solitons using the Sagdeev pseudopotential, Eq. (3.94).

4.2.1 The existence domain of the soliton

Conditions for the existence of electrostatic solitary waves: The following conditions have to be satisfied for the occurrence of a solitary wave solution in Eqs. (3.93-94), (Sagdeev, 1966).

1. $\Psi(\phi = 0, M) = \frac{d\Psi(\phi, M)}{d\phi}|_{\phi=0} = 0$ (at the origin), the overall charge neutrality condition in an undisturbed state at $\eta \rightarrow \pm\infty$.
2. $\frac{d^2\Psi(\phi, M)}{d\phi^2}|_{\phi=0} < 0$, so that the fixed point is unstable at the origin (i.e. $\Psi(\phi, M)$ has maximum at the origin) and
3. $\Psi(\phi, M) < 0$ for $0 < |\phi| < |\phi_0|$; where ϕ_0 is the soliton amplitude.

The condition for the existence of a soliton can be found from the root of $\frac{d^2\Psi(\phi, M)}{d\phi^2}|_{\phi=0} < 0$ (condition 2 above) in terms of the pulse velocity M (Mach number), which is normalized with respect to the thermal speed v_{th} of the hot species. Taking the second derivative of Eq. (3.94) with respect to ϕ , the following equation will be obtained at $\phi = 0$,

$$f_l(M) = \frac{\alpha}{M^2 - 3\sigma} - \frac{\kappa - \frac{1}{2}}{\kappa - \frac{3}{2}} < 0. \quad (4.6)$$

The lower limit of M will be obtained by solving Eq. (4.6), to get

$$M > M_s = \left(\alpha \left[\frac{2\kappa - 3}{2\kappa - 1} \right] + 3\sigma \right)^{1/2}, \quad (4.7)$$

where M_s is the lower limit of the Mach number (acoustic speed). This is the same as the linear phase velocity, normalized to the hot component thermal velocity, found earlier in Eq. (2.75) in the limit that the wavelength is very large (small k), and $\alpha = N_c/N_h$. Furthermore, it follows from Eq. (4.7), that the soliton speed M is greater than the acoustic speed M_s for the existence of an electrostatic potential pulse in the model under investigation. This implies that only super-acoustic solitons can exist in the model. This is in agreement with the result obtained earlier from mKdV analysis in this chapter. For the Maxwellian plasma, i.e, $\kappa \rightarrow \infty$, we recover $M_s = (\alpha + 3\sigma)^{1/2}$, which was obtained by Verheest et al. (1996).

For Eqs. (3.88) and (3.89), it follows that the number densities of the cold electrons and positrons are only real if

$$Z_j 2\phi \leq (M - \sqrt{3\sigma})^2,$$

where $Z_j = +1$ for positrons and $Z_j = -1$ for electrons. Hence, the upper limit on the electrostatic excitation potential which depends on the cold to hot temperature ratio σ and the normalized speed M , will be

$$|\phi_{lm}| \leq \frac{(M - \sqrt{3\sigma})^2}{2} \quad (4.8)$$

where ϕ_{lm} is the critical value of the potential up to which the value of n_{jc} remains real, and beyond this value of the electrostatic potential pulse amplitude n_{jc} becomes complex. Further, from Eq. (4.8) it is seen that the maximum electrostatic potential ϕ_{lm} increases with an increase of the Mach number M and it decreases with σ . Evidence of this effect is seen in Fig. 4.3 (c) and Fig. 4.3 (d), respectively.

The upper limit Mach number M , can be found from the condition (3) above, that is $\Psi(\phi_{lm}) \leq 0$, where ϕ_{lm} is the maximum value of ϕ for which the cold species number

density remains real. It follows that, substituting Eq. (4.8) in place of ϕ in Eq. (3.94), one obtains that

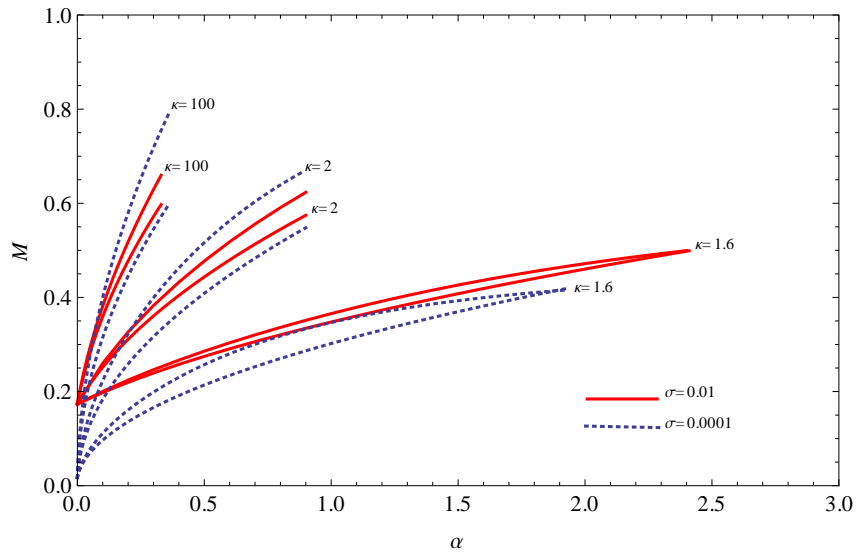
$$f_{ul}(M) = \frac{1}{1+\alpha} \left[2 - \left(1 + \frac{(M - \sqrt{3\sigma})^2}{3 - 2\kappa} \right)^{\frac{3}{2} - \kappa} - \left(1 + \frac{(M - \sqrt{3\sigma})^2}{2\kappa - 3} \right)^{\frac{3}{2} - \kappa} \right] + \frac{\alpha \left[-4 \times 3^{3/4} (M\sqrt{\sigma})^{\frac{3}{2}} + 6\sqrt{3\sigma} (M^2 + \sigma) - \sqrt{2} ((M^2 + 3\sigma)^{3/2} - (M^2 - \sqrt{3\sigma})^3) \right]}{3\sqrt{3\sigma}(1+\alpha)} \leq 0. \quad (4.9)$$

Solving Eq. (4.9) gives us the upper limit Mach number $M_{ul}(\alpha, \kappa, \sigma)$. It follows that the soliton existence domain is confined between the lower Mach number M_s (Eq. (4.7)) and the upper Mach number M_{ul} (Eq. (4.9)), that is, $M_s < M < M_{ul}$, for the selected set of parameter values of α , κ and σ , which satisfy the limit imposed by the model.

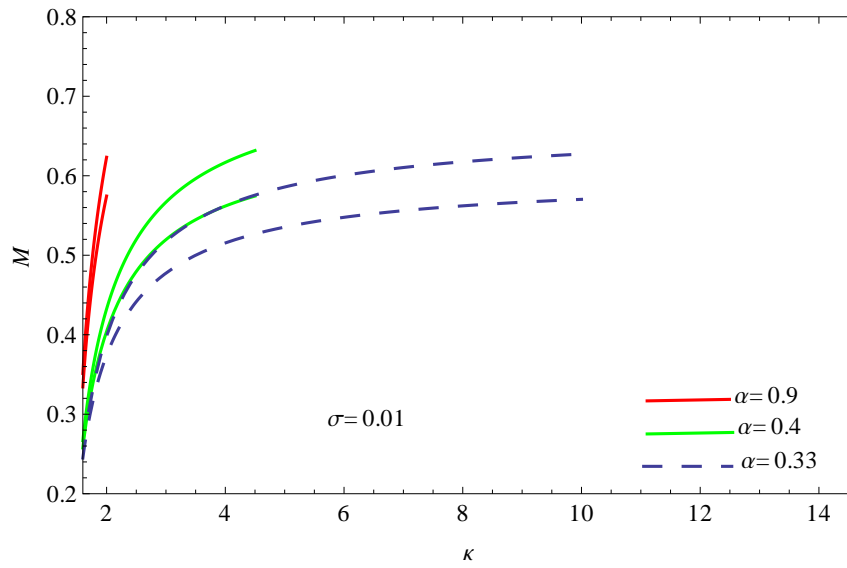
The Mach number domain $[M_s, M_{ul}]$ in which the soliton may exist can be depicted in Fig. 4.4. It shows the existence regions of solitons in the parameter spaces $[\alpha, M]$ and $[\kappa, M]$ at the fixed temperature ratio σ . In each case, the solitons exist in the regions that are bounded by the upper and lower curves of the same style/colour. Note that the lower and upper bounding curves were obtained from the analytically derived Eq. (4.7) and numerically solved Eq. (4.9), respectively, for various set of plasma parameters.

From the $[\alpha, M]$ plane in Fig. 4.4 (a) one can see that the region of existence, which is bounded by the lower and upper curves, has a cut-off at the critical value of α for a given superthermal parameter κ value. For example, at $\kappa = 1.6$ (very high superthermal-ity) it can be seen that solitons exist only in the narrow region bounded by the upper and lower red curves. The cut-off for this region occurs at the critical value of the normalized equilibrium number density ratio of hot to cold species $\alpha \approx 2.42$ ($N_c \approx 0.76$), where the upper and lower curves coincide with each other. This ratio provides an upper limit in α for the existence of a soliton at the chosen values of $\kappa = 1.6$ and $\sigma = 0.01$.

As confirmation, this effect is shown in Fig. 4.5. It can be seen that at the critical value



(a)



(b)

Figure 4.4: Figure shows the existence region of arbitrary amplitude solitons. The upper figure shows the soliton existence domain in the (α, M) space, whereas the lower figure shows the (κ, M) space. Solitons may exist between the lower and upper curves of the same style/color.

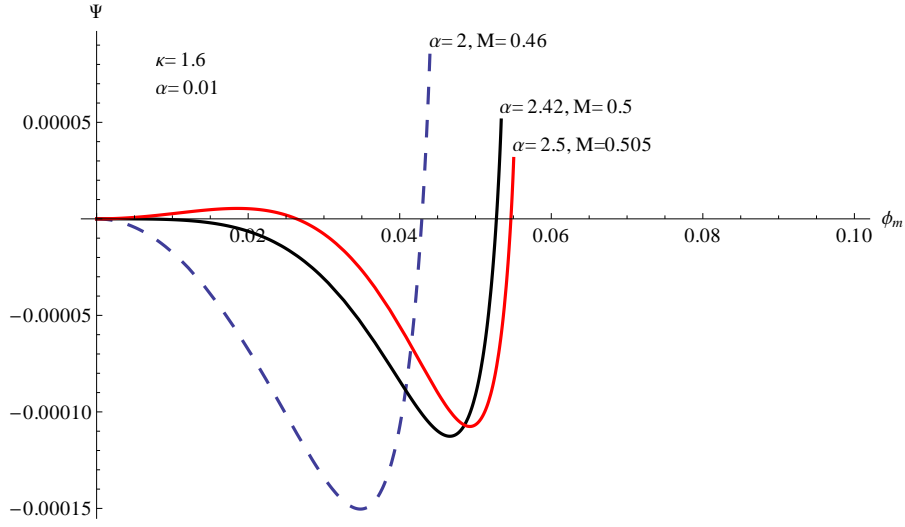


Figure 4.5: Sagdeev pseudopotential confirmation of the existence domain of solitary waves for chosen parametric values of plasma in accordance with our model.

of $\alpha \approx 2.42$, the Sagdeev pseudopotential has a solution, but when α increases slightly to 2.5 we can observe a small hump near the origin on the red curve of Fig. 4.5. This implies that the Sagdeev potential does not have a soliton solution for those particular values of α , κ , σ and M . In other words, it means that a soliton cannot exist for those particular values of the plasma parameters.

On the other hand, the range of α that supports solitons will be reduced when the temperature ratio is increased, as seen in the blue dotted curve of Fig. 4.4 (a). Moreover, from Fig. 4.4 (a) it is clearly seen that the soliton existence region bounded by the blue dotted curves is wider than that of the existence region bounded by the red curves for the same plasma parameter κ . This implies that increasing the temperature ratio will result in a wider region of existence and reduction of the range of number density ratio over which solitons are supported.

Interestingly, it shows that the high superthermality (low $\kappa = 1.6$) allows a higher number density of the cold component, $N_c = \frac{\alpha}{1+\alpha} \approx 0.76$ for $\alpha = 2.42$, to support the solitary

structure in the model. This value ($N_c \approx 0.76$) is well beyond the cut-off value of N_c (≈ 0.2) that was obtained by Verheest et al. (1996) during their investigation which assumed the hot species to be Maxwellian. Although the excess superthermality ($\kappa = 1.6$) permits more cold species to support solitons, it is seen that as the cold species density goes to zero (via $\alpha \rightarrow 0$), the existence region shrinks down to zero. This is because as the cold species tends to zero the model will break down and will not support solitary waves in the absence of the inertial cold species. Moreover, as shown in Fig. 4.4(a), at $\alpha \rightarrow 0$, the cut-off M_s is related to σ , giving lower cutoff in M if σ is smaller.

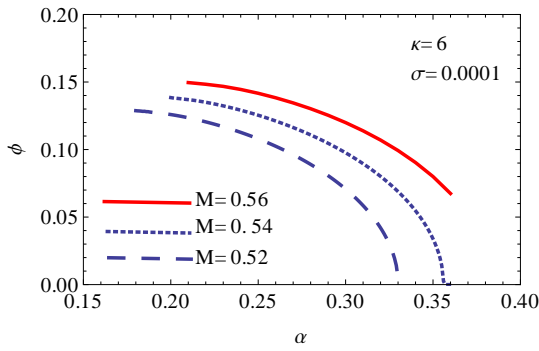
It is observed that the range of α that supports solitary waves decreases as one moves from high superthermality to the Maxwellian regime as depicted in Fig. 4.4(a). At fixed α , increasing κ yields an increase in the limits of both upper and lower curves. This means that the range of speeds of solitary waves increases when the superthermality decreases (increasing κ) at fixed equilibrium cold to hot species number density ratio α .

The soliton existence domain is displayed in Fig. 4.4(b) in $[\kappa, M]$ space. It is seen that the existence regions between different curves of the same style/color shrink down to zero when the superthermality parameter κ is approaching the critical value, $\kappa = 1.5$. It can also be observed that at fixed κ , the limits of both upper and lower curves increases when the α value increased. This implies that increasing the cold species relative to the hot one at fixed κ will result in increasing solitary wave speeds in the plasma model.

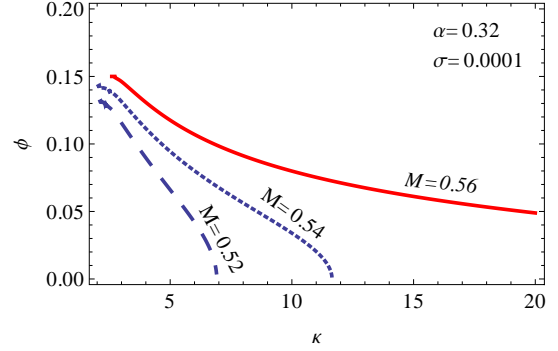
The solitary wave exists in a narrow region that is bounded by the lower and upper curves with cut-offs around $\kappa = 2$ for a chosen value of $\alpha = 0.9$. This means that when the equilibrium number density of the cold component is larger than to that of its hot counterpart (i.e., $\alpha > 1$), the plasma can only support solitary waves for very high superthermality (low κ) region, as shown by the red curves in Fig. 4.4 (b). On the other hand, when κ approaches the Maxwellian regime, that is, $\kappa \rightarrow \infty$, the existence regions becomes wider before the curves show marked flattening for the lower values of α as dis-

played in the dashed curves of Fig. 4.4 (b). Moreover, at fixed κ , increasing α yields larger values of M as seen in Fig. 4.4 (b).

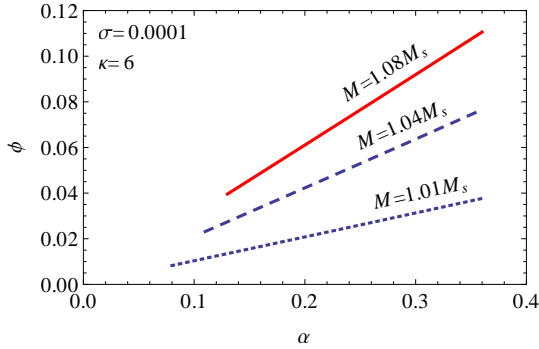
The dependence of the soliton amplitudes ϕ on α and κ for various values of soliton speed M and the true Mach number M/M_s is displayed in Fig. 4.6. From Fig. 4.6 (a)



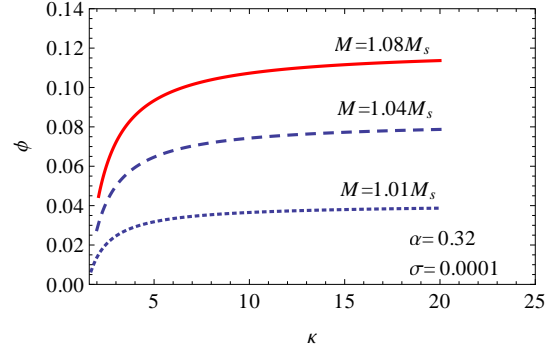
(a) The dependence of ϕ on α for various values of M at the fixed κ and σ .



(b) The dependence of ϕ on κ for various values of M at the fixed α and σ .



(c) The dependence of ϕ on α for various values of M/M_s at the fixed κ and σ .



(d) The dependence of ϕ on κ for various values of M/M_s at the fixed α and σ .

Figure 4.6: The dependence of amplitude on α and κ for various values of M and M/M_s .

it can be seen that at fixed Mach number M , κ and σ , the amplitude of the electrostatic potential pulse decreases as the number density ratio α is increased. It can also be seen that the ranges of α over which solitons can be found are fairly similar for each curve although the cut-offs in soliton amplitude occur at different values of α . Moreover, at fixed α the amplitude of the soliton increases with increasing Mach number M . For a given ampli-

tude, the solitons are seen to have increasing Mach number for increasing α . From this figure one can also see that there is a slight flattening of the curves at lower values of α before the cold species density cut-off has been reached.

In Fig. 4.6 (b) the dependence of soliton amplitude on the superthermal parameter κ is displayed for various M for fixed α and σ . It is seen that the amplitude of the soliton decreases as κ increases. That is, high superthermality (lower κ) enhances the amplitude of the soliton. For the larger values of M , the soliton exists over a wider range of κ (red curve on Fig. 4.6 (b)). Conversely, the range of κ over which the soliton will exist decreases with decreasing M (blue dashed curve on Fig. 4.6 (b)) at fixed α and σ . At constant κ the amplitude increases as the Mach number M increases. For a given amplitude of solitons, M increases with κ .

On the above discussion, the soliton speed M was scaled with respect to the hot species thermal speed v_{th} . Hence, the effects of κ , α and σ on the acoustic speed have not been taken into account. To correct that, we have also measured the normalized soliton speed M (Mach number) relative to the true acoustic speed M_s to see the effect of M/M_s (the true Mach number) on the solitary amplitude, following the ideas of Baluku and Hellberg (2011).

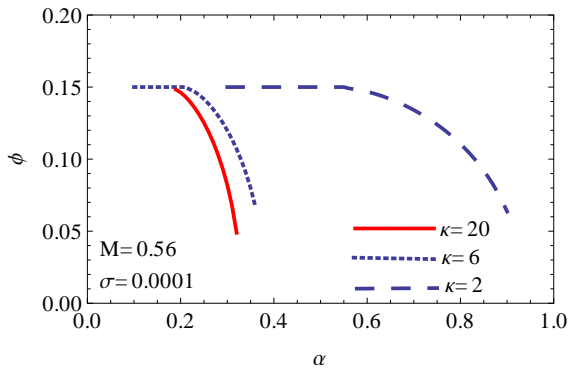
Using that idea, from Fig. 4.6 (c) one can see that the soliton amplitude increases monotonically with increasing number density ratio α for fixed true Mach number M/M_s and temperature ratio σ . This is the opposite effect to that observed in Fig. 4.6 (a). Moreover, from each of the curves it is seen that there are different cut-off points where solitons no longer exist for given parametric values of α at chosen values of M/M_s (Fig. 4.6 (c)). At fixed α , the amplitude of the soliton increases with increasing M/M_s . For given ϕ , the true Mach number decreases with the increasing of α . From Fig. 4.6 (c) it is also seen that solitons are found over a smaller range of α as the true Mach number is increased.

The dependence of ϕ on κ for a given true Mach number at fixed α and σ is displayed in Fig. 4.6 (d). It is shown that the amplitude increases with κ before the curves exhibit marked flattening. At fixed κ the amplitude increases with true Mach number. From the figure it is also observed that the increased superthermality (lower κ) reduces the amplitude of the soliton at fixed M/M_s and σ . This is contrary to the effect observed in Fig. 4.6 (b) in which the soliton amplitude was decreasing under these circumstances.

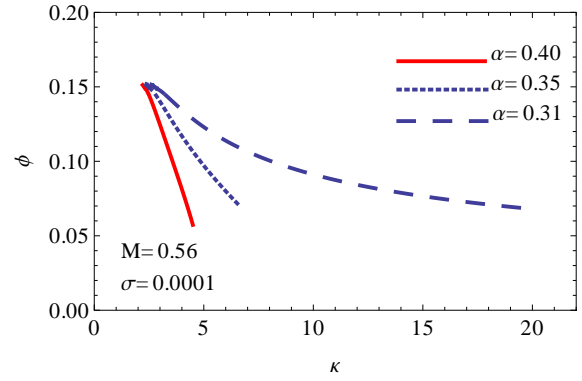
The effect of the variation of κ and α on the soliton amplitude ϕ at fixed Mach number and temperature ratio σ is displayed in Fig. 4.7. The upper panel of this figure shows the dependence of ϕ on α and κ at fixed Mach number M , while the lower panel displays the same parametric effects at the fixed true Mach number M/M_s . From Fig. 4.7 (a) one can see that the soliton amplitude has a constant value of about 0.15 for lower values of α for both $\kappa=2$ and 6. However, this amplitude does not remain constant throughout, but declines with increasing α until the cut-offs occur.

From Fig. 4.7 (a) it is also seen that the range of α over which solitons will be found decreases as κ goes to Maxwellian regime. On the other hand, it is again seen that solitons are supported over a wider range of α for lower κ (high superthermality) shown by the dashed curve of Fig. 4.7 (a). This is in agreement with limits imposed by the model as discussed earlier at the end of Chapter 2. The variation of ϕ with κ for various values of α at fixed M and σ is depicted in Fig. 4.7 (b). It is observed that the amplitude decreases with increasing κ for a given α . For larger α , soliton are supported over a shorter range of κ , whereas they may occur over a wider range of κ when α is smaller. Note that, each of the curves has a different cut-off because of the cold species number density cut-off.

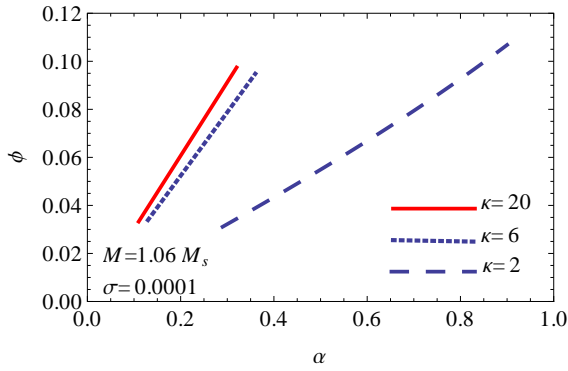
The variations of ϕ with α and κ , respectively, at the fixed true Mach number M/M_s and temperature ratio σ are depicted in Fig. 4.7 (c) and Fig. 4.7 (d). It is observed that the amplitudes of solitons increase sharply with α as shown in Fig. 4.7 (c), but solitons are supported over a wider range of α for higher superthermality as displayed in the dashed



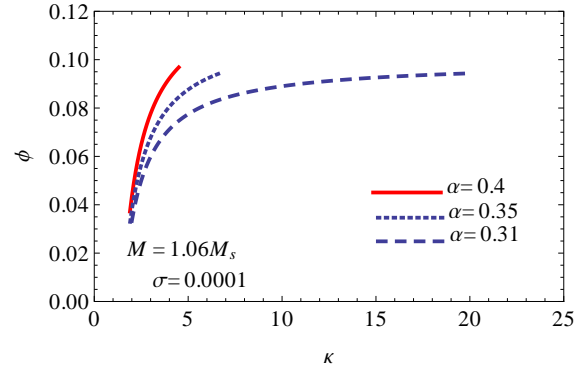
(a) Variation of solitary wave amplitude ϕ with α for various κ values at the fixed σ and M .



(b) Variation of solitary wave amplitude ϕ with κ for various α values at the fixed σ and M .



(c) Variation of solitary wave amplitude ϕ with α for various κ values at the fixed σ and M/M_s .

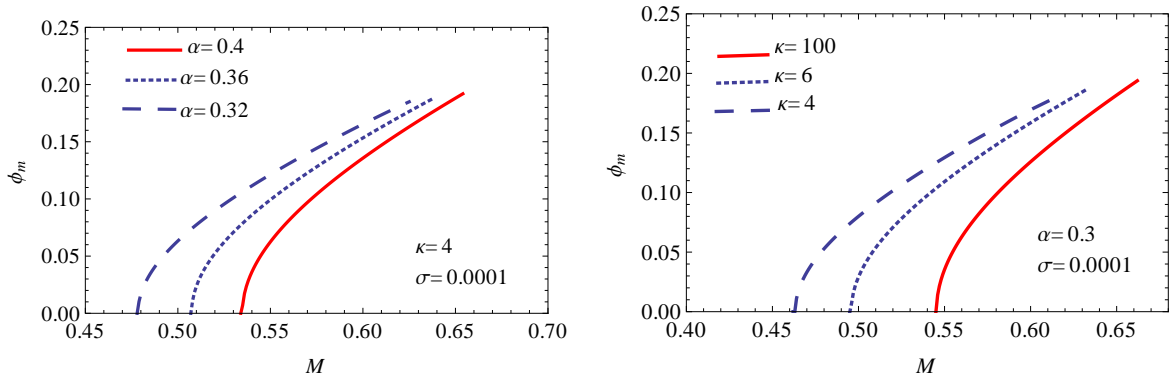


(d) Variation of solitary wave amplitude ϕ with κ for various α values at the fixed σ and M/M_s .

Figure 4.7: The dependence of the solitary wave amplitude ϕ on κ and α for fixed soliton speed, M (upper panels) and fixed Mach number, M/M_s (lower panels).

curve of Fig. 4.7 (c). On the other hand, it is seen that for larger κ solitons exist over a narrower range of α . From Fig. 4.7 (d) it is seen that the amplitudes of solitons increase initially with κ before the curves marked flattening as the α values are getting smaller. One can also observe that the range of κ over which solitons will be supported is reduced with increasing α , as discussed earlier.

Fig. 4.8 shows the dependence of the solitary wave amplitude ϕ on Mach number M for various values of the number density ratio α and superthermal parameter κ . Fig. 4.8 (a) displays the effect of variation of α on ϕ at fixed κ and temperature ratio σ . It shows that the solitary wave amplitude increases monotonically with the increase of M . However, the range of M that supports solitons is slightly reduced when α is larger. Similarly, the dependence of solitary wave amplitude on M for various values of κ is displayed in Fig. 4.8 (b). It is seen that the amplitude of the solitary wave increases when the superthermality effect increases at the fixed M . Moreover, from the dashed curve of Fig. 4.8 (b) it can be seen that solitons are supported over a range of M that is slightly wider as the κ value is getting smaller.

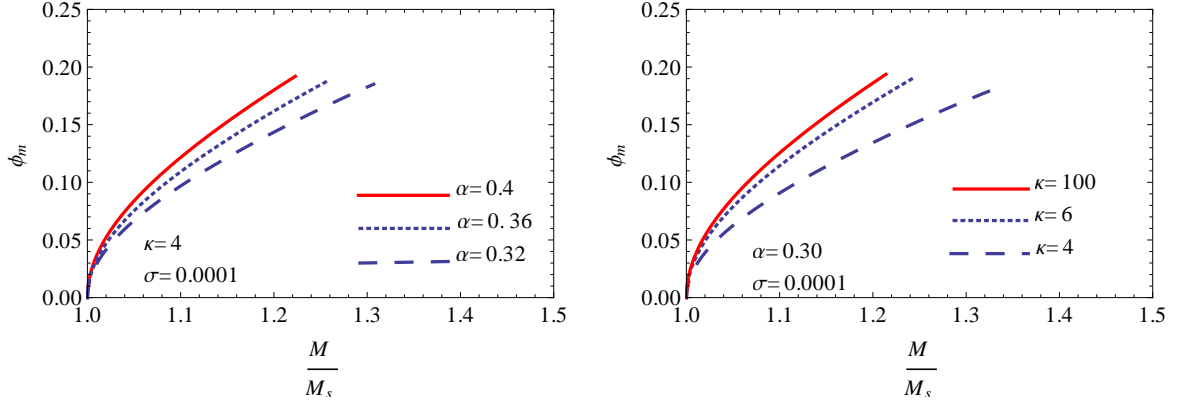


(a) The effect of variation in α on the amplitude ϕ_m of the soliton at fixed σ and κ .

(b) The effect of variation in κ on the amplitude ϕ_m of the soliton at fixed α and σ .

Figure 4.8: Figure shows the variation of ϕ_m with Mach number M for different values of α and κ .

The effect of the true Mach number M/M_s on the solitary amplitude ϕ_m is displayed in Fig. 4.9 for various values of α and κ . It is seen that the solitary wave amplitude is increasing monotonically with the increase of M/M_s before the cut-offs are reached for each of the curves. The amplitude increases slightly with the increase of α at the fixed value of M/M_s (Fig. 4.9 (a)). In the same fashion, the effect of variation of superther-



(a) The effect of variation in α on the amplitude ϕ_m of the soliton at fixed σ and κ .

(b) The effect of variation in κ on the amplitude ϕ_m of the soliton at fixed α and σ .

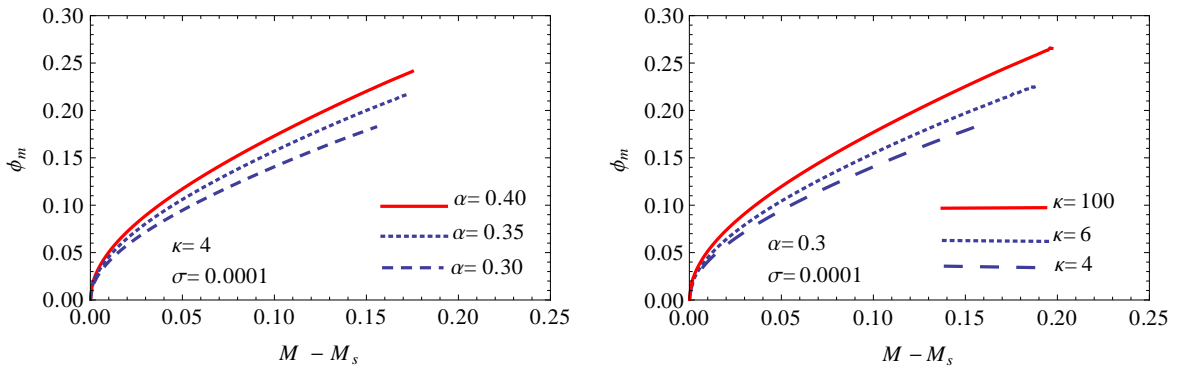
Figure 4.9: Figure shows the variation of the amplitude of soliton of the electrostatic potential ϕ_m with “true” Mach number $\frac{M}{M_s}$.

mality parameter κ on the solitary wave amplitude is seen in Fig. 4.9 (b). It is observed that the amplitude of the wave is decreasing with κ at the fixed M/M_s . However, solitons exist over the relatively wider range of M/M_s when the effect of superthermality increases (lower kappa).

The dependence of the soliton amplitude on δM (that is, $M - M_s$) is displayed in Fig. 4.10. The effect of variation in α on soliton amplitude ϕ at fixed κ and σ is shown in Fig. 4.10 (a). It can be seen that the range of δM over which the soliton can be found increases with α very slightly before the cut-off is reached. Moreover, the amplitude of the soliton increases with α at the fixed δM . As expected, at $M = M_s$ the amplitude of the soliton tends to zero. This result is in agreement with the mKdV analysis. So, it

confirmed that the solitons are superacoustic in our model and they vanish when $M = M_s$.

From Fig 4.10 (b) it can be seen that the amplitude of the soliton increases slightly with the increasing of κ at the fixed δM . The range of δM over which the soliton can be supported increases with κ .



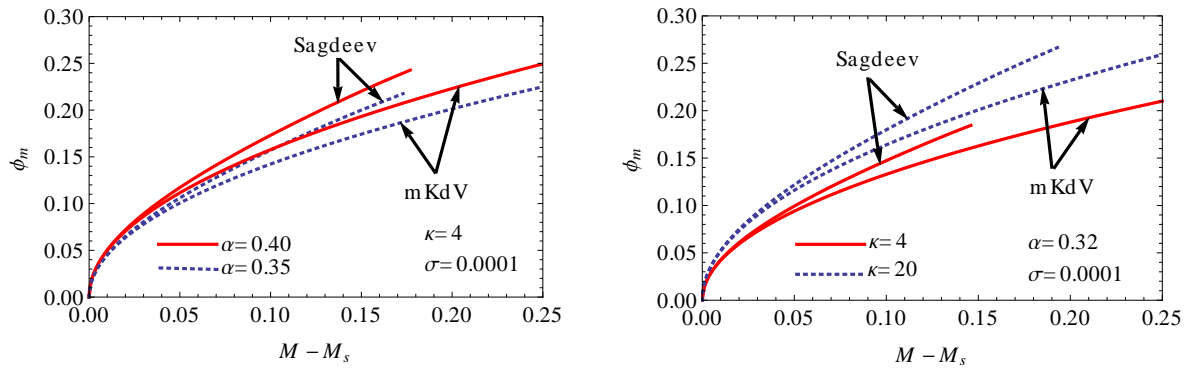
(a) The dependence of ϕ on $M - M_s$ at the fixed κ and σ for various α .

(b) The dependence of ϕ on $M - M_s$ at the fixed κ and σ for various α .

Figure 4.10: The variation of ϕ_m with $M - M_s$ for various values of α and κ .

4.2.2 Comparison between mKdV and arbitrary amplitude results

Fig. 4.11 shows the comparison between small amplitude (mKdV) analysis and an arbitrary amplitude (Sagdeev) soliton solution in $(M - M_s, \phi_m)$ space. Closer examination reveals that both mKdV and arbitrary amplitude solutions agreed for small ϕ_m , where the difference between the Mach number M (normalized solitary wave speed) and the acoustic speed M_s is small. This confirms that the mKdV theory is valid for smaller amplitudes and where the speed of solitary waves is closer to that of the acoustic speed. On the other hand, from Fig. 4.11 (b) it can be seen that increased superthermality (through lower κ) suppresses the amplitude of the solitary waves in both mKdV and Sagdeev solutions at the fixed δM ($M - M_s$). Most importantly, the mKdV theory does not incorporate cut-offs although it shows a good correlation with arbitrary amplitude theory at low soliton amplitudes and Mach numbers.



(a) Comparison between mKdV and Sagdeev theory for different α at the fixed κ and σ .

(b) Comparison between mKdV and Sagdeev theory for different κ at the fixed α and σ .

Figure 4.11: Comparison between the small amplitude and arbitrary amplitude results.

Chapter 5

Conclusion

5.1 Summary

In this thesis we have studied linear and nonlinear electrostatic waves in electron-positron plasmas consisting of hot electrons and positrons which were created by a primary plasma production process, and cool electrons and positrons which were created by a secondary plasma production process in the pulsar magnetosphere. The hot and cool species are found at the hot temperature T_h (number density N_h) and at the cool temperature T_c (number density N_c), respectively. The dynamics of cool species are governed by non-relativistic multi-fluid equations of motion, whereas those of the hot species are assumed to follow a kappa velocity distribution law. This is an extension of the work of Verheest et al. (1996) in that it considers the effects of excess superthermal particles in the hot species distributions, as opposed to the Maxwell-Boltzmann distribution used by them.

We initially investigated linear electrostatic waves in related simple plasma models. For each of these we have derived linear dispersion relations. First, we considered a simple electron-positron plasma model comprising of isothermal electrons and positrons. As expected, this model does not support waves. A plasma consisting of inertial cool electrons and positrons, both at temperature T_c , gave rise to a plasma-like wave for small k , but no

acoustic wave. Next we considered a plasma comprising of hot kappa electrons found at T_h and cool adiabatic positrons at T_c . Although an acoustic wave was found, this model is rejected, because of the asymmetry between the electrons and positrons, bearing in mind the symmetry of the pair creation mechanism. A three-component model, consisting of cold inertial electrons and positrons, together with a component of energetic kappa-distributed positrons at temperature T_h similarly lead to a linear dispersion relation of acoustic form, but, too, suffer from electron-positron asymmetry.

We finally investigated a plasma model that we are mainly concerned with in this thesis, consisting of hot electrons and positrons at T_h (number density N_h), and cool electrons and positrons at T_c (number density N_c). An acoustic wave was found, the dispersion relation being reminiscent of that of the electron-acoustic wave. Moreover, we have found that a non-Maxwellian plasma has a decreased phase velocity compared to that of a Maxwellian plasma as found by Verheest et al. (1996). On the other hand, as the hot species number density tends to zero, the plasma starts to support a plasma-like wave for smaller k . However, this analysis is not valid as the model assumption (i.e., $v_{tc} \ll v_\phi \ll v_{th}$) breaks down. We have set out restrictions of the model on the available range of the density ratio $\alpha = N_c/N_h$ and represented them graphically.

To study nonlinear solitary wave structures in our four-component symmetric electron-positron plasma model we have used two approaches. These are small and arbitrary amplitude analysis, using KdV and Sagdeev potential approaches, respectively. In the small amplitudes approach, the nonlinearity term in the KdV equation vanishes. To avoid such a scenario we have employed the mKdV approach which incorporates more nonlinearity terms in the reductive perturbation technique, and then found a standard soliton solution from the mKdV equation that governs small amplitude solitary waves.

To investigate arbitrary amplitude solitary wave structures in our model we have used the Sagdeev pseudopotential approach. In order to obtain an expression for the number

density of the cool components, that would be easily integrable analytically in finding the corresponding Sagdeev potential, we have used the Ghosh et al. (1996) approach. Using numerical analysis for the analytical results of Sagdeev potential, individual solitons were plotted to observe the effect of variations of different plasma parameters on the solitary wave amplitude.

Interestingly, it was found that high superthermality (lower kappa) permits solitary structures to be supported by plasmas with a larger cool species fraction than is the case for Maxwellian hot species, the range of N_c/N_h going well beyond the upper limit imposed by Verheest et al. (1996) for the Maxwellian hot species. In other words, solitons exist over a wider range of cool-to-hot species number density ratio α if the excess of superthermal particles is increased. Moreover, at fixed “Mach number” M , measured relative to an arbitrary normalizing speed, superthermality parameter κ and temperature ratio σ , it was found that the solitary wave amplitude decreases with increasing α . On the other hand, at fixed “true” Mach number M/M_s , κ and σ , the opposite was observed, that is, the amplitude of the structure increases with increasing α . Soliton amplitudes were observed to decrease as superthermality was decreased (by increasing κ) at fixed α and M . However, at fixed M/M_s low κ values yield larger amplitudes than found for higher kappa values and hence, Maxwellian hot species.

We also conducted a comparison between the mKdV and arbitrary amplitude calculations. We found that, as expected, the two theories agreed for lower amplitude and if the difference between the Mach number M and the acoustic speed M_s is small. Most importantly, the mKdV theory does not incorporate cut-offs although it shows a good correlation with arbitrary amplitude theory at low soliton amplitude and Mach numbers.

Appendix A

Derivation of KdV equation

The normalized basic equations governing the dynamics of the cool-components of the EP plasma will be given by

$$\frac{\partial n_{jc}}{\partial t} + \frac{\partial}{\partial t}(n_{jc}u_{jc}) = 0, \quad (\text{A.1})$$

$$\frac{\partial u_{jc}}{\partial t} + u_{jc} \frac{\partial u_{jc}}{\partial x} + 3\sigma \frac{n_{jc}}{N_c^2} \frac{\partial n_{jc}}{\partial x} = -z_j \frac{\partial \phi}{\partial x}. \quad (\text{A.2})$$

The hot component is governed by the kappa distribution law. For each of the hot species, the number density can take the form

$$n_{eh} = N_h \left[1 - \frac{\phi}{\kappa - \frac{3}{2}} \right]^{-\kappa+1/2} \quad (\text{A.3})$$

$$n_{ph} = N_h \left[1 + \frac{\phi}{\kappa - \frac{3}{2}} \right]^{-\kappa+1/2}. \quad (\text{A.4})$$

For small ϕ we can introduce a Taylor power series expansion to (A.3) and (A.4), giving

$$n_{eh} = N_h(1 + c_1\phi + c_2\phi^2 + c_3\phi^3 + \dots) \quad (\text{A.5})$$

$$n_{ph} = N_h(1 - c_1\phi + c_2\phi^2 - c_3\phi^3 + \dots), \quad (\text{A.6})$$

where c_1 , c_2 , and c_3 are defined in Eq. (2.37), Eq. (2.38) and Eq. (2.39), respectively.

The above set of equations are coupled by Poisson's equation:

$$\frac{\partial^2 \phi}{\partial x^2} = n_{eh} - n_{ph} + \sum_j -Z_j n_{jc} \quad (\text{A.7})$$

Using (A.5) and (A.6) into (A.7), Poisson's equation can take the form

$$\frac{\partial^2 \phi}{\partial x^2} = 2N_h c_1 \phi + 2N_h c_3 \phi^3 + \dots + \sum_j -Z_j n_{jc}. \quad (\text{A.8})$$

Coordinate stretching for KdV analysis

Following Verheest (1988) we can have the following coordinate stretching for KdV analysis:

$$\xi = \varepsilon^{1/2}(x - Vt), \quad \zeta = \varepsilon^{3/2}Vt, \quad (\text{A.9})$$

where ε , ξ and ζ are the parameters that measures the smallness of the non-linearity, space like and time-like quantities in the wave frame, respectively. Hence from (A.9), we have

$$\frac{\partial}{\partial x} = \varepsilon^{3/2} \frac{\partial}{\partial \xi} \quad (\text{A.10})$$

$$\frac{\partial}{\partial t} = -V\varepsilon^{1/2} \frac{\partial}{\partial \xi} + \varepsilon^{3/2} \frac{\partial}{\partial \zeta}. \quad (\text{A.11})$$

Reductive perturbation analysis

Now we can expand the dependent variables n_{jc} , u_{jc} and ϕ near their equilibrium values in a power series in ε as

$$n_{jc} = N_c + \varepsilon n_{jc1} + \varepsilon^2 n_{jc2} + \dots \quad (\text{A.12})$$

$$u_{jc} = \varepsilon u_{jc1} + \varepsilon^2 u_{jc2} + \dots \quad (\text{A.13})$$

$$\phi = \varepsilon \phi_1 + \varepsilon^2 \phi_2 + \dots \quad (\text{A.14})$$

Note that $\phi_o = u_{jco} = 0$ and $n_{jco} = N_c$ in the equilibrium state. So that, using (A.10) and (A.11) into (A.1), (A.2) and (A.8), we have

$$-\varepsilon^{1/2}V \frac{\partial n_{jc}}{\partial \xi} + \varepsilon^{3/2}V \frac{\partial n_{jc}}{\partial \zeta} + \varepsilon^{1/2} \frac{\partial(n_{jc}u_{jc})}{\partial \xi} = 0 \quad (\text{A.15})$$

$$-\varepsilon^{1/2}V \frac{\partial u_{jc}}{\partial \xi} + \varepsilon^{3/2}V \frac{\partial u_{jc}}{\partial \zeta} + u_{jc}\varepsilon^{1/2} \frac{\partial u_{jc}}{\partial \xi} + \frac{3\sigma}{N_c^2} \varepsilon^{1/2} n_{jc} \frac{\partial n_{jc}}{\partial \xi} = -Z_j \varepsilon^{1/2} \frac{\partial \phi}{\partial \xi} \quad (\text{A.16})$$

$$\varepsilon \frac{\partial^2 \phi}{\partial \xi^2} = 2N_h(c_1\phi + c_3\phi^3 + \dots) - \sum_j Z_j n_{jc}. \quad (\text{A.17})$$

Using (A.12), (A.13) and (A.14) into (A.15), (A.16) and (A.17), respectively, and after some algebra, the following set of equations will be obtained:

Continuity equation:

$$\begin{aligned} & -\varepsilon^{3/2}V \frac{\partial n_{jc1}}{\partial \xi} - \varepsilon^{5/2}V \frac{\partial n_{jc2}}{\partial \xi} + \dots + \varepsilon^{5/2}V \frac{\partial n_{jc1}}{\partial \zeta} + \varepsilon^{7/2}V \frac{\partial n_{jc2}}{\partial \zeta} + \dots + \varepsilon^{3/2}N_C \frac{\partial u_{jc1}}{\partial \xi} \\ & + \varepsilon^{5/2}N_C \frac{\partial u_{jc2}}{\partial \xi} + \dots + \varepsilon^{5/2}n_{jc1} \frac{\partial u_{jc1}}{\partial \xi} + \varepsilon^{7/2}n_{jc1} \frac{\partial u_{jc2}}{\partial \xi} + \dots + \varepsilon^{7/2}n_{jc2} \frac{\partial u_{jc1}}{\partial \xi} + \varepsilon^{9/2}n_{jc2} \frac{\partial u_{jc2}}{\partial \xi} \\ & + \dots + \varepsilon^{5/2}u_{jc1} \frac{\partial n_{jc1}}{\partial \xi} + \varepsilon^{7/2}u_{jc1} \frac{\partial n_{jc2}}{\partial \xi} + \dots + \varepsilon^{7/2}u_{jc2} \frac{\partial n_{jc1}}{\partial \xi} + \varepsilon^{9/2}u_{jc2} \frac{\partial n_{jc2}}{\partial \xi} + \dots = 0 \end{aligned} \quad (\text{A.18})$$

Momentum equation:

$$\begin{aligned} & -\varepsilon^{3/2}V \frac{\partial u_{jc1}}{\partial \xi} - \varepsilon^{5/2}V \frac{\partial u_{jc2}}{\partial \xi} + \dots + \varepsilon^{5/2}V \frac{\partial u_{jc1}}{\partial \zeta} + \varepsilon^{7/2}V \frac{\partial u_{jc2}}{\partial \zeta} + \dots + \varepsilon^{5/2}u_{jc1} \frac{\partial u_{jc1}}{\partial \xi} \\ & + \varepsilon^{7/2}u_{jc1} \frac{\partial u_{jc2}}{\partial \xi} + \dots + \varepsilon^{5/2}u_{jc2} \frac{\partial u_{jc1}}{\partial \xi} + \varepsilon^{9/2}u_{jc2} \frac{\partial u_{jc2}}{\partial \xi} + \dots \\ & + \frac{3T_C}{N_c} \varepsilon^{3/2} \frac{\partial n_{jc1}}{\partial \xi} + \frac{3\sigma}{N_c} \varepsilon^{5/2} \frac{\partial n_{jc2}}{\partial \xi} + \dots + \frac{3\sigma}{N_c^2} [\varepsilon^{5/2}n_{jc1} \frac{\partial n_{jc1}}{\partial \xi} + \varepsilon^{7/2}n_{jc1} \frac{\partial n_{jc2}}{\partial \xi} + \dots \\ & + \varepsilon^{7/2}n_{jc2} \frac{\partial n_{jc1}}{\partial \xi} + \varepsilon^{9/2}n_{jc2} \frac{\partial n_{jc2}}{\partial \xi} + \dots] = -Z_j \varepsilon^{3/2} \frac{\partial \phi_1}{\partial \xi} - Z_j \varepsilon^{5/2} \frac{\partial \phi_2}{\partial \xi} + \dots \end{aligned} \quad (\text{A.19})$$

Poisson's equation:

$$\begin{aligned} & \varepsilon^2 \frac{\partial^2 \phi_1}{\partial \xi^2} + \varepsilon^3 \frac{\partial^2 \phi_2}{\partial \xi^2} + \dots = 2N_h c_1 (\varepsilon \phi_1 + \varepsilon^2 \phi_2 + \dots) \\ & + 2N_h c_3 (\varepsilon^3 \phi_1^3 + 3\varepsilon^4 \phi_1^2 \phi_2 + 3\varepsilon^5 \phi_1 \phi_2^2 + \varepsilon^6 \phi_2^3 + \dots) - \sum_j Z_j (N_c + \varepsilon n_{jc1} + \varepsilon^2 n_{jc2} + \dots). \end{aligned} \quad (\text{A.20})$$

Setting the coefficients of like powers of ε equal to zero, the following set of differential equations are obtained:

Continuity equation (i.e., from (A.18))

$$O(\varepsilon^{3/2}) : \quad -V \frac{\partial n_{jc1}}{\partial \xi} + N_c \frac{\partial u_{jc1}}{\partial \xi} = 0 \quad (\text{A.21})$$

$$O(\varepsilon^{5/2}) : \quad -V \frac{\partial n_{jc2}}{\partial \xi} + V \frac{\partial n_{jc1}}{\partial \zeta} + N_c \frac{\partial u_{jc2}}{\partial \xi} + n_{jc1} \frac{\partial u_{jc1}}{\partial \xi} + u_{jc1} \frac{\partial n_{jc1}}{\partial \xi} = 0 \quad (\text{A.22})$$

Momentum equation (i.e., from (A.19))

$$O(\varepsilon^{3/2}) : \quad -V \frac{\partial u_{jc1}}{\partial \xi} + \frac{3\sigma}{N_c} \frac{\partial n_{jc1}}{\partial \xi} = -Z_j \frac{\partial \phi_1}{\partial \xi} \quad (\text{A.23})$$

$$O(\varepsilon^{5/2}) : \quad -V \frac{\partial u_{jc2}}{\partial \xi} + V \frac{\partial u_{jc1}}{\partial \zeta} + u_{jc1} \frac{\partial u_{jc1}}{\partial \zeta} + \frac{3\sigma}{N_c} \frac{\partial n_{jc2}}{\partial \xi} + \frac{3\sigma}{N_c^2} n_{jc1} \frac{\partial n_{jc1}}{\partial \xi} = -Z_j \frac{\partial \phi_2}{\partial \xi} \quad (\text{A.24})$$

Poisson's equation (i.e., from (A.20))

$$O(\varepsilon^0) : \quad \sum_j Z_j N_c = 0 \quad (\text{A.25})$$

$$O(\varepsilon^1) : \quad 2N_h c_1 \phi_1 - \sum_j Z_j n_{jc1} = 0 \quad (\text{A.26})$$

$$O(\varepsilon^2) : \quad \frac{\partial^2 \phi_1}{\partial \xi^2} = 2N_h c_1 \phi_2 - \sum_j Z_j n_{jc2}. \quad (\text{A.27})$$

After integration, (A.21) takes the form

$$n_{jc1} = \frac{N_c}{V} u_{jc1} \implies u_{jc1} = \frac{V}{N_c} n_{jc1}. \quad (\text{A.28})$$

Integrating (A.23), gives

$$-V u_{jc1} + \frac{3\sigma}{N_c} n_{jc1} = -Z_j \phi_1. \quad (\text{A.29})$$

Substituting (A.28) in (A.29), we get

$$n_{jc1} = \frac{Z_j N_c}{V^2 - 3\sigma} \phi_1 \quad (\text{A.30})$$

$$u_{jc1} = \frac{Z_j V}{V^2 - 3\sigma} \phi_1. \quad (\text{A.31})$$

Using (A.30) in (A.26), we have

$$\left(2N_h c_1 - \sum_j \frac{Z_j^2 N_c}{V^2 - 3\sigma} \right) \phi_1 = 0. \quad (\text{A.32})$$

Since $\phi_1 \neq 0$, it follows that its coefficient is equal to zero. Hence,

$$2N_h c_1 - \sum_j \frac{Z_j^2 N_c}{V^2 - 3\sigma} = 0, \quad (\text{A.33})$$

which implies that

$$V^2 = \frac{N_c}{N_h c_1} + 3\sigma. \quad (\text{A.34})$$

In terms of the superthermal parameter κ , (A.24) can be written as

$$V^2 = \left(\frac{2\kappa - 3}{2\kappa - 1} \right) \frac{N_c}{N_h} + 3\sigma. \quad (\text{A.35})$$

By re-arranging (A.22), we obtain

$$N_c \frac{\partial u_{jc2}}{\partial \xi} = V \frac{\partial n_{jc2}}{\partial \xi} - V \frac{\partial n_{jc1}}{\partial \zeta} - \frac{\partial(u_{jc1} n_{jc1})}{\partial \xi}. \quad (\text{A.36})$$

Multiplying both sides of (A.24) with N_c , we have

$$-V N_c \frac{\partial u_{jc2}}{\partial \xi} + N_c V \frac{\partial u_{jc1}}{\partial \zeta} + N_c u_{jc1} \frac{\partial u_{jc1}}{\partial \zeta} + 3\sigma \frac{\partial n_{jc2}}{\partial \xi} + \frac{3T\sigma}{N_c} n_{jc1} \frac{\partial n_{jc1}}{\partial \xi} = -Z_j N_c \frac{\partial \phi_2}{\partial \xi}. \quad (\text{A.37})$$

Using (A.36) in (A.37), gives

$$(V^2 - 3\sigma) \frac{\partial n_{jc2}}{\partial \xi} = N_c V \frac{\partial u_{jc1}}{\partial \zeta} + V^2 \frac{\partial n_{jc1}}{\partial \zeta} + V \frac{\partial(n_{jc1} u_{jc1})}{\partial \zeta} + N_c u_{jc1} \frac{\partial u_{jc1}}{\partial \xi} + \frac{3\sigma}{N_c} n_{jc1} \frac{\partial n_{jc1}}{\partial \xi} + Z_j N_c \frac{\partial \phi_2}{\partial \xi}. \quad (\text{A.38})$$

Applying (A.30) and (A.31) into (A.38), we obtain

$$\frac{\partial n_{jc2}}{\partial \xi} = \frac{2Z_j N_c V^2}{(V^2 - 3\sigma)^2} \frac{\partial \phi_1}{\partial \zeta} + \frac{3Z_j^2 N_c (V^2 + \sigma)}{(V^2 - 3\sigma)^3} \phi_1 \frac{\partial \phi_1}{\partial \xi} + \frac{Z_j N_c}{(V^2 - 3\sigma)} \frac{\partial \phi_2}{\partial \zeta}. \quad (\text{A.39})$$

By taking the derivative of (A.27) with respect to ξ one will have

$$\sum_j Z_j \frac{\partial n_{jc2}}{\partial \xi} = 2N_h c_1 \frac{\partial \phi_2}{\partial \xi} - \frac{\partial^3 \phi_1}{\partial \xi^3}. \quad (\text{A.40})$$

Multiplying both sides of (A.39) by $\sum_j Z_j$, we have

$$\sum_j Z_j \frac{\partial n_{jc2}}{\partial \xi} = 2 \sum_j \frac{Z_j^2 N_c V^2}{(V^2 - 3\sigma)^2} \frac{\partial \phi_1}{\partial \zeta} + 3 \sum_j \frac{Z_j^3 N_c (V^2 + \sigma)}{(V^2 - 3\sigma)^3} \phi_1 \frac{\partial \phi_1}{\partial \xi} + \sum_j \frac{Z_j^2 N_c}{(V^2 - 3\sigma)} \frac{\partial \phi_2}{\partial \zeta}. \quad (\text{A.41})$$

Comparison between (A.40) and (A.41) gives us

$$\frac{\partial^3 \phi_1}{\partial \xi^3} = \left[2N_h c_1 - \sum_j \frac{Z_j^2 N_c}{V^2 - 3\sigma} \right] \frac{\partial \phi_2}{\partial \xi} - \left[2 \sum_j \frac{Z_j^2 N_c V^2}{(V^2 - 3\sigma)^2} \right] \frac{\partial \phi_1}{\partial \zeta} - \left[3 \sum_j \frac{Z_j^3 N_c (V^2 + \sigma)}{(V^2 - 3\sigma)^3} \right] \phi_1 \frac{\partial \phi_1}{\partial \xi}. \quad (\text{A.42})$$

From (A.33) we already know that the coefficient of $\frac{\partial\phi_2}{\partial\xi}$ in (A.42) is zero. Therefore, (A.42) finally takes a KdV form as

$$\boxed{\frac{\partial\phi_1}{\partial\zeta} + A\phi_1\frac{\partial\phi_1}{\partial\xi} + B\frac{\partial^3\phi_1}{\partial\xi^3} = 0}. \quad (\text{A.43})$$

Here

$$A = \frac{3\sum_j Z_j^3 N_c (V^2 + \sigma)}{2\sum_j Z_j^2 N_c V^2} \quad \text{and} \quad B = \frac{1}{2\frac{\sum_j Z_j^2 N_c V^2}{(V^2 - 3\sigma)^2}}. \quad (\text{A.44})$$

However, in general,

$$\sum_j Z_j^n = \begin{cases} 2 & \text{if } n=\text{even} \\ 0 & \text{if } n=\text{odd} \end{cases} \quad (\text{A.45})$$

With this property, the coefficient of the nonlinear term $\phi_1\frac{\partial\phi_1}{\partial\xi}$, that is, $A = 0$, in (A.43). Therefore, Eq. (A.43) becomes

$$\frac{\partial\phi_1}{\partial\zeta} + B\frac{\partial^3\phi_1}{\partial\xi^3} = 0, \quad (\text{A.46})$$

and is not a KdV equation.

Appendix B

Derivation of mKdV equation

The dynamics of the cold components of EP plasma are governed by the fluid equations (normalized continuity and momentum equations):

Normalized continuity equation

$$\frac{\partial n_{jc}}{\partial t} + \frac{\partial(n_{jc}u_{jc})}{\partial t} = 0, \quad (\text{B.1})$$

Normalized momentum equation

$$\frac{\partial u_{jc}}{\partial t} + u_{jc} \frac{\partial u_{jc}}{\partial x} + 3\sigma \frac{n_{jc}}{N_c^2} \frac{\partial n_{jc}}{\partial x} = -z_j \frac{\partial \phi}{\partial x}. \quad (\text{B.2})$$

The hot component is governed by the kappa distribution law. For each of the hot species, the number density can take the form (normalized)

$$n_{eh} = N_h \left[1 - \frac{\phi}{\kappa - \frac{3}{2}} \right]^{-\kappa+1/2}$$

$$n_{ph} = N_h \left[1 + \frac{\phi}{\kappa - \frac{3}{2}} \right]^{-\kappa+1/2}.$$

For small ϕ these equations can be expanded using a Taylor power series law to get

$$n_{eh} = N_h(1 + c_1\phi + c_2\phi^2 + c_3\phi^3 + \dots) \quad (\text{B.3})$$

$$n_{ph} = N_h(1 - c_1\phi + c_2\phi^2 - c_3\phi^3 + \dots). \quad (\text{B.4})$$

These equations are coupled by Poisson's equation

$$\frac{\partial^2 \phi}{\partial x^2} = n_{eh} - n_{ph} + \sum_j -Z_j n_{jc}. \quad (\text{B.5})$$

Substituting (B.3) and (B.4) into (B.5), gives

$$\frac{\partial^2 \phi}{\partial x^2} = 2N_h(c_1 \phi + c_3 \phi^3 + \dots) + \sum_j -Z_j n_{jc}. \quad (\text{B.6})$$

Coordinate stretching for mKdV analysis

In order to allow for the higher degree of symmetry, we thus need to consider the modified Korteweg de Vries equation (Watanabe, 1984) with a different stretching to obtain quadratic and cubic nonlinear terms on an equal footing. Following the approach of Verheest (1988), we thus have the following stretched coordinates

$$\xi = \varepsilon(x - Vt) \quad \text{and} \quad \zeta = \varepsilon^3 Vt \quad .$$

From this stretching, we have

$$\frac{\partial}{\partial x} = \varepsilon \frac{\partial}{\partial \xi} \quad \text{and} \quad \frac{\partial}{\partial t} = -\varepsilon V \frac{\partial}{\partial \xi} + \varepsilon^3 V \frac{\partial}{\partial \tau}. \quad (\text{B.7})$$

Reductive perturbation

Expanding the dependent variables n_{jc} , u_{jc} and ϕ near their equilibrium values in a power series in ε gives

$$n_{jc} = N_c + \varepsilon n_{jc1} + \varepsilon^2 n_{jc2} + \varepsilon^3 n_{jc3} + \dots \quad (\text{B.8})$$

$$u_{jc} = \varepsilon u_{jc1} + \varepsilon^2 u_{jc2} + \varepsilon^3 u_{jc3} \dots \quad (\text{B.9})$$

$$\phi = \varepsilon \phi_1 + \varepsilon^2 \phi_2 + \varepsilon^3 \phi_3 \dots \quad (\text{B.10})$$

Using (B.7) into (B.1), (B.2) and (B.6) we will have the following set of equations in terms of stretched coordinates:

Continuity equation

$$-\varepsilon V \frac{\partial n_{jc}}{\partial \xi} + \varepsilon^3 V \frac{\partial n_{jc}}{\partial \zeta} + u_{jc} \varepsilon \frac{\partial n_{jc}}{\partial \xi} + n_{jc} \varepsilon \frac{\partial u_{jc}}{\partial \xi} = 0 \quad (\text{B.11})$$

Momentum equation

$$-\varepsilon V \frac{\partial u_{jc}}{\partial \xi} + \varepsilon^3 V \frac{\partial u_{jc}}{\partial \zeta} + u_{jc} \varepsilon \frac{\partial u_{jc}}{\partial \xi} + \frac{3\sigma}{N_c^2} \varepsilon n_{jc} \frac{\partial n_{jc}}{\partial \xi} = -Z_j \varepsilon \frac{\partial \phi}{\partial \xi} \quad (\text{B.12})$$

Poisson's equation

$$\varepsilon^3 \frac{\partial^2 \phi}{\partial \xi^2} = 2N_h (c_1 \phi + c_3 \phi^3 + \dots) + \sum_j -Z_j n_{jc}. \quad (\text{B.13})$$

Using (B.8), (B.9) and (B.10) into (B.11), (B.12) and (B.13), respectively, we will have the following set of equations in terms of perturbed plasma parameters :

continuity equation

$$\begin{aligned} & -\varepsilon^2 V \frac{\partial n_{jc1}}{\partial \xi} - \varepsilon^3 V \frac{\partial n_{jc2}}{\partial \xi} - \varepsilon^4 \frac{\partial n_{jc3}}{\partial \xi} + \dots + \varepsilon^4 V \frac{\partial n_{jc1}}{\partial \zeta} + \varepsilon^5 V \frac{\partial n_{jc2}}{\partial \zeta} + \varepsilon^6 V \frac{\partial n_{jc3}}{\partial \zeta} + \dots + \varepsilon^3 u_{jc1} \frac{\partial n_{jc1}}{\partial \xi} \\ & + \varepsilon^4 u_{jc1} \frac{\partial n_{jc2}}{\partial \xi} + \varepsilon^5 u_{jc1} \frac{\partial n_{jc3}}{\partial \xi} + \dots + \varepsilon^4 u_{jc2} \frac{\partial n_{jc1}}{\partial \xi} + \varepsilon^5 u_{jc2} \frac{\partial n_{jc2}}{\partial \xi} + \varepsilon^6 u_{jc2} \frac{\partial n_{jc3}}{\partial \xi} + \dots \\ & + \varepsilon^5 u_{jc3} \frac{\partial n_{jc1}}{\partial \xi} + \varepsilon^6 u_{jc3} \frac{\partial n_{jc2}}{\partial \xi} + \varepsilon^7 u_{jc3} \frac{\partial n_{jc3}}{\partial \xi} + \dots + \varepsilon^2 N_c \frac{\partial u_{jc1}}{\partial \xi} + \varepsilon^3 N_c \frac{\partial u_{jc2}}{\partial \xi} + \varepsilon^4 N_c \frac{\partial u_{jc3}}{\partial \xi} + \dots \\ & + \varepsilon^3 n_{jc1} \frac{\partial u_{jc1}}{\partial \xi} + \varepsilon^4 n_{jc1} \frac{\partial u_{jc2}}{\partial \xi} + \varepsilon^5 n_{jc1} \frac{\partial u_{jc3}}{\partial \xi} + \dots + \varepsilon^4 n_{jc2} \frac{\partial u_{jc1}}{\partial \xi} + \varepsilon^5 n_{jc2} \frac{\partial u_{jc2}}{\partial \xi} + \varepsilon^6 n_{jc2} \frac{\partial u_{jc3}}{\partial \xi} + \dots \\ & + \varepsilon^5 n_{jc3} \frac{\partial u_{jc1}}{\partial \xi} + \varepsilon^6 n_{jc3} \frac{\partial u_{jc2}}{\partial \xi} + \varepsilon^7 n_{jc3} \frac{\partial u_{jc3}}{\partial \xi} + \dots = 0 \quad (\text{B.14}) \end{aligned}$$

momentum equation

$$\begin{aligned} & -\varepsilon^2 V \frac{\partial u_{jc1}}{\partial \xi} - \varepsilon^3 V \frac{\partial u_{jc2}}{\partial \xi} - \varepsilon^4 \frac{\partial u_{jc3}}{\partial \xi} + \dots + \varepsilon^4 V \frac{\partial u_{jc1}}{\partial \zeta} + \varepsilon^5 V \frac{\partial u_{jc2}}{\partial \zeta} + \varepsilon^6 V \frac{\partial u_{jc3}}{\partial \zeta} + \dots \\ & + \varepsilon^3 u_{jc1} \frac{\partial u_{jc1}}{\partial \xi} + \varepsilon^4 u_{jc1} \frac{\partial u_{jc2}}{\partial \xi} + \varepsilon^5 u_{jc1} \frac{\partial u_{jc3}}{\partial \xi} + \dots + \varepsilon^4 u_{jc2} \frac{\partial u_{jc1}}{\partial \xi} + \varepsilon^5 u_{jc2} \frac{\partial u_{jc2}}{\partial \xi} \\ & + \varepsilon^6 u_{jc2} \frac{\partial u_{jc3}}{\partial \xi} + \dots + \varepsilon^5 u_{jc3} \frac{\partial u_{jc1}}{\partial \xi} + \varepsilon^6 u_{jc3} \frac{\partial u_{jc2}}{\partial \xi} + \varepsilon^7 u_{jc3} \frac{\partial u_{jc3}}{\partial \xi} + \dots \\ & + \frac{3\sigma}{N_c} \left[\varepsilon^2 \frac{\partial n_{jc1}}{\partial \xi} + \varepsilon^3 \frac{\partial n_{jc2}}{\partial \xi} + \varepsilon^4 \frac{\partial n_{jc3}}{\partial \xi} + \dots \right] + \frac{3\sigma}{N_c^2} \left[\varepsilon^3 n_{jc1} \frac{\partial n_{jc1}}{\partial \xi} + \varepsilon^4 n_{jc1} \frac{\partial n_{jc2}}{\partial \xi} \right. \\ & + \varepsilon^5 n_{jc1} \frac{\partial n_{jc3}}{\partial \xi} + \dots + \varepsilon^4 n_{jc2} \frac{\partial n_{jc1}}{\partial \xi} + \varepsilon^5 n_{jc2} \frac{\partial n_{jc2}}{\partial \xi} + \varepsilon^6 n_{jc2} \frac{\partial n_{jc3}}{\partial \xi} + \dots \\ & \left. + \varepsilon^5 n_{jc3} \frac{\partial n_{jc1}}{\partial \xi} + \varepsilon^6 n_{jc3} \frac{\partial n_{jc2}}{\partial \xi} + \varepsilon^6 n_{jc3} \frac{\partial n_{jc3}}{\partial \xi} + \dots \right] = -Z_j \varepsilon^2 \frac{\partial \phi_1}{\partial \xi} - Z_j \varepsilon^3 \frac{\partial \phi_2}{\partial \xi} - Z_j \varepsilon^4 \frac{\partial \phi_3}{\partial \xi} + \dots \quad (\text{B.15}) \end{aligned}$$

Poisson's equation

$$\begin{aligned}
\varepsilon^3 \frac{\partial^2 \phi_1}{\partial \xi^2} + \varepsilon^4 \frac{\partial^2 \phi_2}{\partial \xi^2} + \varepsilon^5 \frac{\partial^2 \phi_3}{\partial \xi^2} + \dots &= 2N_h c_1 (\varepsilon \phi_1 + \varepsilon^2 \phi_2 + \varepsilon^3 \phi_3 + \dots) \\
&+ 2N_h c_3 [\varepsilon^3 \phi_1^3 + 3\varepsilon^4 \phi_1^2 \phi_2 + 3\varepsilon^5 \phi_1^2 \phi_3 + 3\varepsilon^5 \phi_1 \phi_2^2 + 6\varepsilon^6 \phi_1 \phi_2 \phi_3 \\
&+ \varepsilon^6 \phi_2^3 + 3\varepsilon^7 \phi_1 \phi_3^2 + 3\varepsilon^7 \phi_2^2 \phi_3 + 3\varepsilon^8 \phi_2 \phi_3^2 + \varepsilon^9 \phi_3^3 + \dots] \\
&+ \sum_j (-Z_j) [N_c + \varepsilon n_{jc1} + \varepsilon^2 n_{jc2} + \varepsilon^3 n_{jc3} + \dots]. \quad (\text{B.16})
\end{aligned}$$

Rearranging the terms order by order in ε the following set of equations are obtained from:

continuity (i.e., from (B.14))

$$O(\varepsilon^2) : \quad -V \frac{\partial n_{jc1}}{\partial \xi} + N_c \frac{\partial u_{jc1}}{\partial \xi} = 0 \quad (\text{B.17})$$

$$O(\varepsilon^3) : \quad -V \frac{\partial n_{jc2}}{\partial \xi} + u_{jc1} \frac{\partial n_{jc1}}{\partial \xi} + N_c \frac{\partial u_{jc2}}{\partial \xi} + n_{jc1} \frac{\partial u_{jc1}}{\partial \xi} = 0 \quad (\text{B.18})$$

$$O(\varepsilon^4) : \quad V \frac{\partial n_{jc2}}{\partial \xi} - V \frac{\partial n_{jc3}}{\partial \xi} + u_{jc1} \frac{\partial n_{jc2}}{\partial \xi} + u_{jc2} \frac{\partial n_{jc1}}{\partial \xi} + N_c \frac{\partial u_{jc3}}{\partial \xi} + n_{jc1} \frac{\partial u_{jc2}}{\partial \xi} + n_{jc2} \frac{\partial u_{jc1}}{\partial \xi} = 0 \quad (\text{B.19})$$

momentum (i.e., from (B.15))

$$O(\varepsilon^2) : \quad -V \frac{\partial u_{jc1}}{\partial \xi} + \frac{3\sigma}{N_c} \frac{\partial n_{jc1}}{\partial \xi} = -Z_j \frac{\partial \phi_1}{\partial \xi} \quad (\text{B.20})$$

$$O(\varepsilon^3) : \quad -V \frac{\partial u_{jc2}}{\partial \xi} + u_{jc1} \frac{\partial u_{jc1}}{\partial \xi} + \frac{3\sigma}{N_c} \frac{\partial n_{jc2}}{\partial \xi} + \frac{3\sigma}{N_c^2} n_{jc1} \frac{\partial n_{jc1}}{\partial \xi} = -Z_j \frac{\partial \phi_2}{\partial \xi} \quad (\text{B.21})$$

$$O(\varepsilon^4) : \quad -V \frac{\partial u_{jc3}}{\partial \xi} + V \frac{\partial u_{jc1}}{\partial \xi} + \frac{\partial (u_{jc1} u_{jc2})}{\partial \xi} + \frac{3\sigma}{N_c} \frac{\partial n_{jc3}}{\partial \xi} + \frac{3\sigma}{N_c^2} \frac{\partial (n_{jc1} n_{jc2})}{\partial \xi} = -Z_j \frac{\partial \phi_3}{\partial \xi} \quad (\text{B.22})$$

Poisson's (i.e., from (B.16))

$$O(\varepsilon^0) : \quad \sum_j Z_j N_c = 0 \quad (\text{B.23})$$

$$O(\varepsilon^1) : \quad 2N_h c_1 \phi_1 - \sum_j Z_j n_{jc1} = 0 \quad (\text{B.24})$$

$$O(\varepsilon^2) : \quad 2N_h c_1 \phi_2 - \sum_j Z_j n_{jc2} = 0 \quad (\text{B.25})$$

$$O(\varepsilon^3) : \quad 2N_h c_1 \phi_3 + 2N_h c_3 \phi_1^3 - \sum_j Z_j n_{jc3} = \frac{\partial^2 \phi_1}{\partial \xi^2}. \quad (\text{B.26})$$

Through integration, (B.17) becomes

$$V n_{jc1} = N_c u_{jc1},$$

which implies that

$$n_{jc1} = \frac{N_c}{V} u_{jc1} \quad \text{and} \quad u_{jc1} = \frac{V}{N_c} n_{jc1}. \quad (\text{B.27})$$

After integration, (B.18) can be written as

$$-V n_{jc2} + u_{jc1} n_{jc1} + N_c u_{jc2} = 0. \quad (\text{B.28})$$

Applying integration to (B.20) and (B.21), we have, respectively,

$$\frac{3\sigma}{N_c} n_{jc1} - V u_{jc1} = -Z_j \phi_1 \quad (\text{B.29})$$

and

$$-V u_{jc2} + \frac{u_{jc1}^2}{2} + \frac{3\sigma}{N_c} n_{jc2} + \frac{3\sigma}{2N_c^2} n_{jc1}^2 = -Z_j \phi_2. \quad (\text{B.30})$$

Substituting (B.27) into (B.30), we get

$$u_{jc1} = \frac{Z_j V}{V^2 - 3\sigma} \phi_1 \quad (\text{B.31})$$

$$n_{jc1} = \frac{Z_j N_c}{V^2 - 3\sigma} \phi_1. \quad (\text{B.32})$$

Using (B.32) in (B.33), we have

$$\left(2N_h c_1 - \sum_j \frac{Z_j^2 N_c}{V^2 - 3\sigma} \right) \phi_1 = 0.$$

Since $\phi_1 \neq 0$, this equation becomes

$$2N_h c_1 - \sum_j \frac{Z_j^2 N_c}{V^2 - 3\sigma} = 0, \quad (\text{B.33})$$

where V is the normalized sound speed which satisfies the long wave equation. Rearranging (B.28), gives us

$$N_c u_{jc2} = V n_{jc2} - u_{jc1} n_{jc1}. \quad (\text{B.34})$$

Multiplying both sides of (B.30) with N_c , we obtain that

$$-V N_c u_{jc2} + N_c \frac{u_{jc1}^2}{2} + 3\sigma n_{jc2} + \frac{3\sigma}{2N_c} n_{jc1}^2 = -Z_j N_c \phi_2. \quad (\text{B.35})$$

Substituting (B.31), (B.32) and (B.34) into (B.35), gives

$$(V^2 - 3\sigma) n_{jc2} = Z_j N_c \phi_2 + \frac{Z_j^2 N_c V^2}{(V^2 - 3\sigma)^2} \phi_1^2 + \frac{Z_j^2 N_c V^2}{2(V^2 - 3\sigma)^2} \phi_1^2 + \frac{3\sigma}{2} \frac{Z_j^2 N_c V^2}{(V^2 - 3\sigma)^2} \phi_1^2,$$

which implies that

$$n_{jc2} = \frac{Z_j N_c}{V^2 - 3\sigma} \phi_2 + \frac{3Z_j^2 N_c}{2(V^2 - 3\sigma)^3} (V^2 + \sigma) \phi_1^2. \quad (\text{B.36})$$

Substituting (B.36) into (B.25), we have

$$2N_h c_1 \phi_2 - \sum_j Z_j \left[\frac{Z_j N_c}{V^2 - 3\sigma} \phi_2 + \frac{3Z_j^2 N_c}{2(V^2 - 3\sigma)^3} (V^2 + \sigma) \phi_1^2 \right] = 0. \quad (\text{B.37})$$

By rearranging, (B.37) takes the form

$$\overbrace{\left[2N_h c_1 - \frac{\sum_j Z_j^2 N_c}{V^2 - 3\sigma} \right]}^0 \phi_2 - \frac{3}{2} \frac{\sum_j Z_j^3 N_c}{(V^2 - 3\sigma)^3} (V^2 + \sigma) \phi_1^2 = 0, \quad (\text{B.38})$$

where we have used (B.33) to make the coefficient of ϕ_2 zero in (B.38) above. Hence, by using the property of Eq. (3.32), the coefficient of ϕ_1^2 in the above equation also becomes zero. Then,

$$\frac{3}{2} \frac{\sum_j Z_j^3 N_c}{(V^2 - 3\sigma)^3} (V^2 + \sigma) \phi_1^2 = 0. \quad (\text{B.39})$$

Using (B.31), (B.33) and (B.36) into (B.35), we obtain

$$\begin{aligned} & -V u_{jc2} + \frac{1}{2} \left[\frac{Z_j V}{V^2 - 3\sigma} \phi_1 \right]^2 \\ & + \frac{3\sigma}{N_c} \left[\frac{Z_j N_c}{V^2 - 3\sigma} \phi_2 + \frac{3}{2} \frac{Z_j^2 N_c}{(V^2 - 3\sigma)^3} (V^2 + \sigma) \phi_1^2 \right] + \frac{3\sigma}{2N_c^2} \left[\frac{Z_j N_c}{V^2 - 3\sigma} \phi_1 \right]^2 = -Z_j \phi_2. \end{aligned}$$

After some rearrangement, this can be written as

$$-Vu_{jc2} + \left[\frac{Z_j^2 V^2}{2(V^2 - 3\sigma)^2} + \frac{9T_c Z_j^2}{2(V^2 - 3\sigma)^3} (V^2 + \sigma) + \frac{3Z_j^2 \sigma}{2(V^2 - 3\sigma)^2} \right] \phi_1^2 + Z_j \left[1 + \frac{3\sigma}{V^2 - 3\sigma} \right] \phi_2 = 0.$$

By simplifying this equation one obtains that

$$u_{jc2} = \frac{1}{2} Z_j^2 \left[\frac{V(V^2 + 9T_c)}{(V^2 - 3\sigma)^3} \right] \phi_1^2 + \frac{Z_j V}{V^2 - 3\sigma} \phi_2. \quad (\text{B.40})$$

Rearranging (B.19), gives us

$$N_c \frac{\partial u_{jc3}}{\partial \xi} = V \frac{\partial n_{jc3}}{\partial \xi} - V \frac{\partial n_{jc2}}{\partial \zeta} - \frac{\partial(u_{jc1} n_{jc2})}{\partial \xi} - \frac{\partial(u_{jc2} n_{jc1})}{\partial \xi}. \quad (\text{B.41})$$

Multiplying both sides of (B.22) by N_c , one obtain that

$$-VN_c \frac{\partial u_{jc3}}{\partial \xi} + VN_c \frac{\partial u_{jc1}}{\partial \zeta} + N_c \frac{\partial(u_{jc1} u_{jc2})}{\partial \xi} + 3\sigma \frac{\partial n_{jc3}}{\partial \xi} + \frac{3\sigma}{N_c} \frac{\partial(n_{jc1} n_{jc2})}{\partial \xi} = -Z_j N_c \frac{\partial \phi_3}{\partial \xi}. \quad (\text{B.42})$$

Inserting (B.41) into (B.42), and after some rearrangement, we obtain

$$(V^2 - 3\sigma) \frac{\partial n_{jc3}}{\partial \xi} = VN_c \frac{\partial u_{jc1}}{\partial \zeta} + V^2 \frac{\partial n_{jc1}}{\partial \zeta} + V \frac{\partial}{\partial \xi} (u_{jc1} n_{jc2} + n_{jc1} u_{jc2}) + N_c \frac{\partial}{\partial \xi} (u_{jc1} u_{jc2}) + \frac{3\sigma}{N_c} \frac{\partial}{\partial \xi} (n_{jc1} n_{jc2}) + Z_j N_c \frac{\partial \phi_3}{\partial \xi}. \quad (\text{B.43})$$

Using (B.31), (B.32), (B.36) and (B.40) into (B.41), we then have

$$\begin{aligned} (V^2 - 3\sigma) \frac{\partial n_{jc3}}{\partial \xi} &= VN_c \frac{\partial}{\partial \zeta} \left[\frac{Z_j V}{V^2 - 3\sigma} \phi_1 \right] + V^2 \frac{\partial}{\partial \zeta} \left[\frac{Z_j N_c}{V^2 - 3\sigma} \phi_1 \right] \\ &+ V \frac{\partial}{\partial \xi} \left[\frac{Z_j V}{V^2 - 3\sigma} \phi_1 \left(\frac{Z_j N_c}{V^2 - 3\sigma} \phi_2 + \frac{3Z_j^2 N_c}{2(V^2 - 3\sigma)^3} (V^2 + \sigma) \phi_1^2 \right) \right] \\ &+ V \frac{\partial}{\partial \xi} \left[\frac{Z_j N_c}{V^2 - 3\sigma} \phi_1 \left(\frac{1}{2} Z_j^2 \left[\frac{V(V^2 + 9\sigma)}{(V^2 - 3\sigma)^3} \right] \phi_1^2 + \frac{Z_j V}{V^2 - 3\sigma} \phi_2 \right) \right] \\ &+ N_c \frac{\partial}{\partial \xi} \left[\frac{Z_j V}{V^2 - 3\sigma} \phi_1 \left(\frac{1}{2} Z_j^2 \left[\frac{V(V^2 + 9\sigma)}{(V^2 - 3\sigma)^3} \right] \phi_1^2 + \frac{Z_j V}{V^2 - 3\sigma} \phi_2 \right) \right] \\ &+ \frac{3\sigma}{N_c} \frac{\partial}{\partial \xi} \left[\frac{Z_j N_c}{V^2 - 3\sigma} \phi_1 \left(\frac{Z_j N_c}{V^2 - 3\sigma} \phi_2 + \frac{3Z_j^2 N_c}{2(V^2 - 3\sigma)^3} (V^2 + \sigma) \phi_1^2 \right) \right] + Z_j N_c \frac{\partial \phi_3}{\partial \xi}. \end{aligned}$$

This can be written as

$$\begin{aligned} \frac{\partial n_{jc3}}{\partial \xi} &= 2 \frac{Z_j N_c V^2}{(V^2 - 3\sigma)^2} \frac{\partial \phi_1}{\partial \zeta} \\ &+ \frac{Z_j^3 N_c}{(V^2 - 3\sigma)^2} \left[\frac{(V^2 + 3\sigma)}{(V^2 - 3\sigma)^2} + \frac{9\sigma(V^2 + \sigma)}{(V^2 - 3\sigma)^3} + \frac{3(V^2 + 3\sigma)(V^2 + \sigma)}{2(V^2 - 3\sigma)^3} \right] \frac{\partial \phi_1^3}{\partial \xi} \\ &+ \frac{Z_j^2 N_c}{(V^2 - 3\sigma)^2} \left[3 \frac{(V^2 + \sigma)}{V^2 - 3\sigma} \right] \frac{\partial}{\partial \xi} (\phi_1 \phi_2) + \frac{Z_j^2 N_c}{V^2 - 3T_c} \frac{\partial \phi_3}{\partial \xi}. \end{aligned}$$

Multiplying both sides of the above equation by $\sum_j Z_j$, we have

$$\begin{aligned} \sum_j Z_j \frac{\partial n_{jc3}}{\partial \xi} &= 2 \frac{\sum_j Z_j^2 N_c V^2}{(V^2 - 3\sigma)^2} \frac{\partial \phi_1}{\partial \xi} \\ &+ \frac{\sum_j Z_j^4 N_c}{(V^2 - 3\sigma)^2} \left[\frac{(V^2 + 3\sigma)}{(V^2 - 3\sigma)^2} + \frac{9\sigma(V^2 + \sigma)}{(V^2 - 3\sigma)^3} + \frac{3(V^2 + 3\sigma)(V^2 + \sigma)}{2(V^2 - 3\sigma)^3} \right] \frac{\partial \phi_1^3}{\partial \xi} \\ &+ \frac{\sum_j Z_j^3 N_c}{(V^2 - 3\sigma)^2} \left[3 \frac{(V^2 + \sigma)}{V^2 - 3\sigma} \right] \frac{\partial}{\partial \xi} (\phi_1 \phi_2) + \frac{\sum_j Z_j^3 N_c}{(V^2 - 3\sigma)} \frac{\partial \phi_3}{\partial \xi}. \quad (\text{B.44}) \end{aligned}$$

Taking the derivative of (B.26) with respect to ξ , we get

$$\sum_j Z_j \frac{\partial n_{jc3}}{\partial \xi} = 2N_h c_1 \frac{\partial \phi_3}{\partial \xi} + 2N_h c_3 \frac{\partial \phi_1^3}{\partial \xi} - \frac{\partial^3 \phi_1}{\partial \xi^3}. \quad (\text{B.45})$$

Comparison between (B.44) and (B.45), gives us

$$\begin{aligned} -\frac{\partial^3 \phi_1}{\partial \xi^3} &+ \overbrace{\left[2N_h c_1 - \frac{\sum_j Z_j^2 N_c}{(V^2 - 3\sigma)^2} \right]}^0 \frac{\partial \phi_3}{\partial \xi} - 2 \frac{\sum_j Z_j^2 N_c V^2}{(V^2 - 3\sigma)^2} \frac{\partial \phi_1}{\partial \zeta} \\ &+ \left[2N_h c_3 - \frac{\sum_j Z_j^4 N_c}{(V^2 - 3\sigma)^2} \left(\frac{(V^2 + 3\sigma)}{(V^2 - 3\sigma)^2} + \frac{9\sigma(V^2 + \sigma)}{(V^2 - 3\sigma)^3} + \frac{3(V^2 + 3\sigma)(V^2 + \sigma)}{2(V^2 - 3\sigma)^3} \right) \right] \frac{\partial \phi_1^3}{\partial \xi} \\ &- \overbrace{\left[\frac{\sum_j Z_j^3 N_c}{(V^2 - 3\sigma)^2} \left[3 \frac{(V^2 + \sigma)}{V^2 - 3\sigma} \right] \right]}^0 \frac{\partial}{\partial \xi} (\phi_1 \phi_2) - \overbrace{\left[\frac{\sum_j Z_j^3 N_c}{(V^2 - 3\sigma)} \right]}^0 \frac{\partial \phi_3}{\partial \xi} = 0 \quad (\text{B.46}) \end{aligned}$$

Here we have used (B.39) and the property in Eq. (3.32) to make the coefficients of $\frac{\partial}{\partial \xi}(\phi_1 \phi_2)$ and $\frac{\partial \phi_3}{\partial \xi}$ in (B.46) equal to zero, respectively. With this, (B.46) takes the form

$$\begin{aligned} & -\frac{\partial^3 \phi_1}{\partial \xi^3} - 2 \frac{\sum_j Z_j^2 N_c V^2}{(V^2 - 3\sigma)^2} \frac{\partial \phi_1}{\partial \zeta} \\ & + \left[2N_h c_3 - \frac{\sum_j Z_j^4 N_c}{(V^2 - 3\sigma)^2} \left(\frac{(V^2 + 3\sigma)}{(V^2 - 3\sigma)^2} + \frac{9\sigma(V^2 + \sigma)}{(V^2 - 3\sigma)^3} + \frac{3(V^2 + 3\sigma)(V^2 + \sigma)}{2(V^2 - 3\sigma)^3} \right) \right] \frac{\partial \phi_1^3}{\partial \xi} \\ & = 0. \end{aligned}$$

This can also be written as

$$\begin{aligned} \frac{\partial \phi_1}{\partial \zeta} + \left[\frac{\frac{\sum_j Z_j^4 N_c}{(V^2 - 3\sigma)^2} \left(\frac{(V^2 + 3\sigma)}{(V^2 - 3\sigma)^2} + \frac{9\sigma(V^2 + \sigma)}{(V^2 - 3\sigma)^3} + \frac{3(V^2 + 3\sigma)(V^2 + \sigma)}{2(V^2 - 3\sigma)^3} \right) - 2N_h c_3}{2 \frac{\sum_j Z_j^2 N_c V^2}{(V^2 - 3\sigma)^2}} \right] \frac{\partial \phi_1^3}{\partial \xi} \\ + \frac{1}{2 \frac{\sum_j Z_j^2 N_c V^2}{(V^2 - 3\sigma)^2}} \frac{\partial^3 \phi_1}{\partial \xi^3} = 0. \end{aligned} \quad (\text{B.47})$$

Let

$$b = \frac{\sum_j Z_j^4 N_c}{(V^2 - 3\sigma)^2} \left(\frac{(V^2 + 3\sigma)}{(V^2 - 3\sigma)^2} + \frac{9T_c(V^2 + \sigma)}{(V^2 - 3\sigma)^3} + \frac{3(V^2 + 3\sigma)(V^2 + \sigma)}{2(V^2 - 3\sigma)^3} \right) - 2N_h c_3 \quad (\text{B.48})$$

and

$$a = 2 \frac{\sum_j Z_j^2 N_c V^2}{(V^2 - 3\sigma)^2}. \quad (\text{B.49})$$

With these substitutions (B.47) can be rewritten as

$$\frac{\partial \phi_1}{\partial \zeta} + \frac{b}{a} \frac{\partial \phi_1^3}{\partial \xi} + \frac{1}{a} \frac{\partial^3 \phi_1}{\partial \xi^3} = 0. \quad (\text{B.50})$$

Or

$$\boxed{\frac{\partial \phi_1}{\partial \zeta} + B \frac{\partial \phi_1^3}{\partial \xi} + C \frac{\partial^3 \phi_1}{\partial \xi^3} = 0}, \quad (\text{B.51})$$

where $B = \frac{b}{a}$ and $C = \frac{1}{a}$. Thus, the modified Korteweg de Vries (mKdV) equation can take the form expressed in (B.51).

Using the property of Eq. (3.32), (B.48) and (B.49) becomes

$$b = \frac{2N_c}{(V^2 - 3\sigma)^2} \left(\frac{V^2 + 3\sigma}{(V^2 - 3\sigma)^2} + \frac{9\sigma(V^2 + \sigma)}{(V^2 - 3\sigma)^3} + \frac{3(V^2 + 3\sigma)(V^2 + \sigma)}{2(V^2 - 3\sigma)^3} \right) - 2N_h c_3 \quad (\text{B.52})$$

and

$$a = \frac{4N_c V^2}{(V^2 - 3\sigma)^2}, \quad (\text{B.53})$$

respectively. Thus, the dispersive term coefficient C in the mKdV equation is defined as

$$C = \frac{(V^2 - 3\sigma)^2}{4N_c V^2}.$$

Using the definition for c_1 , we get

$$C = \frac{N_c}{4N_h^2} \left[\frac{2\kappa - 3}{2\kappa - 1} \right]^2 \left[\frac{1}{\frac{N_c}{N_h} \left[\frac{2\kappa - 3}{2\kappa - 1} \right] + 3\sigma} \right].$$

Applying the definition,

$$\frac{N_c}{N_h} = \alpha \quad \text{and} \quad N_c + N_h = 1 \implies N_h = \frac{1}{\alpha + 1} \quad \text{and} \quad N_c = \frac{\alpha}{\alpha + 1}$$

the expression for C reads,

$$C = \frac{\alpha(\alpha + 1)}{4} \left[\frac{2\kappa - 3}{2\kappa - 1} \right]^2 \left[\frac{1}{\alpha \left[\frac{2\kappa - 3}{2\kappa - 1} \right] + 3\sigma} \right]. \quad (\text{B.54})$$

After rearranging (B.52), we have

$$b = \left[\frac{N_c(5V^4 + 30V^2\sigma + 9\sigma^2) - N_h(V^2 - 3\sigma)^5 c_3}{(V^2 - 3\sigma)^5} \right]. \quad (\text{B.55})$$

So using (B.53) and (B.55), we then have

$$B = \frac{b}{a} = \left[\frac{N_c(5V^4 + 30V^2\sigma + 9\sigma^2) - N_h(V^2 - 3\sigma)^5 c_3}{(V^2 - 3\sigma)^5} \right] \left[\frac{(V^2 - 3\sigma)^2}{4N_c V^2} \right]. \quad (\text{B.56})$$

Applying an expression for an acoustic mode speed V which is obtained in Eq. (2.75) so far for four species EP plasma into (B.56), we get

$$B = - \left[\frac{2 \frac{c_3}{c_1^3} \left(\frac{N_c}{N_h} \right)^4 - 5 \frac{1}{c_1^2} \left(\frac{N_c}{N_h} \right)^2 - 60\sigma \left(\frac{1}{c_1} \right) \left(\frac{N_c}{N_h} \right) - 144\sigma^2}{4 \left(\frac{N_c}{N_h} \frac{1}{c_1} + 3\sigma \right) \left(\frac{N_c}{N_h} \frac{1}{c_1} \right)^3} \right]. \quad (\text{B.57})$$

Since we have already defined that $\alpha = \frac{N_c}{N_h}$, the coefficient of nonlinear term in a mKdV equation can take be written as

$$B = - \left[\frac{2 \frac{c_3}{c_1^3} \alpha^4 - 5 \frac{\alpha^2}{c_1^2} - 60\sigma \left(\frac{\alpha}{c_1} \right) - 144\sigma^2}{4 \left(\frac{\alpha}{c_1} + 3\sigma \right) \left(\frac{\alpha}{c_1} \right)^3} \right]. \quad (\text{B.58})$$

In terms of the superthermal parameter, this equation finally takes the form

$$B = - \frac{\left[\left(\frac{16\kappa^4 - 16\kappa^3 - 48\kappa^2 + 36\kappa + 27}{16\kappa^4 - 32\kappa^3 + 24\kappa^2 - 8\kappa + 1} \right) \alpha^4 - \left(\frac{2\kappa - 3}{2\kappa - 1} \right)^2 15\alpha^2 - \left(\frac{2\kappa - 3}{2\kappa - 1} \right) 180\sigma\alpha - 432\sigma^2 \right]}{12 \left[\left(\frac{2\kappa - 3}{2\kappa - 1} \right) \alpha + 3\sigma \right] \left[\left(\frac{2\kappa - 3}{2\kappa - 1} \right) \alpha \right]^3}. \quad (\text{B.59})$$

Bibliography

- Alinejad, H., Sobhanian, S., and Mohamoodi, J. (2006). *Phys. Plasmas*, 13(012304).
- Baboolal, S., Bharuthram, R., and Hellberg, M. A. (1988). *Phys. Plasmas*, 40(1):163–178.
- Baboolal, S., Bharuthram, R., and Hellberg, M. A. (1990). *Phys. Plasmas*, 44(1):1–23.
- Baluku, T. K. and Hellberg, M. A. (2008). *Phys. Plasmas*, 15(123705).
- Baluku, T. K. and Hellberg, M. A. (2011). *Plasma. Phys. Control. Fusion*, 53(095007).
- Baluku, T. K., Hellberg, M. A., Kourakis, I., and Saini, N. S. (2010a). *Phys. Plasmas*, 17(053702).
- Baluku, T. K., Hellberg, M. A., and Verheest, F. (2010b). *Europhysics Letters*, 91(15001).
- Beskin, V. S. (2010). *MHD Flows in Compact Astrophysical Objects*, page 93. Springer-Verlag, Berlin Heidelberg.
- Beskin, V. S., Gurevich, A. V., and Istomin, Y. N. (1983). *Sov. Phys.JETP.*, 58(235).
- Beskin, V. S., Gurevich, A. V., and Istomin, Y. N. (1993). *Physics of the Pulsar Magnetosphere*, pages 92 – 93, 101. Cambridge University Press, The Edinburgh building, Cambridge CB2 2RU, UK.
- Bharuthram, R. (1992). *Astrophys. Space Sci.*, 189:213 – 139.
- Chen, F. F. (1983). *Introduction to Plasma Physics and Controlled Fusion*. Plenum Press, New York.

- Danehkar, A., Nareshpal, S. S., Hellberg, M. A., and Kourakis, I. (2011). *Phys. Plasmas*, 18(072902).
- Drazin, P. G. (1983). *London Mathematical Society Lecture Note Series. 85*, page 1. Cambridge University Press, Cambridge.
- El-Awady, E. I., El-Tantawy, S. A., Moslem, W. M., and Shukla, P. K. (2010). *Phys. Lett A*, 91:3216 – 3219.
- Formisano, V., Moreno, G., and Palmiotto, F. (1973). *Journal of Geophysical Research*, 78(3714).
- Ghosh, S. and Bharuthram, R. (2008). *Space. Sci.*, 314(121).
- Ghosh, S. S., Ghosh, K. K., and Iyengar, A. N. S. (1996). *Phys. Plasmas*, 3(11):3940.
- Goldreich, P. and Julian, W. H. (1969). *Astrophysical Journal*, 157:889.
- Gray, G. J. (1998). *Electrostatic Waves and Solitons in Electron-Positron Plasmas*. MSc Thesis, University of Natal, Durban, South Africa.
- Greaves, R. G. and Surko, C. M. (1995). *Phys. Rev. Lett.*, 75(3846).
- Greaves, R. G., Tinkle, M. D., and Surko, C. M. (1994). *Phys. Plasmas*, 1(5).
- Guo, S., Mei, L., and and, A. S. (2012). *Annals of Phys.*, 332:38 – 55.
- Gurevich, A. V. and Istomin, Y. N. (1985). *Sov. Phys. JETP*, 62(1).
- Hammond, C. M., Feldman, W. C., Phillips, J. L., Goldstein, B. E., and Balogh, A. (1995). *Journal of Geophysical Research*, 100(A5):7881 – 7889.
- Hellberg, M. A. and Mace, R. L. (2002). *Phys. Plasmas*, 9(5).
- Hellberg, M. A., Mace, R. L., Baluku, T. K., Kourakis, I., and Saini, N. S. (2009). *Phys. Plasmas*, 16(094701).
- Istomin, Y. N. (2008). *Physics-USpekhi*, 51(8):847.

- Istomin, Y. N. and Sobyenin, D. N. (2007). *Astronomy Letters*, 33(10):660–672.
- Jehan, N., Masood, W., and Mirza, A. M. (2009). *Physica Scripta*, 80(035506):6.
- Lazarus, I. J., Bharuthram, R., Singh, S. V., Pillay, S. R., and Lakhina, G. S. (2012). *Phys. Plasmas*, 78:621 – 628.
- Leubner, M. P. (2004). *Phys. Plasmas*, 11(1308).
- Livadiotis, G. and McComas, D. J. (2010). *The Astrophysical Journal*, 714:971 – 987.
- Livadiotis, G. and McComas, D. J. (2011). *The Astrophysical Journal*, 741:28 pp.
- Livadiotis, G. and McComas, D. J. (2013). *Space Science Reviews*, 175:215 – 215.
- Lu, D., Li, Z. L., Abdukerim, N., and Xie, B. S. (2014). *Phys. Plasmas*, 21(022108).
- Mace, R. L. (1991). *Linear and Nonlinear Electron Acoustic Waves in Plasmas with Two Electron Components*. Ph.D Thesis, University of Natal, Durban, South Africa.
- Mace, R. L. and Hellberg, M. A. (1993). *Journal of Geophysical Research*, 98(4):5881–5891.
- Mace, R. L. and Hellberg, M. A. (1995). *Phys. Plasmas*, 2(2098).
- Marsch, E., Muhlhauser, K. H., Schwenn, R., Rosenbauer, H., Phillip, W., and Neubauer, F. M. (1982). *Journal of Geophysical Research*, 87:6331.
- McKenzie, J. F. and Doyle, T. (2003). *New Journal of Physics*, 5(26):1–10.
- Misner, W., Throne, K. S., and Wheeler, J. A. (1973). *Gravitation*, page 763. W. H. Freeman, San Francisco.
- Moslem, W. M., Kourakis, I., Shukla, P. K., and Schlickeiser, R. (2007). *Phys. Plasmas*, 14(102901).
- Pierrard, V. and Lazar, M. (2010). *Kappa Distributions: Theory and Applications in Space Plasmas*, pages 153–174. Springer Science+ Business Media B. V.
- Pillay, R. and Bharuthram, R. (1992). *Astrophys. Space Sci.*, 198.

- Popel, S. I., Vladimirov, S. V., and Shukla, P. K. (1995). *Phys. Plasmas*, 2(3):716–719.
- Roychoudhury, R. and Maitra, S. (2002). *Phys. Plasmas*, 9(10):4161.
- Roychoudhury, R. K. and Bhattacharrya, S. (1987). *Can. Journal of Phys.*, 65:699.
- Sagdeev, R. Z. (1966). *Cooperative phenomena and shock waves in collisionless plasmas*, In M. A. Leontovich, editor, pages 23–91. Consultants Bureau, New York.
- Scudder, J. D., Sittler, E. C., and Bridge, H. S. (1981). *Journal of Geophysical Research*, 86(8157).
- Shukla, P. K., Eliasson, B., and Stenflo, L. (2011). *Phys. Rev. E*, 84(037401-1).
- Shukla, P. K. and Mamun, A. A. (2002). *Introduction to Dusty Plasma Physics*, page 195. IOP, Bristol, UK.
- Shukla, P. K., Rao, N. N., Yu, M. Y., and Tsintsadze, N. L. (1986). *Phys. Rev.*, 135(1).
- Sturrock, P. K. (1971). *Astrophysical Journal*, 164.
- Summers, D. and Thorne, R. M. (1991). *Physics of Fluids B: Plasma Physics*, 3:1835–1847.
- Swanson, D. G. (2003). *Plasma Waves*, page 355. IOP Publishing, Bristol, UK.
- Urpin, V. (2011). *Astronomy and Astrophysics*, 535(L5).
- Vasyliunas, V. M. (1968). *Journal of Geophysical Research*, 73:5810 – 5810.
- Verheest, F. (1988). *Phys. Plasmas*, 39(1):4012.
- Verheest, F. (2000). *Waves in Dusty Space Plasmas*. Kluwer, Dordrecht, Netherlands.
- Verheest, F. and Hellberg, M. A. (1999). *Physics Scripta*, T82:99.
- Verheest, F., Hellberg, M. A., Gray, G. J., and Mace, R. L. (1996). *Astrophys. Space Sci.*, (239):125 – 139.
- Verheest, F., Hellberg, M. A., and Kourakis, I. (2008). *Phys. Plasmas*, 15(112309).

- Verheest, F. and Pillay, S. R. (2008). *Phys. Plasmas*, 15(013703).
- Wang, H. and Zhang, K. B. (2014). *Journal of the Korean Physical Society*, 64(11):1677–1682.
- Washimi, H. and Taniuti, T. (1966). *Physical Review Letters*, 17(19):996.
- Watanabe, K. and Taniuti, T. (1977). *Journal of the Physical Society of Japan*, 43:1819–1820.
- Watanabe, S. (1984). *Journal of the Physical Society of Japan*, 53:950–956.
- Zabusky, N. J. and Kruskal, M. D. (1965). *Physical Review Letters*, 15(6):240–243.
- Zank, G. P. and Greaves, R. G. (1995). *Physical Review E*, 51:6079–6090.
- Zheleznyakov, V. V. (1996). *Radiation process in astrophysical plasmas*, page 231. Kluwer, Dordrecht.